

PhD Dissertation 05/2014

Modelling and Analysing the Structure and Dynamics of Species-rich Grasslands and Forests

Franziska Taubert



**Modelling and Analysing
the Structure and Dynamics of
Species-rich Grasslands and Forests**

Dissertation for the degree of Doctor of Natural Sciences (Dr. rer. nat.)

University of Osnabrück

Department of Mathematics/Computer Science

submitted by
Franziska Taubert
from Borna

Osnabrück 2013

Modelling and Analysing the Structure and Dynamics of Species-rich Grasslands and Forests

PhD Dissertation, University of Osnabrück, 2013

Author's address: Franziska Taubert, Helmholtz Centre for Environmental Research – UFZ,
Department of Ecological Modelling, Leipzig, Germany.

Homepage: <http://www.ufz.de/index.php?en=20718>

Supervised by:

Prof. Dr. Andreas Huth (UFZ Leipzig/University of Osnabrück)

Prof. Dr. Karin Frank (UFZ Leipzig/University of Osnabrück)

Defense committee (21.02.2014):

Prof. Dr. Andreas Huth (UFZ Leipzig/University of Osnabrück, 1st reviewer)

Prof. Dr. Frank Hilker (University of Osnabrück, 2nd reviewer)

Prof. Dr. Karin Frank (UFZ Leipzig/University of Osnabrück)

Dr. Jörg Klasmeier (University of Osnabrück)

Abstract

Ecosystems provide important functioning and services, like biomass for bioenergy production or storage of atmospheric carbon. Two examples of such ecosystems are temperate grasslands and tropical forests. Both vegetation are rich of various species, whereby each of the respective ecosystem benefits from its species-richness concerning their functioning, i.e. productivity. In this thesis both vegetation are in the focus of the investigations. In the first chapter, a review of existing grassland and vegetation models provides an overview of important aspects, which have to be considered for modelling temperate grasslands in the context of biomass production. Based on the review, new conceptual modelling approaches for temperate grasslands are proposed. In the third chapter, derived from the suggested concept, the process-oriented and individual-based grassland model Grassmind is presented. In the fourth chapter, the model Grassmind is used in order to parameterize and simulate the annual dynamics of a typical Central European grass species. Grassmind is able to reproduce the structure and dynamics of a temperate grass species. With reference to the parameterized grass species, a simulation study using defined species groups is performed in order to investigate on the effect of the richness of species groups on aboveground productivity. We do not observe a significant positive effect of species group richness on productivity, which is explained by limitations of using the parameterized grass species as a reference. In the fifth chapter, comprehensive investigations are carried out on the example of stem size distributions in forests concerning their statistical analyses, i.e. by using maximum likelihood estimation. The effects of uncertainties, i.e. binning of measured stem sizes or random measurement errors, are examined in detail. Uncertainties bias the analyses of maximum likelihood estimations. It is shown, that the use of modified likelihood functions, which include either binning or measurement errors, reduce these biases to a large extent. For both studies, i.e. modelling of temperate grasslands and analysing stem size distributions of forests, the presented investigations are discussed and possible examinations are suggested for future research in the last chapter.

Brief contents

Abstract	2
Contents.....	5
1. Introduction.....	7
2. A Review of Grassland Models in the Biofuel Context.....	21
3. Grassmind – Model Description.....	42
4. Simulating the Structure and Dynamics of Temperate Grasslands in the Context of Diversity-Productivity Relationships	66
5. On the Challenge of Fitting Tree Size Distributions in Ecology	79
6. Discussion and Future Perspectives	96
Appendices	104
Figures.....	127
Tables.....	130
Bibliography.....	131

Contents

Abstract	2
Brief contents	4
1. Introduction.....	7
1.1 <i>Species-rich temperate grasslands</i>	7
1.2 <i>Modelling the structure and dynamics of grasslands</i>	14
1.3 <i>Analysing the structure and dynamics of species-rich forests</i>	15
1.4 <i>Research objectives</i>	17
1.5 <i>The chapters at a glance</i>	18
2. A Review of Grassland Models in the Biofuel Context.....	21
2.1 <i>Introduction</i>	22
2.2 <i>Review and evaluation methods</i>	23
2.3 <i>Brief review of grassland modelling concepts</i>	25
2.4 <i>Discussion</i>	39
3. Grassmind – Model Description.....	42
3.1 <i>Overview</i>	42
3.2 <i>The geometry of an individual</i>	44
3.3 <i>Model processes</i>	47
3.4 <i>Model inputs and outputs</i>	60
3.5 <i>Coupling Grassmind with a soil model</i>	63
4. Simulating the Structure and Dynamics of Temperate Grasslands in the Context of Diversity-Productivity Relationships	66
4.1 <i>Introduction</i>	66
4.2 <i>Material and methods</i>	68
4.3 <i>Results</i>	73
4.4 <i>Discussion</i>	76
5. On the Challenge of Fitting Tree Size Distributions in Ecology	79
5.1 <i>Introduction</i>	80

5.2	<i>Materials and methods</i>	82
5.3	<i>Results</i>	87
5.4	<i>Discussion</i>	93
6.	Discussion and Future Perspectives	96
6.1	<i>The approach developed in this thesis</i>	96
6.2	<i>Main results</i>	100
6.3	<i>Outlook</i>	101
	Appendices	104
	Figures.....	127
	Tables.....	130
	Bibliography.....	131

Chapter 1

Introduction

Vegetation plays an important role either harvested for purposes like biomass conversion to energy products (e.g. electricity) or seen as a key position in storing atmospheric carbon sources. The diversity of species in different vegetation types influences the potential of such possible uses. Various types of vegetation are present ranging from highly diverse forests in the tropics to less species-rich steppes or savannahs to human influenced ecosystems in the temperate zone like semi-natural grasslands. This work focuses mainly on two of them: (a) species-rich grasslands in the temperate zone and (b) species-rich forests in the tropics. Both vegetation types are predominantly characterised by the occurrence of various plant species and their interactions. Site-specific factors like climate and soil conditions, the biotic environment, and human-based activities have an influence often resulting in observable patterns on the ecosystem-level. Two prominent examples represent the diversity-productivity relationships in grasslands and the functional relationship of tree size distributions in tropical forests. Attempts to understand such emerging patterns of an ecosystem's structure and functioning, profit from simulation models and statistical analysis tools. In this work, we address (a) the discrepancies between the variety of existing process-based modelling approaches or analysis tools and (b) the need for novel attempts for both techniques on the example of semi-natural grasslands in Central Europe within the bioenergy context and measured tree size distributions of species-rich tropical forests.

1.1 Species-rich temperate grasslands

1.1.1 Diversity of grasslands in the temperate zone

There is a large variety of different herbaceous species occurring in temperate grasslands. In Central Europe, approximately 80.3 % of the species of vascular plants are attributed to herbaceous species (Ellenberg & Leuschner 2010; Ellenberg *et al.* 1992). Most grasslands in Central Europe consist mainly of so-called *hemi-cryptophytes* – a class of species, which have their renewal buds near the soil surface (Ellenberg & Leuschner 2010). About 56 % of the herbaceous species are *hemi-cryptophytes* (Ellenberg & Leuschner 2010;

Ellenberg *et al.* 1992). By their low positioned buds, they are best adapted to the Central European climatic conditions (Ellenberg & Leuschner 2010). For example in winter, their survival is ensured as a closed snow cover protects their buds (Ellenberg & Leuschner 2010). Examples of such species comprise meadow and red fescue (*Festuca pratensis* and *Festuca rubra*), timothy (*Phleum pratense*) or perennial and Italian ryegrass (*Lolium perenne* and *Lolium multiflorum*).

Different types of grasslands exist in Central Europe – the so-called *plant associations*. About 13.2 % of the European land surface area has been covered in the year 2007 by permanent grasslands and meadows (Eurostat Yearbook 2012). Examples are Nardus grasslands, dry to semi-dry grasslands and permanent cultivated grasslands (Ellenberg & Leuschner 2010; Fig. 1.1). Nardus grasslands are typical for soils with low nutrient concentrations, dominated by the tussock-forming species *Nardus stricta* in combination with extensive management (Nitsche & Nitsche 1994; Ellenberg & Leuschner 2010). This grassland type is often found on cool and humid sites, for example in North-West-Germany and the Netherlands (Ellenberg & Leuschner 2010). Those Nardus grasslands of the lowlands and low mountain ranges are characterized by a poor species-richness (Ellenberg & Leuschner 2010). For example, a subtype of Nardus grasslands, i.e. the *Galium-saxatile-Nardus-stricta* association, of heavy acidic sandy soils reveals only 17 species (Ellenberg & Leuschner 2010; Pott & Hüppe 1991). Typical species coexisting with the dominant species *Nardus stricta* comprise *Holcus lanatus*, *Danthonia decumbens* and others (Ellenberg & Leuschner 2010). In contrast, Nardus grasslands of the high mountain ranges or alpine zone reveal a higher species-richness with the typical occurring species *Anthoxanthum alpinum*, *Pseudorchis albida* and others (Ellenberg & Leuschner 2010; Peppeler-Lisbach & Petersen 2001).

Only a small fraction of grasslands in Central Europe occurs as nutrient-poor, dry or semi-dry grasslands, also called *xerothermic grasslands* (Ellenberg & Leuschner 2010). But these types of grasslands are highly important due to their great species-richness. Ellenberg & Leuschner (2010) state that more than 10 % of the Central European vascular plants occur mainly on nutrient-poor, dry grasslands. For example, on alkaline soils up to 80 species per 4 m² can be found (Ellenberg & Leuschner 2010; Dengler 2005). This high species-richness is explained by resource limitations, which promote weak competitive species and hinder ones that are more competitive (Grime 1981; Keel 1995; Ellenberg & Leuschner 2010).

Species with high competitive strength often occur on permanent cultivated grasslands (Ellenberg & Leuschner 2010). This type of grassland forms the majority of all occurring types in Central Europe (Ellenberg & Leuschner 2010). About one third of all vascular plants are mainly found on permanent pastures (Ellenberg & Leuschner 2010). Extensively cultivated grasslands differ from intensively cultivated ones not only according to the cultivation intensity, but also according to species-richness. Extensive meadows can show up

to 70 vascular species per 20 m², whereby intensively used ones reveal only 25 species per 20 m² (Ellenberg & Leuschner 2010). About one third to 50 % of species composition is usually designated by grass species (Ellenberg & Leuschner 2010; Klapp 1971). A typical example of cultivated grasslands is the *Molino-Arrhenatheretea grassland association* with the presence of grass species like *Poa pratensis* and *Anthoxanthum odoratum*, herbs like *Viccia cracca* and *Lathyrus pratensis* or legumes *Trifolium pratense* (Ellenberg & Leuschner 2010).

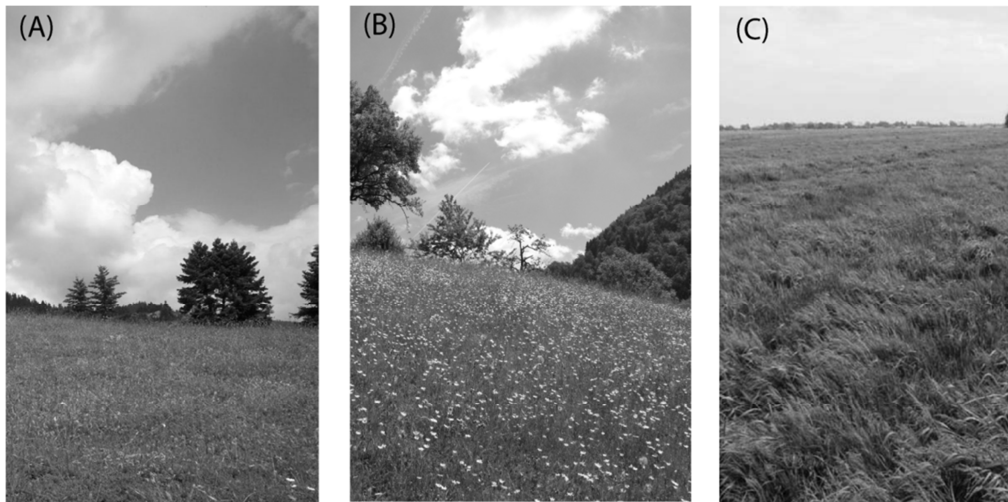


Figure 1.1: Pictures of the three types of grasslands: (A) Nardus grassland on Mount Oiti, Greece (picture from www.foropenforests.org), (B) dry grassland in Beinwil, Switzerland (picture from L. Pfiffner, www.fibl.org), (C) permanent cultivated grassland in Germany (picture from Artenagentur, <http://artenagentur-sh.lpv.de/>)

Aboveground net productivity rates of the mentioned grassland associations span a broad range between 100 and 1500 g dry matter per m² and year (Ellenberg & Leuschner 2010). For example, dry and Nardus grasslands can yield approximately 100 to 300 g dry matter per m² and year, whereby intensively cultivated permanent grasslands can achieve a productivity rate of 1000 to 1200 g dry matter per m² and year (Ellenberg & Leuschner 2010). This shows that aboveground productivity of grasslands is highly dependent on the species diversity and composition, soil properties and human cultivation activities.

1.1.2 The diversity-productivity relationship and its understanding

Various experimental studies have been performed in the last decades, which investigated on the effect of species richness on the aboveground net productivity of grassland communities. Large biodiversity experiments have been established across Europe and the

United States of America. In 1994 Tilman and colleagues initiated an experimental design in the Cedar Creek Ecosystem Science Reserve in the USA by planting various mixtures of different diversity levels (Tilman *et al.* 2001). The large-scale BIODEPTH network of eight European experiments is composed of several investigations of various sites across Europe (Kinzig *et al.* 2002; Spehn *et al.* 2005; Hector *et al.* 1999). Study sites range from northern areas in Sweden to southern ones in Greece (Diemer *et al.* 1997; Lawton *et al.* 1998; Hector *et al.* 1999; Mulder *et al.* 1999; Scherer-Lorenzen 1999; Spehn *et al.* 2000a, 2000b, 2005; Troumbis & Memtas 2000). The experiments have been designed such that not only the effect of species composition, but also site conditions can be investigated (Spehn *et al.* 2005). The latest established large biodiversity experiment - the *Jena Experiment*, is located in Central Germany in Thuringia (Weigelt *et al.* 2010). Its study design comprises main experiments of different species combinations on 20 x 20 m plots and additional small-scale experiments (Roscher *et al.* 2004). Besides the large biodiversity experiments, several small-scale experimental studies on the diversity-productivity relationship have also been carried out (McNaughton 1993; Swift & Anderson 1993; Naeem *et al.* 1995, 1996; Hooper & Vitousek 1997, 1998; Symstad *et al.* 1998). For example, Naeem *et al.* (1995, 1996) performed greenhouse experiments of random species assemblages from one to 16 species diversity and observed a significant positive effect within the diversity-productivity relationship.

In general, the large biodiversity experiments revealed a positive effect of species richness on productivity. Net productivity has been estimated from aboveground biomass of the vegetation (Tilman *et al.* 1997, 2001, 2006b; Weigelt *et al.* 2009; Spehn *et al.* 2005). Experiments differ in the extent to which productivity increases with higher species-richness. For example, Tilman *et al.* (1997) found from his experimental studies in 1996 an increase of mean aboveground biomass from 20 g dry matter per m² for monocultures to 160 g dry matter per m² for 32-species-mixtures. For the consecutive years 1997 to 2000, Tilman and colleagues observed higher biomass values on average up to 300 g dry matter per m² for 16-species-mixtures and even steeper slopes of the diversity-productivity relationship for the years 1999 and 2000 (Tilman *et al.* 2001). Similar results have been observed in the *Jena Experiment*, which show for the years 2003 and 2004 an increase of mean productivity from 500 g dry matter per m² and year for monocultures to 750 g dry matter per m² and year (Marquard *et al.* 2009a). For the consecutive years of observation, mean monoculture productivities reduce by one half and average net productivity rates of the 16-species-mixtures reduce to a range between approximately 400 to 700 g dry matter per m² and year (Marquard *et al.* 2009a; Weigelt *et al.* 2009). The different study sites of the BIODEPTH network show variable results - for some sites positive and for others neutral effects of species diversity (Spehn *et al.* 2005). The site in Germany reveals an increase of aboveground biomass from approximately 400 g dry matter per m² for monocultures to 500 g dry matter per m² for 16-species-mixtures, increasing even up to 1250 g dry matter per m² for the second and

third year of observation (Spehn *et al.* 2005). In contrast, the site in Greece shows a constantly remaining aboveground biomass of 250 g dry matter per m², irrespective of year and species-richness (Spehn *et al.* 2005).

Currently, concepts explaining the mechanisms responsible for the observed effects comprise on the one hand stochastic mechanisms and on the other hand deterministic mechanisms (Loreau & Hector 2001, Loreau *et al.* 2001). The stochastic ones include random sampling of the species mixtures designed within the experiments (Kinzig *et al.* 2002; Loreau & Hector 2001; Loreau *et al.* 2001) in combination with the dominance of a highly competitive species. That means, with a rising species-richness the probability of the presence of higher competitive species dominating the community is increasing (Kinzig *et al.* 2002; Loreau & Hector 2001; Loreau *et al.* 2001). As a result, biomass of species, suppressed by the dominating species, decreases in highly diverse mixtures (Kinzig *et al.* 2002). This mechanism reveals in the diversity-productivity curves, if no multi-species-mixture performance exceeds the best monoculture performance (Kinzig *et al.* 2002; Loreau & Hector 2001; Loreau *et al.* 2001). In contrast, the complementarity mechanisms would reveal species performances in the mixtures higher than expected from their performance in monocultures (Kinzig *et al.* 2002; Loreau & Hector 2001; Loreau *et al.* 2001). Complementarity explains positive diversity effects by niche differentiation – that means species differ in their functional traits, thus occupying different niches in the resource space (Kinzig *et al.* 2002; Loreau & Hector 2001; Loreau *et al.* 2001). This implies that biomass of single species increases with increasing diversity (Kinzig *et al.* 2002). Incorporated in the complementarity could also be facilitation between species. Facilitation occurs for example in grass-legume mixtures. Legumes are in symbiosis with rhizobia fixing atmospheric nitrogen. By this, legumes do not compete with grass species for soil nitrogen resources, but contribute additional nitrogen to soil by death or litterfall. Loreau & Hector (2001) proposed a standard statistical method to distinguish selection and complementarity effects within the diversity-productivity relationship. Positive complementarity effects can explain a higher importance of interspecific interactions rather than intraspecific interactions (Reich *et al.* 2012). In turn, a negative complementarity effect can reveal that intraspecific interactions are more important (Reich *et al.* 2012). In contrast, a positive selection effect can show that the most productive species reaches higher productivity values in the mixtures than expected from its monoculture (Reich *et al.* 2012). A negative selection effect reveals that the least productive species exceeds its expected monoculture productivity in mixtures (Reich *et al.* 2012).

Following the above-mentioned concepts, several studies calculated the complementarity and selection effect using the additive partitioning of both biodiversity effects proposed by Loreau & Hector (2001). In all biodiversity experiments, generally both effects have been observed. Loreau & Hector (2001) applied the additive partitioning first to the measurements of the BIODEPTH network experiments. Results differ between the study

sites. Generally, positive complementarity effects are revealed, which increased on average with species-richness for nearly all site (Loreau & Hector 2001; Spehn *et al.* 2005). Instead, selection effects vary broadly around zero remaining on average constant with increasing species diversity (Loreau & Hector 2001; Spehn *et al.* 2005). The BioCON and BioDIV experiments of Tilman *et al.* (1997; 2001; 2006a; Reich *et al.* 2001, 2006) show both a positive complementarity effect increasing on average with time and species-richness and a neutral selection effect slightly decreasing on average with time and species-richness (Fargione *et al.* 2006; Reich *et al.* 2012). Investigations in the *Jena Experiment* show on average a positive complementarity and selection effect (Marquard *et al.* 2009a). Complementarity effects increase on average with species-richness and time, whereby diversity and time have no influence on the selection effect (Marquard *et al.* 2009a).

Strategies other than applying the additive partitioning approach by Loreau & Hector (2001) comprise detailed individual-level measurements of species. For example, Marquard *et al.* (2009b) measured the density and aboveground biomass on the individual-level of each species of the mixtures. They suggest that species, which revealed higher biomass in mixtures than expected from their respective monocultures, increased in their densities and thus, play a key role in the positive diversity-productivity relationships (Marquard *et al.* 2009b). Nevertheless, the role of single species for the diversity-productivity relationships remains almost unknown.

1.1.3 Managing grasslands for biomass production

In the course of the debate on sustainable energy supply, the observed positive effects of biodiversity on the productivity of grasslands open up new perspectives. Currently, the worldwide primary energy demands are estimated of more than 400 EJ per year, whereby it has been estimated that only 7.5 % can be provided by energy converted from forest biomass (e.g. short rotation coppices) and agriculturally produced biomass (McKendry 2002a, 2002b). Thereby, biomass derived from crop monocultures like maize, wheat or rapeseed provokes conflicts between food and fuel production (Gelfand *et al.* 2013).

In 2006 Tilman and colleagues proposed the use of grassland mixtures of high species diversity for sustainable biomass production on abandoned land (Tilman *et al.* 2006b). Within the bioenergy context, Tilman and colleagues compared two types of systems: (a) extensively managed grassland mixtures denoted as *Low-Input-High-Diversity (LIHD)* and (b) intensively managed mixtures denoted as *High-Input-Low-Diversity (HILD)* grasslands (Tilman *et al.* 2006b). They represent two extreme sides along a management and diversity gradient (Fig. 1.2). Management options can be applied with different frequency of use and intensity of

input. A variety of management options, which differ in frequency and intensity of application, ranges from no or low extent (extensive management) to high magnitudes (intensive management). Frequency and intensity of management activities generally modify competition for resources between all plants (e.g by increasing the availability of light, soil nutrients and soil water; Ellenberg & Leuschner 2010). By this, highly productive or disturbance tolerant species are favoured, which suppress other species, gradually reducing species diversity of the ecosystem (Ellenberg & Leuschner 2010). As a result, *LIHD* grasslands show usually a higher species richness, whereas *HILD* grasslands tend to have less species diversity. Based on the experiments of Tilman *et al.* (2006b) in the Cedar Creek Ecosystem Science Reserve they calculate that the biomass harvests from *LIHD* grasslands can reach a gross energy yield of 68.1 GJ per hectare and year. Further, the use of natural grasslands can mitigate greenhouse gas emissions (Tilman *et al.* 2006b) and decrease competition for land as their cultivation is possible on abandoned or agriculturally unsuitable land (Tilman *et al.* 2006b; Gelfand *et al.* 2013).



Figure 1.2: Schematic view of different management option affecting the diversity of grasslands.

Next to the benefits of species diversity for biomass productivity in *LIHD* grasslands, several positive side effects concerning ecosystem functioning reveal with increasing species richness. For example, Tilman *et al.* (2006b) observe also an increase of annual carbon sequestration in soil and plant roots with increasing species diversity. Monocultures store approximately 0.62 MG per hectare and year in their roots, whereby 16-species-mixture reach 160 % more carbon storage of atmospheric carbon dioxide (Tilman *et al.* 2006b). Services provided by such ecosystem functions can be broadly classified into provisioning, regulating, supporting, and cultural services (according to the TEEB Ecological and Economic Foundations; TEEB 2010; de Groot *et al.* 2002). For example, regulating services include the maintenance of natural soil by nutrient regulation and provisioning services comprise the energy supply by biomass production (de Groot *et al.* 2002).

Major factors for assessing the relevance of semi-natural grasslands in the bioenergy context comprise economic aspects like maximized biomass production, low inputs of energy and nutrients as well as low cost for their production (McKendry 2002a, 2002b). These aspects are generally dependent on environmental conditions of the biomass producing system, on the chemical composition of the produced biomass material and on the conversion technology (McKendry 2002a, 2002b). Concerning the two latter ones, herbaceous plants can be categorized, for example, into low-moisture-material able for gasification or combustion and into high-moisture-material suitable for fermentation processes (McKendry 2002a, 2002b). Further characteristics of the biomass material influencing the energy potential comprise amongst other the calorific value, the ash or residue content and cellulose-lignin ratio (McKendry 2002a, 2002b). Including *LIHD* grasslands in the renewable and sustainable energy production, pays additional attention to ecological aspects such as biodiversity. Long-term advantages of biodiversity, for example increased soil fertility, could affect economic aspects indirectly. For example, increasing species diversity could accompany with a positively influenced nutrient cycle. By this, lower fertilization would be needed, which in turn would reduce costs for purchase and input of fertilizers.

1.2 Modelling the structure and dynamics of grasslands

Current modelling approaches of grassland ecosystems focus mainly on a few species. Interactions and competition is often only considered on the population-level for one or two resources. Nevertheless, temperate conditions across Central Europe are characterized by changing light, nitrogen and water resource availabilities. For assessing and understanding changes in the diversity-productivity relationships as well as its underlying mechanisms like complementarity and selection, a detailed view on intra- and interspecific interactions on the individual-level is needed. Following the behaviour of single individuals concerning their inter- or intra-specific interactions requires process-oriented and individual-based modelling approaches.

Individual-based and process-oriented modelling techniques experienced numerous and comprehensive applications to various ecosystems. Typical examples of such applications are forest models including gap dynamics. That means, a forest exposed to disturbances like falling of big trees or wildfire, is composed of a mosaic of gaps in different successional stages (Shugart 1998). Successional stages are differentiated by the temporal rearrangement of occurring species and their composition. For example, in forests usually pioneer species occupy an area under full sunlight at first. In the shade of such pioneers, shade-tolerant species are able to establish, which reach increasing abundance within time. Due to

disturbances, for example the falling of large trees, gaps in the canopy with full light resources are created, which again firstly are occupied by sun-loving pioneers starting the process cycle of succession again. Modelling of such gap dynamics in forests refers to a long history. Various works originate in those of Botkin *et al.* (1972). The model called JABOWA introduced the gap-concept, in which the dynamics of individual trees are simulated on independent and horizontally homogenous patches (Botkin *et al.* 1972; Bugmann 2001). Several forest gap-models like FORSKA, FORMIX, FORMIND and others developed during the last decades based on the origin gap-model but modifying some assumptions (Bugmann 2001; Pacala *et al.* 1993; Pacala *et al.* 1996; Leemans & Prentice 1989; Bugmann *et al.* 1997; Huth *et al.* 1998; Köhler & Huth 2004).

This work focuses on modelling of temperate species-rich grasslands following the principles of forest gap models. Applying the gap-approach to temperate grasslands turns out to be a major challenge. Several characteristics different to forests have to be considered. Firstly, temperate grasslands generally contain species of widely varying growth forms. For example, some species grow in tussock, while others do form dense sod-forming swards. Defining an individual is thus more complicated for temperate grasslands than for forest, in which all individual trees can be characterized by a conical stem and crown (Köhler & Huth 2004). As a secondary aspect, forests and grasslands show contrasting priorities according to above- and belowground resource use and competition (Coffin & Urban 1993). For example, in forests asymmetric competition for aboveground light plays a major role, whereby in grasslands symmetric competition for soil resources is more decisive. Thus, competition for belowground resources has to be included in the classical gap approach. Thirdly, a species performance is dependent on temporally changing site conditions like seasonal climate or soil properties (Breckle 1999). Resource availabilities can further change according to human management activities. By these factors, the strength of resource competition of individuals switches temporally between soil water, soil nutrients and light. For example, mowing of grasslands immediately reduces shading within the canopy and thus, competition for light resources becomes less important. Competition for soil water would be dominating in times of heavy drought events.

1.3 Analysing the structure and dynamics of species-rich forests

Species diversity, human management activities, soil and climatic site conditions play an important role in shaping an ecosystem's structure and dynamics. Besides dynamic forest models, analyses of structural characteristics are important elements for estimating the

functioning of forest ecosystems, for example the aboveground carbon storage in the forest community.

1.3.1 A functional relationship for stem size distributions of forests

Observation studies of uneven-aged forest communities collect structural properties usually on discrete observation times or in time intervals. For example, in a Panamanian tropical forest the stem diameter at breast height is measured for each tree every five years (Hubbell *et al.* 1999; Condit 1998; Hubbell *et al.* 2005). Breast height is located at 1.3 m aboveground, which is more easily accessible for measurements than the height of a tree and thus, replications or time-series observations can be handled less cost- and time-expensive.

The observed stem diameters are aggregated in a so-called *stem size distribution* – a histogram, which shows the number of stems per hectare within distinct diameter classes of certain width. Empirical stem size distributions are observed to follow a skewed decaying shape for several examined forests, which is reminiscent of an ‘inverse *J*’ or an ‘*L-shape*’ (Niklas *et al.* 2003). Such a decaying distribution shows in detail a huge fraction of trees with small stem diameters and a highly variable small fraction of trees with big stem diameter.

Measurements and analyses of stem size distributions in tropical forests play a key role in estimating a forest’s biomass and productivity. Functional relationships exist to calculate the biomass content of a single tree by assuming a cylindrical stem (Yamakura *et al.* 1986). Using this in combination with the stem diameter distribution of a forest, the forest’s biomass can easily be estimated in a non-destructive way. For example, forests in an early successional stage consist of a large fraction of small stem diameters and only very few large ones, which results in a relatively low biomass compared to late successional forests. These are characterized by an increased fraction of larger stems and a decreased amount of smaller stem diameters. Similar observations of the decaying shape of stem size distributions across several undisturbed natural forests led to the research question, whether general functional relationships for stem size distributions in forests exist (Muller-Landau *et al.* 2006).

To answer this question, various approaches either in a statistical or in a theoretical context emerged. Theoretical approaches include the works of West *et al.* (2009), Enquist *et al.* (2009), Kohyama *et al.* (1995; 2003), Kohyama (1991; 1993) and Muller-Landau *et al.* (2006). In this thesis, a statistical analysis is used. In the last decades, statistical analyses have primarily been chosen based on plotting histograms of field measurements on double logarithmic axes. Field data appeared then as an almost straight line. Such empirical observations on double logarithmic axes have led to the assumption of a power-law

relationship. A power-law distribution is typically characterized by a probability density function, which also appears as a straight line on a double logarithmic scale. In general, linear regression analyses have been performed on double logarithmic scales to estimate the slope of empirical size distributions (Niklas *et al.* 2003). Later, maximum likelihood estimation has been prioritized, as their estimators are generally unbiased in contrast to those of linear regression analyses.

1.3.2 Uncertainties in the analysis of stem size distributions

During the procedure of observing stem diameters in tropical forests several uncertainties could be included in the measurements. These can be broadly classified into systematic and random uncertainties. Systematic uncertainties comprise, for example, binning of field measurements into stem diameter classes of certain width, i.e. 1 cm or 10 cm. Such a systematic classification of field data is often required to perform linear regression analyses. An example for random uncertainties includes the deviation of a stem's cross-section shape from a spherical form.

Difficulties in the observation can lead to biases within the measurements, which may propagate across the statistical analyses applied and the resulting conclusions drawn from these (Chave *et al.* 2004). Several investigations have already shown a negative effect of increasing binning on the estimation results of the maximum likelihood approach (White *et al.* 2008). Modified likelihood approaches including the extent of binning have already been proposed, which are able to reduce these negative effects (Muller-Landau *et al.* 2006). However, such investigations have not yet been performed for random measurement uncertainties in ecology.

1.4 Research objectives

Current research on the diversity-productivity relationships in grasslands is mainly based on experimental studies. Sufficient simulation studies following an individual's behaviour as well as the role of certain species according to the diversity-productivity relationship have not been presented so far. Comprehensive investigations on further understanding the emerging effects of diversity on aboveground productivity require simulation studies. The main research objectives are:

- I. To review on various existing grassland models and select suitable modelling approaches, which help to investigate on diversity-productivity relationships
- II. To build a simulation model for species-rich temperate grasslands, which is able to reproduce the observed structure and dynamics of experimental grassland studies
- III. To investigate on the change of aboveground productivity from monocultures to 2-species-mixtures in the context of diversity-productivity relationships by using the developed grassland model

Besides our analyses on grasslands, we also investigate methods for analysing the size structure of vegetation on the example of species-rich forests. Statistical analyses like maximum likelihood estimation used to analyse stem size distributions in tropical forests currently lack of including further uncertainties arising in the measurement procedure. Thereby, different forms of uncertainties may affect analysis results differently. In this thesis, we develop new methods by considering such errors in the analysis. Our research objectives are:

1. To examine the effects of systematic and random uncertainties in measurements of stem size distributions on the analysis of assumed functional relationships using maximum likelihood estimation
2. To assess whether we can improve the reliability of maximum likelihood estimation by considering uncertainties in the analysis methods

1.5 The chapters at a glance

1.5.1 Synopsis

Within the following chapters of this work, we will analyse modelling approaches in detail. Based on this review, an individual-based and process-oriented grassland model is developed. A simulation study based on a parameterized typical grass species is used to provide insights into the processes and mechanisms responsible for the emerging relationships between diversity and productivity. Concerning the structure of forests, we will concentrate on current measurement techniques, which provoke systematic and random uncertainties. We analyse the effect of such uncertainties on the estimation of relationships for stem size distributions. Consequently, we will develop new methods for reducing negative effects of measurement uncertainties on analysis results and increasing their reliability. A

comprehensive discussion of the approaches and methods developed within this thesis is presented at the end including future perspectives and application.

1.5.2 Chapter 2

We review already existing grassland models and beyond, modelling approaches for describing vegetation dynamics in general. Thereby, we give an overview on simulation models and modelling approaches of species-rich temperate grasslands, which include aspects needed to investigate on the diversity-productivity relationships in the context of biomass related energy production. We will present new conceptual approaches for individual-based and process-oriented modelling of species-rich grasslands, where needed and assess comprehensively modelling techniques of already existing models.

1.5.3 Chapter 3

Based on the literature review in chapter 2, we will present a new temperate grassland model in this chapter. The model aims at simulating species-rich temperate grasslands by using individual-based and process-oriented modelling approaches. A full description of this model is presented in detail in this chapter. We will introduce the modelled geometry of an individual plant. Afterwards, we will describe the main modelled processes an individual passes through during its life cycle. The grassland model is coupled with a soil model, of which a brief overview is given. As a last part, the scheduling of the coupling of both models is presented.

1.5.4 Chapter 4

First, we will parameterize the model for a representative Central European grass species. We will test the simulated parameterization with published field data from literature and biodiversity experiments with regard to reproducing observed structure and dynamics. Based on the parameterization, we perform a simulation study by creating virtual species types. The defined species types differ in their functionality of acquiring and competing for resources. We will simulate them in monocultures and 2-species-mixtures in order to assess the effect of diversity on productivity.

1.5.5 Chapter 5

In chapter 5, we will address statistical methods for analysing stem size distributions of tropical forests. For our investigations, we will create virtual field data sets from three selected distributions, which are typically used for describing empirical stem size distributions of forests. We will consider two different uncertainties. These comprise on the one hand binning of field data into stem diameter classes and on the other hand random uncertainties, for example caused by measurement errors. We analyse the created data sets using three different likelihood functions – one assuming accurately measured stem diameter and two other, which each of them includes the respective uncertainty in the estimation method.

1.5.6 Chapter 6

In the last chapter, we discuss methods and approaches used in this thesis. First, we debate chances and limitations of the included modelling approaches of our grassland model Grassmind. We present possible extension for future applications. The main results of our simulation study using the developed grassland model are discussed with regard to published field measurements in the context of diversity-productivity relationships and current hypothesis of underlying mechanisms explaining the shape of these relationships. Future perspectives of important research questions concerning additional simulation studies of diversity-productivity relationships in grasslands will be suggested at the end. Secondly, we focus in our investigations on the analysis methods of stem size distributions of forests. Concerning our findings in analysing stem size distributions of tropical forests using maximum likelihood methods, we discuss their relevance and applicability in practice. An outlook on future analysis methods of ecosystem structures will be proposed at last.

Chapter 2

A Review of Grassland Models in the Biofuel Context¹

Abstract

Various studies have suggested that semi-natural grasslands could be a more ecologically beneficial source for biofuel production than intensively managed monocultures. In particular, it has been observed that the high level of species diversity in grasslands has a positive effect on several ecosystem functions (e.g. productivity). Ecological models are useful tools for analysing the interactions of different processes in grasslands, which are assumed to be the underlying drivers of this positive effect. In this paper we present a review of the main processes included in existing grassland models and discuss the strength and limitations of existing approaches in the context of biofuel production. Most of the existing models (a) focus solely on one or a few single species, (b) do not consider competition processes adequately, or (c) do not follow the individual's development in the grassland community. This hinders a detailed analysis of the mechanisms and conditions that govern the ecosystem functions that are relevant for biofuel production such as productivity, stability, and carbon fixation. To bridge this gap, we propose a concept for a novel individual-based grassland model for temperate regions. Our approach covers a high number of species/functional groups, above- and below-ground intra- and inter-specific competition for different resources (light, water, nitrogen, space), and disturbances (due to management or climate change). Hence, it could facilitate comprehensive mechanistic analyses of the dynamics of semi-natural grasslands and their efficiency in biofuel production.

¹ A review paper with analogous content has already been published (Taubert *et al.* 2012).

2.1 Introduction

The global demand for renewable biofuels continues to grow. Currently, intensively managed monocultures of energy crops such as rapeseed, soybean or maize are often used to meet this demand. This leads to land-use conflicts and propagates competition between food and fuel production (Koh & Ghazoul 2008). A new path has been proposed by Tilman and colleagues. (Cedar Creek Ecosystem Science Reserve USA; Tilman *et al.* 2001). Tilman *et al.* (2006b) also suggest using multi-species mixtures of perennial grassland species (*Low-Input High-Diversity (LIHD)*) for biofuel production. Other biodiversity experiments, such as the Jena Experiment, substantiate these results by observing equal productivity of *LIHD* grassland mixtures and *High-Input Low-Diversity (HILD)* grassland mixtures (Weigelt *et al.* 2009). However, whether *LIHD* grasslands are better able to meet energy demands than crop monocultures also depends on the soil properties of the land used, on the regional climate and on the management strategy. Furthermore, it can be assumed that the results of these experiments cannot be simply transferred to natural systems (Grace *et al.* 2007). In addition, climate change, especially the expected increase in drought events in Central Europe, may cause additional effects (IPCC 2007). Hence, reasonable statements on the potential of grasslands for biofuel production under changing conditions are needed. Experiments addressing this question can be supported by simulation models.

Here, we review 13 existing grassland models. These models are used (a) to simulate productivity and dynamics of grasslands and (b) to analyse the grassland's response to changing factors and disturbances. However, most of the investigated models fit only partially into the biofuel context. For example, the Hurley-Pasture model is too complex in its entire model structure for simulating species-rich sites (Thornley & Verberne 1989; Thornley 1998). This is reflected in a higher degree of detail (e.g. structural and substrate mass is distinguished) and thus, a higher number of parameters. Another limitation of several grassland models is the exclusion of one or more resources from the modelled competition processes. As an example, the model of Schippers & Kropff (2001) is developed to include inter-specific competition for light and nitrogen, but not for water. However, due to the expected increase of drought events in Central Europe (Beniston *et al.* 2007; IPCC 2007), competition for limited water also becomes an important factor for grassland model development. In this study we present in detail grassland models which provide sufficient modelling approaches for essential processes, reveal their lack of additional important characteristics in terms of biofuel production, and propose new conceptual approaches for certain processes.

This review results in our proposal for a new grassland model concept called Grassmind, consisting of approaches adopted from already existing grassland models and

novel approaches for modelling specific vegetation processes. A new perspective for simulating temperate, species-rich grasslands can thus be provided. Our model concept focuses on the one hand on the full involvement of characteristics and processes which were partly absent in existing grassland models. On the other hand, proven modelling approaches for processes from existing models are partially adopted (e.g. production and allocation).

2.2 Review and evaluation methods

We investigated 19 vegetation models, 13 of which describe the dynamics of grasslands (see Appendix A1 for a detailed list). Because global vegetation models also include grasses, and forest models often use simple approaches, we consider these additionally in our review of specific processes. The review is conducted by (1) describing the main aspects of the grassland models such as focus and structure and (2) evaluating the models with regard to their potential use for simulating *LIHD* and *HILD* grasslands. For this evaluation, we used patterns we identified as being important to be reproduced by a grassland model in the biofuel context.

Temperate grasslands are important in the biofuel context as they produce harvestable biomass. As is typical for temperate regions, the above-ground biomass production of the ecosystem shows inter-seasonal variability. So, e.g. the influence of the abiotic environment on seasonal and inter-annual variations of net ecosystem CO₂ exchange, leaf area index or nitrogen content were investigated in some studies (Flanagan *et al.* 2002). This climatically dependent variability arises mainly from the growth of plant tissue, the establishment of new plants and their tillers, and the mortality of plants and their tillers by self-thinning and harvest. Several studies showed that the dynamics of tiller density, species abundances or other vegetation characteristics is highly dependent not just on the abiotic environment, but also on management activities such as sowing, mowing, plant removal or fertilization. For example, the studies of two grass species populations showed a decline in tiller density after harvest and an increase following the winter season until the next harvest (Lonsdale & Watkinson 1983).

Concerning *LIHD* or *HILD* grasslands in the biofuel context, different species abundances and cover can be expected, especially when induced under different management regimes. With no or rare management considered, one can initially expect to observe an increasing number of grasses and a decreasing number of small herbs and legumes in grasslands (Deák *et al.* 2011; Török *et al.* 2011). With no or rare mowing, grasses grow higher than small herbs and thus shade them the more they grow. Smaller species get less light for photoproduction and may die due to lowered net primary production. The fewer legumes in

the grassland, the less nitrogen is fixed by them in the soil. As a consequence, a lack of nitrogen for grasses might occur (Temperton *et al.* 2007). It can be assumed that grass species suffer from such a nitrogen deficiency, leading to higher stress and thus higher mortality. Dying grass shoots, which contribute to the litter pool, create gaps with high incoming irradiance intensity, giving legumes the opportunity to establish. So, a state of equilibrium of a grass-legume community with reduced occurrences of herbs and a high variance of the equilibrium due to the interplay of the grasses and legumes can be expected. With management, different results would be expected. Mowing offers small herbs a greater chance of survival due to equal non-attenuated irradiance input for all species, which means competition for light, is of minor importance. Due to their more horizontal leaf position some herbs and legumes usually have higher light absorption rates and thus may have an advantage over grasses (Lantinga *et al.* 1999). In the case of infrequent mowing and non-limiting water and nitrogen resources in soil, a well-mixed community of species sown can be presumed. With their shoots growing more and more, light competition is reactivated and may become dominant again. In the case of frequent mowing and additional supply of e.g. fertilizers, grasses may become dominant due to an increased vegetative propagation. Following these patterns specific criteria for our evaluation of grassland models can be defined:

- (1) Species-richness (or functional group richness)
- (2) Resource limitations (water, nutrients, light, space)
- (3) Complex above- and below-ground competition processes between individual species for these resources
- (4) Management activities disturbing or supporting the system
- (5) Simplicity of the model, meaning the inclusion of essential, but not all aspects
- (6) Linkage of competition for resources.

Following our set-up criteria, we explored the reviewed grassland models in further detail. In doing so, we identified the key processes and characteristics for simulating *LIHD* and *HILD* grasslands. We then determined whether or not one or more of the existing grassland models provide sufficient information for modelling the processes adequately (in terms of our criteria). If not, we propose new conceptual approaches for modelling those processes or integrating specific characteristics.

2.3 Brief review of grassland modelling concepts

2.3.1 Description of existing grassland models and evaluation of their potential in the biofuel context

The 13 grassland models varied broadly in their objectives, structure and complexity. The objectives range from detailed reproduction of the architecture of plants to the analysis of below-ground resource use or impacts of climate change or management on grasslands. The structural design of the models including their time steps, main variables, abiotic factors, considered competition processes and management activities are listed in Table 2.1 and Table 2.2.

The Hurley Pasture Model comprises a dynamic, mechanistic ecosystem model with a great deal of complexity (Thornley & Verberne 1989; Thornley & Cannell 2000; Thornley 1998). The process-based model structure simulates daily fluxes of carbon, nitrogen and soil water by coupling soil, plant and grazing sub-models. Central variables of, e.g. the plant sub-model, comprise structural dry matter, carbon and nitrogen substrate, and leaf area, additionally structured by age and plant components. As a result, the plant sub-model already covers 21 state variables and 60 parameters inducing a high degree of complexity, which may cause difficulties in the parameterization of species-rich sites (Thornley & Cannell 2000). Therefore, in simulation studies of the Hurley Pasture Model only a generic C3 grass species was assumed (Thornley & Cannell 2000; Thornley 1998).

The daily working PaSim model is based to a large extent on the Hurley Pasture Model, but it also includes certain processes such as leaf stomatal resistance or the dynamic change of a plant's fractional nitrogen content in greater detail (Riedo *et al.* 1998, 2000). Additionally, some new aspects, e.g. the reproductive developmental stage and the non-linear temperature dependence of the shoot and root growth rates, were introduced. As in the Hurley Pasture Model, a plant's state is described by the structural dry matter of the plants in different compartments (e.g. leaves, stem, and sheaths) as well as the nitrogen content. Due to the high degree of complexity, as in the Hurley Pasture Model, simulation studies assumed only a single species representing a kind of a mean species for the entire community.

Table 2.1: Overview of the reviewed models concerning time step, model structure, main variables and management activities considered.

Model	Timestep	Individual-(I) or population-(P) based calculations	Spatially explicit	Main variables	Management activities considered
Schippers & Kropff	daily	P	✓	above- and below-ground biomass and nitrogen content	cutting, fertilization
Hurley-Pasture model	minutes (variable)	P	✗	above- and below-ground biomass and nitrogen content, leaf area	fertilization, cutting, grazing
PaSim	minutes (variable)	P	✗	above- and below-ground biomass and nitrogen content, leaf area	cutting, fertilization, grazing
Coughenour <i>et al.</i>	2 days	P	✗	above- and below-ground biomass	-
Detling <i>et al.</i>	daily	P	✗	above- and below-ground biomass	irrigation, fertilization
Coffin & Lauenroth	annual	I	✗	number of individuals, above-ground biomass	-
Duru <i>et al.</i>	daily	P	✗	leaf area index, above-ground biomass	cutting
Acevedo & Raventos	0.1 months	I	✓	above-ground shoot or leaf length	-
LINGRA	daily	P	✗	above- and below-ground biomass, tiller number, leaf area index	cutting, irrigation
GEM	days (variable)	P	✗	above- and below-ground biomass and nitrogen	-
GREENLAB	days to years (variable)	I	✓	above-ground biomass, physiological age	-
Reuss & Innis	daily	P	✗	above- and below-ground nitrogen, biomass	fertilization
GraS-Model	daily	P	✓	above-ground occupied area/cover	cutting, grazing and trampling

In a less complex way, the process-based GraS-Model simulates daily species-specific vegetation cover dynamics (Siehoff *et al.* 2011). Different single species as well as various plant groups (e.g. tufted plants or erect forbs) are simulated on the population-level by coupling a simple plant competition model and a land use model, each of them raster-based. Utilization indicator values for trampling, cutting and grazing allow the incorporation of management activities. However, in this model species compete only for space, but the

influence of different abiotic factors as well as competition between species for e.g. soil water would lend further insight.

Table 2.2: Overview of abiotic factors considered in the reviewed models, the resources species compete for and the number and type of species represented (single species (S) e.g. *Lolium perenne*, plant functional types (PFT) e.g. grasses or legumes, or generic mean species (GMS) for an entire community). For each model the number of simulated species is given in brackets.

Model	Abiotic factors included	Modelled intra- /inter-specific competition for which resources	Species representation		
			S	PFT	GMS
Schippers & Kropff	radiation, air temperature, soil nitrogen content	light, nitrogen	✓(3)		
Hurley Pasture Model	radiation, air and soil temperature, soil water and nitrogen content, wind speed, atmospheric CO ₂ concentration, precipitation, vapour pressure, (non-symbiotic and symbiotic N fixation)	light, nitrogen, water			✓(1)
PaSim	radiation, air and soil temperature, soil water and nitrogen content, wind speed, atmospheric CO ₂ concentration, precipitation, vapour pressure, snow cover, (symbiotic nitrogen fixation)	light, nitrogen, water			✓(1)
Coughenour <i>et al.</i>	soil nitrogen content	light, nitrogen		✓(3)	
Detling <i>et al.</i>	radiation, air and soil temperature, soil water content, precipitation, photoperiod	light	✓(1)		
Coffin & Lauenroth	air temperature, precipitation	water		✓(15)	
Duru <i>et al.</i>	radiation, air temperature, soil water, nitrogen and phosphor content, seasonality	light		✓(3)	
Acevedo & Raventos	-	-	✓(1)		
LINGRA	radiation, air temperature, soil water content, precipitation	light, water			✓(1)
GEM	radiation, air and soil temperature, soil water and nitrogen content, wind speed, atmospheric CO ₂ concentration, precipitation, vapour pressure, (symbiotic N fixation)	nitrogen, water	✓(1)		
GREENLAB	air temperature, soil water content	-	✓(1)		
Reuss & Innis	air and soil temperature, soil water content, soil nitrogen content, (symbiotic N fixation)	nitrogen			✓(1)
GraS-Model	-	space		✓(10)	

In contrast, the grassland model developed by Schippers & Kropff (2001) does include such abiotic factors as radiation and temperature. This daily working model also shows a less complex model structure including dry mass of the plants in different compartments (flower, shoot, root, and reserves) and nitrogen content as state variables. This lower level of complexity allows the simulation of several single species competing with each other. Competition processes are considered to take place above-ground for light and below-ground for nitrogen. An extended spatially explicit model version enables an individual-oriented modelling concept based on the self-thinning law (Yoda *et al.* 1963). Overall, this model provides a potential tool for simulating species-rich herbaceous communities. The model of Schippers & Kropff (2001) does not consider water stress and competition for water between individuals, which would also be of great interest.

The LINGRA grassland model, on the other hand, includes water stress by using a water shortage factor, which influences light-use efficiency (Schapendonk *et al.* 1998). The calculation of light-use efficiency is part of the source-sink concept of the model. Within this scope, light-use efficiency is used for simulating the daily source carbon flow, while temperature-driven leaf area and tiller dynamics are used for modelling the daily sink carbon flow. Interactions between both fluxes are integrated via the plant's storage pool. Simulation studies were carried out for single species populations throughout Europe. The model shows some important characteristics needed for simulating *LIHD* and *HILD* grasslands. Tiller and leaf area dynamics are modelled dependent on radiation intensity, temperature, soil water content and defoliation. Although water stress is considered, the inclusion of nitrogen stress as well as inter-specific competition for water and nitrogen between individual tillers would increase the informative value of the model.

Also based on the light-use efficiency concept, the model of Duru *et al.* (2009) follows a contrary strategy. They focus mainly on the daily accumulation of above-ground herbage mass by taking into account the temperature-driven growth of green leaf area and the reduction of leaf area due to senescence. Factors considering water and nutrient stress are integrated by limiting the growth of herbage mass. Simulations showed herbage growth accumulation of a community consisting of three plant functional groups, but do not include an individual's tiller dynamic and resource use. However, this would be interesting for a detailed view of intra- and inter-specific competition processes between individual tillers, especially for water and nitrogen.

The model developed by Coughenour *et al.* (1984) considers senescence and maturation. It simulates the daily primary production of biomass of perennial grasses. For modelling processes like photosynthesis or senescence potential rates are modified with reduction factors. Additionally, a shoot sub-model including different stages of aging allows the simulation of tiller dynamics per plant. Simulations were carried out using three different

height groups (plant functional types) of tufted perennial grass species. Species that differ in growth form and characteristics are currently not included in this model. However, this would be useful for simulating European species-rich grasslands.

Semi-arid models like the individual-oriented model of Coffin & Lauenroth (1990) focus mainly on competition for water resources between individual plants and a resulting water stress affecting the number of individuals per plant functional group. It uses the gap approach usually applied in forest models and focuses on below-ground resource use of 5 resource groups, which again were divided into 15 plant functional/species groups for simulation. Dynamics are simulated annually by the resource space proportionally assigned to the individual plants in the community and the below-ground gaps in the resource space produced by dying individual plants. As it is a semi-arid grassland model, the resource space is mainly determined by the soil water content or precipitation. However, for temperate regions competition for nitrogen and light and the resulting effects on the individual's growth and survival are as important as competition for water resources.

Detling *et al.* (1979) incorporate in their model structure the intra-seasonal impact of temperature, moisture, light and nitrogen on the biomass dynamics of the species *Bouteloua gracilis*. The daily simulated processes covered in the model comprise among others spring regrowth and the translocation of carbohydrates between leaves, crowns and roots. These are important aspects for temperate regions. The model is tested for one species only. But the consideration of detailed inter-specific competition for e.g. water, light, nitrogen and space would be revealing.

The GEM model (Hunt *et al.* 1991) presents a producer-decomposer model comprising (1) the impact of abiotic factors on the primary production sub-model and (2) feedbacks of the nitrogen flux. The model includes a water sub-model, a plant sub-model, a decomposer sub-model as well as a fauna sub-model and is designed for investigating climate change impacts on the daily carbon and nitrogen dynamics. Simulation studies were only carried out using a dominant single species and do not examine the inter-specific competition processes of species-rich communities.

2.3.2 Identification of key processes and comparison of suitable process modelling approaches

After reviewing and evaluating existing grassland models, we were able to identify the processes and characteristics that should be included in the context of *LIHD* grasslands for biofuel production. The inclusion of abiotic factors in the production and their reduction due

to limitations is important for tracking an individual's dynamic in the community and thus for evaluating population-based tiller and vegetation cover dynamics. Mortality is as important as plant production. Important mortality aspects are mainly crowding mortality (e.g. self-thinning) and mortality due to harvest (i.e. mowing). The potential to simulate species-rich herbaceous communities induces several important mechanisms. Central European herbaceous species differ widely in characteristics such as growth form and architecture, temporal reproduction, and strategy depending on (a) allocation of produced biomass via photosynthesis in terms of their life cycle and (b) inter- and intra-specific competition for resources in a species-rich, competitive environment. Thus, a suitable model should allow the inclusion of these different growth forms and architectures. In the context of biofuel production senescence plays an important role. In terms of different biofuel production technologies, only certain proportions of fresh green biomass and/or senescent biomass can be used. Species differ in their ability to maintain senescent biomass as standing dead material within the community dependent on their architectural stability.

Resource-dependent production

Among the most common concepts for modelling the production process are those that calculate gross photosynthesis and net photosynthesis. Gross photosynthesis models constitute primarily the Farquhar photosynthesis model (Farquhar *et al.* 1980; LPJDGVM, Sitch *et al.* 2003) and the single-leaf photosynthesis model based on the light response function (Thornley & Johnson 1990; FORMIND, Köhler & Huth 2004; Seib-DGVM, Sato *et al.* 2007). The Farquhar model calculates assimilation in a detailed biochemical way, whereas the approach using the light response function performs a more aggregated calculation of the single-leaf photosynthesis integrated over the canopy or individual's projection area. Another option is to use just an average gross photosynthetic rate per unit leaf area (Coughenour *et al.* 1984) as is done in net photosynthesis models, which are mainly based on such a potential net photosynthetic rate (Detling *et al.* 1979). Other models just calculate the absorbed amount of radiation, which is subsequently converted to organic dry matter either after subtracting maintenance costs (Schippers & Kropff 2001) or directly using the light-use efficiency (LINGRA, Schapendonk *et al.* 1998; Duru *et al.* 2002, 2009). There are also models that aggregate several production processes by focusing on the relative growth rate of the plant's biomass or size (Coffin & Lauenroth 1990) or growth equations for biomass or size (Acevedo & Raventós 2002; Damgaard *et al.* 2002; Damgaard & Weiner 2008). The latter ones take an equation-based approach rather than a process-based approach as described above.

All the above mentioned production model types can be multiplied by the respective reduction factors for irradiance, water, nutrients, temperature, age, etc. The concepts differ widely in models depending on the goal of the study. But all these reduction factors either

decrease from 1 to 0 with decreasing availability of the respective resource (e.g. for water; Granier *et al.* 1999; Reuss & Innis 1977) or reach an optimum in the middle of their range between 0 and 1 (e.g. for temperature; Larcher 1976).

In the context of biofuel production, we propose as part of our conceptual model Grassmind the single-leaf photosynthesis approach integrated over the individual leaf area (Thornley & Johnson 1990). An individual can produce biomass via photosynthesis of its above-ground green shoot parts. So it is not only the producing green parts that compete for light, but also the senescent or dead shoot parts. These can no longer produce biomass via photosynthesis, but they can shade the green parts which are still producing. Reduction factors according to soil water and soil nitrogen availability as well as air temperature can be sufficiently taken into account by multiplication with the gross primary production:

$$R = R_w(\text{soil water}) \cdot R_T(\text{temperature}) \cdot R_N(\text{soil nitrogen}), \quad (2.1)$$

whereby R_w is an increasing function from 0 to 1 of increasing available soil water (e.g. Granier *et al.* 1999), R_T is a function accounting for unfavourable temperatures (e.g. Schippers & Kropff 2001), and R_N is an increasing function of available soil nitrogen content. It can be clearly seen, that R_w and R_N are greatly influenced by competition with other individuals and abiotic conditions. In contrast, the reduction factor R_T only reflects abiotic stress situations.

Respiration

There are numerous possibilities accounting for the different levels of detail describing respiration. Most models only distinguish between growth respiration and maintenance respiration (Hurley Pasture, Thornley & Verberne 1989; Thornley 1998; LPJ-GUESS, Smith *et al.* 2001; LPJ-DGVM, Sitch *et al.* 2003). Three different concepts for modelling such respiration sub-processes can be distinguished (Thornley & Cannell 2000): (a) Most commonly assumed is the priority of maintenance respiration over growth respiration and its proportionality to plant biomass (FORMIND, Köhler & Huth 2004; LPJ-DGVM, Sitch *et al.* 2003). Therefore, the produced biomass is primarily used for maintaining all important plant processes; the remaining biomass is utilized for growth of new plant tissue. (b) Secondly, growth respiration can also be assumed to have priority over maintenance respiration. After reducing assimilation for growth processes, the produced organic material is partially used for maintaining already existing components and processes (Thornley & Cannell 2000). (c) Thirdly, the concept of plant tissue partially feeding back to assimilation can be applied, whereby both are then used to fulfil total respiration costs (Thornley & Cannell 2000). In the

context of biofuel production, we propose using the concept of primarily maintaining already existing green plant tissue and secondly creating new plant tissue:

$$NPP = (1 - r_g) \cdot (R \cdot P_B - r_m \cdot f_T \cdot (B_{shoot}^{green} + B_{root}^{alive})), \quad (2.2)$$

whereby NPP is the net primary production, r_g is a dimensionless growth respiration factor, r_m is the maintenance respiration rate. As part of the Grassmind model concept we consider that maintenance is only needed for living green plant parts, which means green shoot biomass B_{shoot}^{green} and living root biomass B_{root}^{alive} . Further, the function f_T can account for increasing demands for maintenance with increasing temperature (e.g. Schippers & Kropff 2001) and R consists of the three dimensionless reduction factors considered for the plant production (cf. Eq. 2.1).

Allocation strategies

Dependent on the type of respiration modelled, biomass produced by photosynthesis can be subsequently allocated to different plant pools where new tissue is growing. There can be differences in the pools considered ranging from one plant pool to several ones describing different components of a plant such as the leaves or the stem. In grassland models these different pools mostly comprise above- and below-ground plant parts, storage or reserve organs, and reproduction pools. The degree of resolution differs in the models. Differentiations from coarse pools such as above- and below-ground pools to more detailed ones such as leaf lamina or sheaths are possible (Hurley Pasture, Thornley & Verberne 1989; Thornley 1998). There is also the possibility to distinguish different ages of plant parts, to which different amounts of produced biomass can be allocated (Detling *et al.* 1979).

Besides the number of pools the model takes as a basis, different allocation strategies can be assumed. For example, a grassland model of annual species would assume a strategy that allocates more biomass to reproductive parts than to storage organs. On the contrary, a model of perennial species would imply that greater amounts are allocated to reserves than to the reproduction pool. Mostly allocation strategies are modelled statically, that means the allocation fractions remain constant over time (FOREST-BGC, Running & Gower 1991). Other concepts include the compliance of functional relationships between the pool masses summarized in the pipe theory (LPJ-GUESS, Smith *et al.* 2001; LPJ-DGVM, Sitch *et al.* 2003; Seib-DGVM, Sato *et al.* 2007) or the source-sink strength of the plants (Coughenour *et al.* 1984; Schippers & Kropff 2001). However, especially in the context of climate change, a dynamic allocation process that adapts to climatic or managerial changes might be important (Detling *et al.* 1979). Nevertheless, in most cases not enough information is available for modelling the adaption process.

In the context of biofuel production and in the course of the development of the Grassmind concept, we propose to assign the following state variables to an individual: (a) above-ground shoot biomass B_{shoot} , (b) below-ground root biomass B_{root} , (c) storage biomass B_{store} and (d) reproduction biomass B_{rep} . Geometrical properties of an individual describing its spatial structure should be related to some of those state variables (Fig. 2.1). The calculated net primary production NPP of Eq. (2.2) can be allocated to those plant pools. Thereby, the connection of an individual between its above-ground shoot biomass B_{shoot} and its below-ground root biomass B_{root} should be assumed to follow a species-specific allometric relationship that remains constant over time (Niklas 2005):

$$B_{shoot} = a \cdot B_{root}^b, \quad (2.3)$$

whereby a and b are species-specific parameters. The remaining biomass can then be partitioned between the storage pool and the reproduction pool. Dependent on the species' strategy or life cycle, an individual either invests more in its reproduction or more in the storage of biomass for maintaining itself in times of stress. For example, an annual species would invest more biomass in its reproduction. In contrast, a perennial species would invest more in the storage biomass to ensure its maintenance over its entire life span. There is a necessity for an individual to use its storage biomass in times when its gross primary production P_B cannot meet the required maintenance respiration.

Architecture (allometry and geometry)

Forest models and global vegetation models use allometric relationships and an underlying geometric architecture (FORMIND, Köhler & Huth 2004; LPJ-GUESS, Smith *et al.* 2001; Seib-DGVM, Sato *et al.* 2007; SILVA, Pretzsch *et al.* 2002). Usually grassland models try to avoid modelling the architectural characteristics of their plants. This results mostly from the great diversity of different growth forms and characteristics of herbaceous plant species, especially in temperate ecosystems. As a consequence, processes are often modelled on the population level, making it difficult to explore individual plant or tiller development. However, a few models do include geometry in their model framework (Acevedo & Raventós 2002; Schippers & Kropff 2001; Yan *et al.* 2004). Hence, for example, the transformation of the above-ground accumulated biomass into cuboids for all shoots using a species-specific relationship between height and width and the self-thinning rule is possible (Schippers & Kropff 2001). Of course, geometrical parameters are difficult to estimate on the individual level due to a lack of field data.

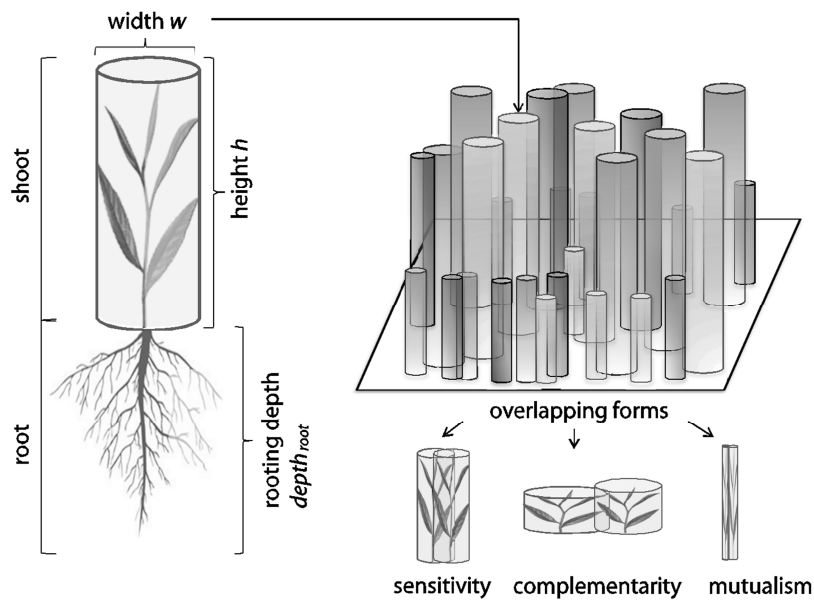


Figure 2.1: The individual's and community architectural concept. (A) On the left side an individual is presented. Its above-ground shoot is covered by a cylinder of height h and width w . Within the cylinder the shoot parts are divided between green photosynthetic active parts and orange senescent parts. The below-ground root system is characterized by its total root length and rooting depth, whereby the system is also divided between living (brown) and dead (orange) parts. (B) On the right side the community consisting of several individuals on a gap is demonstrated. The different colours of the shoots indicate different species or plant functional types. The individuals may overlap concerning their geometry (cylinder), whereby three different forms can be differentiated: (i) sensitivity: individuals do overlap in a way that either one of them or both suffer due to their sensitivity to space competition, (ii) complementarity: individuals do overlap in a way that both of them can share space efficiently without suppressing each other, (iii) mutualism: individuals do not overlap in the true sense, they moreover support each other. This support by holding each other upright is essential for their competitive strength; otherwise they would fall to the ground.

In the development of the conceptual framework of the individual-based model Grassmind, we propose a novel view of individuals in grasslands. The assignment of an 'individual' is thereby chosen contrarily to other models, where it is assumed as a plant individual in the biological or genetic sense. Here, we propose a plant's ramet or tiller to be treated as a kind of virtual individual. This may simplify the structure of an individual-based grassland model, because a differentiation between sod-forming and bunch-growing grasses is not necessary.

We further assume that the individual's above-ground shoot is covered by a cylinder of certain height and width, following a species-specific relationship which is constant over time (adapted from Schippers & Kropff 2001; Fig. 2.1). This relationship is an important factor for the individual's competitive strength in the light and space competition process within the

community. The volume of the covering cylinder $V_{cylinder}$ includes the shoot biomass of plant tissue corrected by a factor f_s accounting for free space within an individual's shoot system:

$$B_{shoot} = V_{cylinder} \cdot f_s \cdot \quad (2.4)$$

The shoot system of an individual captures a region which represents simply the ground area of the covering cylinder. Please note, that the shoot system contains free space between its leaves, the extent of which depends on the particular species. The depth of an individual's roots $depth_{root}$ can be modelled via a functional relationship to the above-ground volume of the shoot covering cylinder (Schenk & Jackson 2002):

$$depth_{root} = r_1 \cdot V_{cylinder}^{r_2}, \quad (2.5)$$

whereby r_1 and r_2 represent species-specific parameters. Therefore, the assumption that all individual ramets or tillers are treated equally as biologically individual plants is needed. Ramets, which are usually connected via below-ground rhizomes, are now considered to have their own individual rooting system, rooting as deep as the biological mother plant would.

The nitrogen absorption from soil is modelled using the total root length of the system (Schippers & Kropff 2001). The greater the summed up lengths of all root sections of an individual's root system, the higher its absorption rate. For calculating an individual's root length the below-ground root biomass is simply multiplied by the specific root length SRL . It also has to be considered that most of the nutrients are available in the upper horizon of the soil. Shallower root systems with high total root length have greater advantages in the absorption of nutrients over those with less root length in the upper soil (Garwood & Williams 1967a, 1967b). As a consequence, the vertical distribution of the rooting system in soil is important for both the competition for water and nitrogen of an individual. Thus, it can be seen that factors specifying the competitive ability of an individual in the competition process for nitrogen and water are strongly related to the root system. The deeper the below-ground system of an individual is rooting, the greater is its access to water resources in soil. Especially in times of drought its competitive strength in the water competition process will be higher.

Changes in the geometry and allometry of an individual can occur when grasslands are cut. This activity changes the species-specific functional relationships between height and width as well as between above- and below-ground biomass, which are assumed to remain constant over time. To be consistent with the proposed conceptual structure and for the sake of simplicity, we assume that the produced biomass is allocated solely to the shoot system until the original relationship between above- and below-ground biomass is reached. Additionally, the biomass allocated to the shoot should only affect the growth in height, but not the width of

the individual, as long as the original height-to-width ratio is not reached. Subsequently, the growth of height and width as well as the allocation fractions to above- and below-ground biomass pools follow the original system.

Mortality and senescence

In most models only one type of mortality is considered. But there can be different reasons for mortality. Plants die off, for example, because they have reached their maximum age, from heat stress, frost or drought. These causes of mortality can be modelled either by testing whether net primary production falls below a threshold (LPJ-GUESS, Smith *et al.* 2001; LPJ-DGVM, Sitch *et al.* 2003) or by directly considering temperature thresholds (Schippers & Kropff, 2001). When mortality occurs, usually the entire plant dies off. But there are also models that distinguish between shoot and root mortality. This is based on the assumption that roots are less sensitive to e.g. freezing (Hunt *et al.* 1991).

Senescence is mentioned explicitly in only a few models and is mostly included in the mortality rate (Coughenour *et al.* 1984; Detling *et al.* 1979). It has to be considered that dead plant material contributes to the dynamics of grassland communities (Deák *et al.* 2011). There are different ways of handling dead plant material. Some models assume that it goes directly into the litter pool, while others assume that it remains standing above ground (Detling *et al.* 1979). Standing dead material can afterwards be transferred to the litter pool e.g. as a function of precipitation (Detling *et al.* 1979).

In the context of biofuel production, we propose considering multiple mortality sources in the course of the Grassmind model concept. For example, it is important to differentiate mortality due to harvest from basic mortality due to fulfilled life span as well as from crowding mortality. We propose to model crowding mortality by using the geometrical framework of covering cylinders with their individual ground or projection area. Considering all individual shoots on an area, the community coverage $\text{cov}_{community}$ cannot just be calculated by adding up all individuals' coverage or projection areas (Fig. 2.1). This would lead to an overestimation by ignoring leaf overtopping and overlapping of individuals. To account for this, the individual shoot coverage cov is modified using a species-specific “overlapping factor” $f_{overlap}$:

$$\text{cov}_{community} = \sum_{\text{individuals } i} f_{overlap}^i \cdot \text{cov}^i . \quad (2.6)$$

This correction factor $f_{overlap}$ gives a broader perspective on the interactions between species and their competition for space (Fig. 2.1). Some species are sensitive to space competition ('sensitivity'), others complement each other by leaf overtopping ('complementarity') and

some species are only competitive when they are held up by other ones ('mutualism'). The latter case can usually be seen in grass tillers, which cover a small area, but have a great height.

By using this framework, crowding mortality can be carried out by setting species-specific and total thresholds for the community cover on a predefined area. Tillers or shoots are deleted from the area until community cover falls below the defined thresholds. Under certain conditions this can be interpreted as self-thinning (Hernández-Garay *et al.* 1999; Kays & Harper 1974; Matthew *et al.* 1995; Yoda *et al.* 1963).

In terms of senescence the transformation process is modelled using a linear rate dependent on the leaf life span. To ensure the conformity of the modelled geometry, we assume that the senescent or dead shoot parts are still standing within the shoot's geometry. The same process of transforming living parts of an individual to dying ones is also assumed to be existent in the below-ground root system. So, using a linear rate dependent on the root life span, living root parts are transformed to dying root parts at each time step. The dying root sections can no longer take up water or nitrogen. In contrast to the above-ground senescent shoot parts, the belowground dying root parts are assumed to go directly into the belowground litter pool.

Temporal reproduction

Nearly all models make use of environmental conditions, which have to be fulfilled for e.g. successful establishment of new individuals (FORMIND, Köhler & Huth 2004; LPJ-DGVM, Sitch *et al.* 2003). Therefore, models that operate on the population level can assume e.g. tiller reproduction rates (LINGRA, Schapendonk *et al.* 1998) whereas individual-based models usually simulate the seedling establishment of individual plants (Coffin & Lauenroth 1990). In the context of biofuel production and for reproducing patterns of tiller dynamics in temperate grasslands it is important to consider establishment via vegetative and generative reproduction. Environmental factors such as temperature, water and nutrient availability and irradiance determine seedling germination. Further, species-specific differences in the temporal initiation of generative and vegetative reproduction may depend on environmental conditions such as the photoperiodic length of a day.

Storage use

The use of biomass from the storage pool, if considered at all, is often included for regrowth in spring or in times of stress e.g. after cutting (Detling *et al.* 1979; Schippers & Kropff 2001). Thereby, the uptake is not only possible from storage organs or reserves, but

also from the roots (Detling *et al.* 1979). The process of reserve uptake is mostly initiated by some event such as the exceedance of a temperature threshold (Detling *et al.* 1979) or the occurrence of a cutting event (LINGRA, Schapendonk *et al.* 1998). In the context of biofuel production, especially with regard to mowing or other stress situations, it is important to include the process of storage use of individuals. For simplicity it can be assumed that an individual needs to use its storage biomass in times when its gross primary production P_B cannot meet the required maintenance respiration or in spring for regrowth.

Inter- and intra-specific competition and their linkages

The reviewed grassland models provide a differentiated view of competition. Limited resources are only considered to affect the growth of individuals or the entire community. However, in most models detailed inter- and intra-specific competition between individual plants or shoots is not described sufficiently. A few models include competition processes, but focus solely on specific resources. For example, the model of Schippers & Kropff (2001) includes inter-specific competition for nitrogen and light. Species compete for light by shading other ones due to their leaf area index, while they compete for nitrogen due to their total root length relative to the sum of all other species. Another example is shown by the model of Siehoff *et al.* (2011) where species explicitly compete for space based on their potential growth rates, their current occupied area and the available space. Table 2.2 summarizes the abiotic factors that may limit growth and the resources for which species explicitly compete for all of the reviewed models. It also shows the number and type of species represented (i.e. single species, plant functional types or a generic mean species) for the entire community in the model simulations.

As part of the conceptual framework of Grassmind, we propose that individuals are competing for water, nitrogen, light and space. The uptake or use of resources of the individuals should be linked. Gross primary production strongly depends on how well the demand for water and nitrogen can be met by the soil. If an individual produces a lower amount of biomass due to reduced incoming linear rate dependent on the root life span, living irradiance or less leaf area, its demand for water and nitrogen is reduced. The other way around, an individual is forced to reduce its photosynthetic production when uptake of water or nitrogen is limited. Uptake of soil nitrogen is highly dependent on the uptake of soil water resources. Resource limitations can occur due to the presence of several competitors or due to environmental changes. If limitations are caused by other individuals competing for the same resources, then the limited resources have to be distributed among the individuals following certain rules. These rules can be defined by the species-specific traits characterizing their success in competition with other species (Fig. 2.2). So, e.g. in times of drought individuals with deep rooting systems may have an advantage in the water competition process, whereas

individuals with fine shallower rooting systems may absorb more nitrogen in the upper soil layer. Competition for space (crowding) is also an important factor in grassland communities. Whether and how individuals compete for space is highly dependent on the overlapping of the different plants within the community. Crowding can result in an increase in individual shoot mortality.

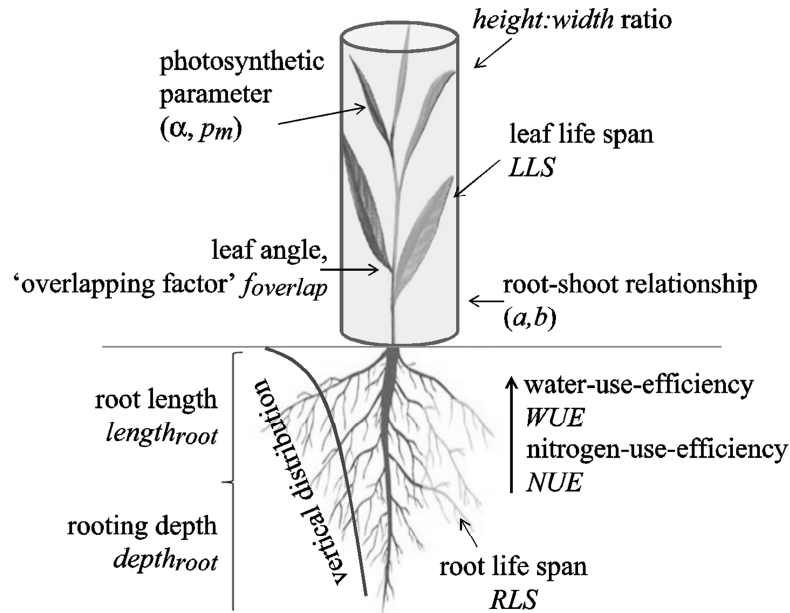


Figure 2.2: Exemplary representation of an individual's traits characterizing its success in resource uptake and in competition with other individuals. The above-ground traits are reflected (a) in the height-to-width ratio of the cylinder covering the shoot, (b) in the leaf life span LLS of the green shoot parts transferred to senescent ones, (c) in photosynthetic parameters as the maximum photosynthetic rate p_m and the initial slope of the light response curve α , (d) in the leaf angle, (e) in the "overlapping factor" $f_{overlap}$ accounting for leaf overlapping between individuals and (f) the relationship between root and shoot biomass using the parameter a and b . For success in below-ground competition (g) the total length of all branches of the root systems $length_{root}$, (h) the rooting depth $depth_{root}$, (i) the vertical distribution of root biomass in soil, (j) the root life span RLS , (k) the water- and nitrogen-use-efficiency (WUE and NUE) are important traits of an individual.

2.4 Discussion

We reviewed 13 existing grassland models concentrating on how suitable they are for simulating species-rich temperate grasslands in the context of biofuel production. In the course of the process-oriented review we presented conceptual approaches for a novel grassland model, where needed from our perspective.

Existing grassland models do not cover the entire range of essential processes needed for investigating the suitability of species-rich grasslands for biofuel production. In particular,

how exactly individuals interact when competing for water, nitrogen, light and space constitutes an important aspect, which has not been modelled sufficiently in recent models. The proposed modelling approaches of the Grassmind concept combine detailed competition modelling with simplified plant growth modelling adopted from recent grassland models. In doing so, a special emphasis is placed on competition for light, water, nitrogen and space, which operates on the individual-level.

Parameterizing vegetation models can always be difficult due, for instance, to restrictions in the availability of field data. Concerning grasslands, measurements of the entire above-ground biomass, coverage and leaf area index on the community or population level have been published (Tilman *et al.* 2001; Weigelt *et al.* 2010) or even performed. This is where the parameterization of detailed competition processes or individual-based growth and death processes can get complicated. To address these problems, either calibration of the full model or separate sub-models, if at all possible, or modern modelling techniques such as inverse parameterization using *MCMC methods* or pattern-oriented modelling are useful tools (Hartig *et al.* 2011; Grimm & Railsback 2012).

From our perspective there is a need for a new grassland modelling approach which offers new possibilities for analysing theoretical concepts and empirical results on the relationship between biodiversity and ecosystem functions (e.g. productivity). The detailed modelling of competition processes raises opportunities to investigate niche differentiation, sampling or facilitation theories in species-rich grasslands (Kinzig *et al.* 2002; Loreau *et al.* 2001). Such a model like the Grassmind concept might contribute to a more comprehensive understanding of the mechanisms underlying the positive effect of biodiversity on ecosystem functioning.

In the context of climate change, increasing drought events in Central Europe also have to be considered (Beniston *et al.* 2007; IPCC, 2007). In periods of drought, nutrients like nitrogen barely infiltrate deeper soil layers. Deep-rooting plants with a high fraction of roots in deeper soil layers may then be at a disadvantage compared to shallow-rooting plants (Garwood & Williams 1967a, 1967b). Although they have access to more soil water resources, their uptake of nitrogen can be very low. In contrast to long drought periods, extreme rainfall events with a high amount of precipitation can lead to nutrient leaching. Thus, not only climate but also management plays an important role in the development of grasslands. In particular, management is responsible for obtaining *Low-Input High-Diversity (LIHD)* or *High-Input Low-Diversity (HILD)* grasslands.

With moderate mowing and fertilizer application only when absolutely essential, *LIHD* grasslands can be created. Here, we expect increased light competition with decreasing management activity. In contrast, increasing the mowing frequency per year along with

fertilization or irrigation would result in *HILD* grasslands. A grassland model such as the Grassmind concept could also be used to elaborate guidelines for the management of grasslands in Central Europe according to a combination of biofuel production and nature conservation. As already mentioned, *LIHD* grasslands were proposed as a biofuel resource to be seriously considered as an alternative to monocultures of annual energy crops (Tilman *et al.* 2006b).

In Central Europe biogas production systems, or biogas plants, are used mainly by farmers. Currently, these systems are mostly fed with fresh maize biomass. The use of *LIHD* grasslands for these production systems may be difficult due to the different temporal niches of various grassland species. Some species become senescent or die at a time when others are still green and alive. Beside innovative biofuel production technologies, an alternative way to produce biofuel is the traditional biomass combustion of lignified plant material. Concerning grasslands, this should be done at the end of the vegetation period, when nearly all plants are senescent or dead, but still standing. However, different temporal niches may also pose a problem for this system of production. Plants that become senescent at a much earlier stage may already be decomposed and no longer standing, while at the very same time others have just become senescent or have transformed into dead material.

To confront these problems, the proposed Grassmind conceptual framework provides an opportunity to look at certain community compositions in terms of their suitability for biofuel production. Such grassland communities could then be used for different biofuel production systems, e.g. in spring after the first cut for biogas production and in late summer/autumn after the second cut for combustion. The results from this type of model can also contribute to a more diverse use of land (Jordan *et al.* 2007). While some areas can be planted traditionally with annual crops, the use of other land areas with species-rich, semi-natural grasslands can open up new opportunities. The negative effects of the high input needed for the cultivation of monocultures may be compensated on a regional scale by the positive effects of low-input systems.

Chapter 3

Grassmind – Model description²

3.1 Overview

The model Grassmind is designed in order to simulate species-rich, temperate grasslands on a daily basis to identify their potential for biomass production. The model focuses on competition between species or functional groups for the aboveground resources light and space as well as for the belowground resources water and nitrogen. Grassmind is coupled with the soil model Candy, which simulates carbon, nitrogen and water dynamics in soil, also on a daily basis (Franko *et al.* 1995).

Grassmind is an individual-based, process-oriented vegetation model following the gap approach typically applied in forest models (Shugart 1998; FORMIND, Köhler & Huth 2004). Just as on a gap in a forest, all individuals interact and compete for resources on a patch, without further assignment of explicit spatial positions for each individual on the patch. Individuals consist of an aboveground shoot (i.e. stem and leaves) and a belowground root system (i.e. root branches). Individuals of different age or species/functional group can differ in the size of these components.

We simulate a landscape of quadratic patches, with a patch size ($area = 10000 \text{ cm}^2$). The time step is set to one day ($\Delta t = 1$). The main processes calculated on the individual- as well as population-level are simulated within one time step according to a specific schedule (Fig. 3.1; Fig. 3.2). These processes comprise: (a) reproduction of new individuals and their (b) emergence as seedlings, (c) mortality of individuals including competition for space, (d) photosynthesis, which can be reduced due to shading and leads to the gross primary production, (e) competition for water and nitrogen, (f) maintenance and growth respiratory costs, (g) senescence of leaves and root branches and (h) the allocation of the resulting net primary production leading to the growth of an individual.

² This model description is based on a concept proposal, which has been published online (Taubert *et al.* 2012, supplementary material).

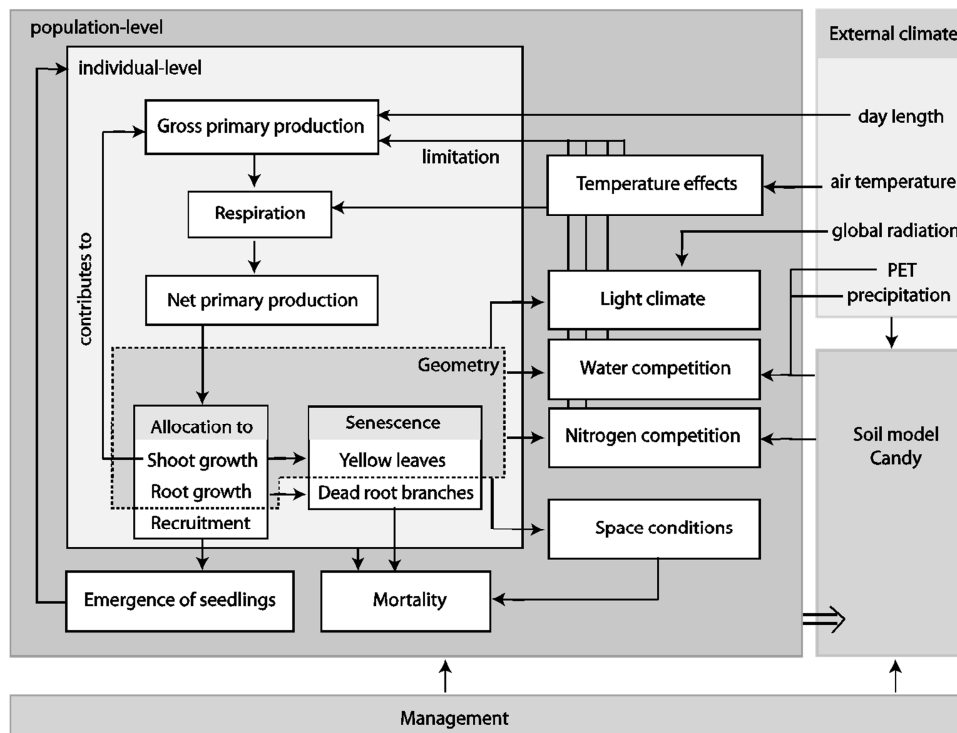


Figure 3.1: Block diagram of one time step (one day) in Grassmind. The block diagram shows the main processes acting on the individual- and population-level. Further, links to external climate data, the soil model Candy and management activities are presented. Arrows indicate an input.

In the beginning, recruited seeds (e.g. sown or produced via an individual's reproduction one time step before) emerge as new seedlings. After the emergence of new seedling, mortality of already established as well as newly emerged individuals is considered. Those individuals, which survive, can shade each other. As individuals can differ in their height, the incoming radiation is reduced from the top to the bottom of a patch stepwise to a certain extent, which is determined by calculating the light climate using an aboveground discretization. Limited space conditions are calculated based on the fraction each individual is covering on a patch. Requirements exceeding the available space can result in a higher mortality in the next time step. Based on the calculated light conditions, each individual performs photosynthesis resulting in its gross primary production. This gross productivity can be exposed to temperature, water and nitrogen limitations. Limitations of water and nitrogen can also be caused by reduced resource availabilities due to competition with other individuals on a patch. As well, respiratory costs can be changed due to daily air temperature. The net primary production of an individual is calculated by the difference between the (eventually reduced) gross production and respiratory costs. Before the net production is used for growth or reproduction, older leaves and root branches become senescent. That means leaves get yellow and root branches partly die. Yellowed leaves are still part of the shoot, whereby dead root branches are directly starting to decompose. After senescence, net productivity is allocated to reproduction of new seedlings and growth of the respective

individual, the latter one resulting in new geometrical properties of an individual's shoot and root. At last, management activities (e.g. mowing down to a height of 10 cm) are performed.

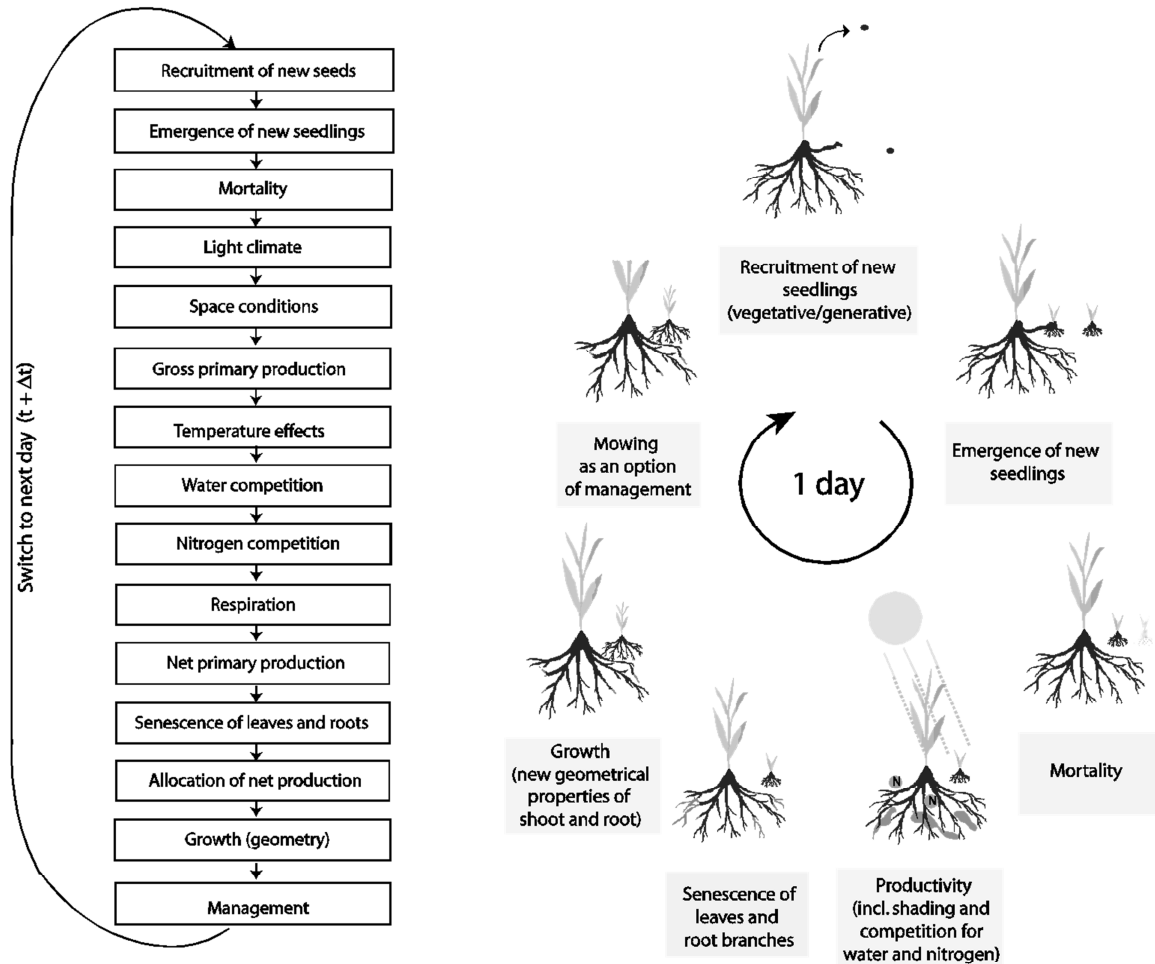


Figure 3.2: Flow diagram of one time step (one day) in Grassmind. The left flow diagram shows the main processes acting within one time step. The right life cycle illustrates again the main processes.

3.2 The geometry of an individual

The following main state variables are supposed to be associated with an individual: (1) aboveground shoot biomass B_{shoot} [g dry matter (DM)], (2) belowground root biomass B_{root} [g(DM)] and (3) reproduction biomass B_{rep} [g(DM)]. The aboveground shoot biomass is divided into biomass of fresh green leaves B_{shoot}^{green} [g(DM)] and biomass of senescent yellow

leaves B_{shoot}^{sen} [g(DM)]. Further state variables, which describe the geometry of an individual, can be derived from relationships with species-specific attributes (Fig. 3.3).

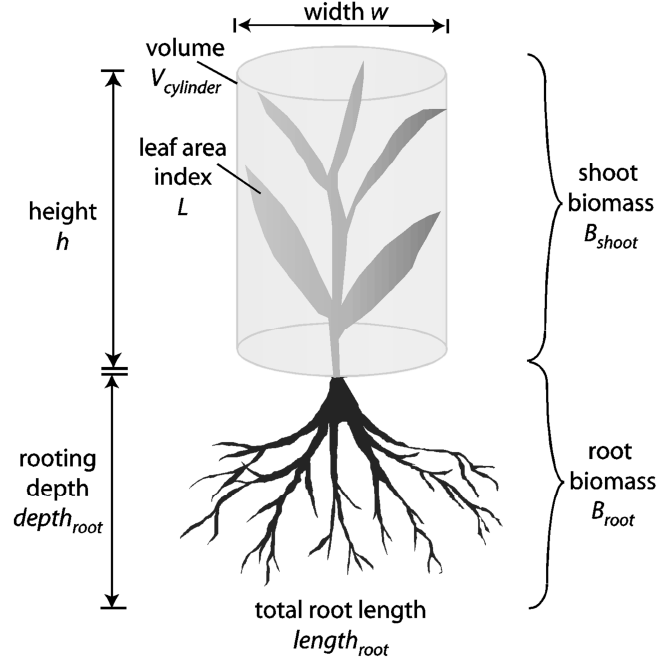


Figure 3.3: Display of the state variables, which correspond with the geometrical characteristics of an individual. The presented state variables can be derived from the aboveground shoot biomass and the belowground root biomass.

3.2.1 The aboveground shoot

We model the aboveground shoot of an individual as encased by a cylinder. The volume of the encasing cylinder $V_{cylinder}$ [cm^3] is directly related to the shoot biomass:

$$V_{cylinder} = \frac{B_{shoot}}{f_s}, \quad (3.1)$$

where the species-specific correction factor f_s [g(DM)/cm^3] accounts for free space within the cylinder not filled with biomass. The species-specific constant *height:width ratio* defines the height h [cm] and width w [cm] for a given cylinder volume.

The space an individual shoot occupies on a patch is determined by the ground area cov [cm^2] of the encasing cylinder. To calculate a patch's *community cover* CC [$\text{cm}^2(cov)/\text{cm}^2(\text{area})$], - that is the area occupied by all individuals relative to the patch area, it is

necessary to take leaf overtopping or overlapping among individuals into account. For this, each individual shoot cover is corrected by a species-specific *overlapping factor* f_o []. This factor accounts for overlapping in an implicit manner since the individuals do not have spatially explicit positions within the patch. The corrected covers of all individuals on the patch are summed up and normalized by the patch area:

$$CC = \frac{1}{area} \cdot \sum_{all\ individuals} (cov \cdot f_o). \quad (3.2)$$

The leaf area of the aboveground shoot is obtained by multiplying the biomass B_{shoot} with the constant *specific leaf area* SLA [$cm^2(leaves)/g(DM)$] leading to the leaf area index L [$cm^2(leaves)/cm^2(cov)$]:

$$L = \frac{B_{shoot} \cdot SLA}{cov}. \quad (3.3)$$

By using only the green shoot biomass B_{shoot}^{green} instead of B_{shoot} in Eq. (3.3), we obtain the green leaf area index L_{green} important for photosynthesis.

3.2.2 The belowground root

We assume a species-specific allometric relationship between an individual's aboveground shoot biomass B_{shoot} and belowground root biomass B_{root} – determined by the parameters s_1 and s_2 (cf. Niklas, 2005):

$$B_{shoot} = s_1 \cdot B_{root}^{s_2}. \quad (3.4)$$

As a reasonable approximation, we set s_2 to 1 and define s_1 as the species-specific *shoot:root ratio* as in literature often these ratios are determined from field measurements.

The individual's ability to access and compete for soil nitrogen and water resources strongly depends on its root system. In addition to the root biomass, the root system's vertical distribution in soil is important. Shallow and highly branched root systems are beneficial for nutrient uptake as most nutrients predominantly occur in the upper soil layers (Garwood & Williams 1967a, 1967b). In contrast, deeper root systems strongly increase the access to soil water resources, particularly during drought periods.

To calculate the rooting depth $depth_{root}$, which is required for water uptake (cf. Sec. 3.3.8), we adapt the approach of Schenk & Jackson (2002), to functionally relate rooting depths to the aboveground ellipsoidal canopy volume. Using the same relationship for the

volume of an individual's aboveground shoot cylinder (Eq. 3.1) and including the *shoot:root ratio* (Eq. 3.4) leads to:

$$depth_{root} = r_1 \cdot \left(\frac{s_1}{f_s} \cdot B_{root} \right)^{r_2}, \quad (3.5)$$

where the species-specific parameters r_1 and r_2 define the dependence of the rooting depth on root biomass. Each individual has an own rooting system, irrespective of the fact, whether the individual has been recruited via generative or vegetative reproduction. The total branching root length $length_{root}$ [cm], which is required for nitrogen uptake (cf. Sec. 3.3.9), is related to the root biomass via the *specific root length SRL* [cm/g(DM)]:

$$length_{root} = B_{root} \cdot SRL. \quad (3.6)$$

3.3 Model processes

In the following, we are going to describe details of the modelled processes important within the life cycle of an individual. These have already been introduced shortly at the beginning (cf. Sec. 3.1; Fig. 3.1; Fig. 3.2).

3.3.1 Reproduction

We do not distinguish between vegetative and generative reproduction. We assume that the single seed biomass produced via generative reproduction equals the biomass investment also required for vegetative reproduction of one individual (e.g. by rhizomes or stolones).

The number of potential seedlings N_{seed} produced by a reproductive individual is dependent on the individual's net production allocated to its reproduction pool B_{rep} and the species-specific single seed biomass B_{seed} [g(DM)]:

$$N_{seed} = \frac{B_{rep}}{B_{seed}}. \quad (3.7)$$

These potential seedlings can emerge in the next time step dependent on a species-specific germination rate (cf. Sec. 3.3.2). Only for seeds sown on a bare field, we include a time t_{em} [days] since the sowing date t_{sow} , that is needed for a single seed to germinate in soil until its emergence (at time $t_{sow} + t_{em}$).

3.3.2 Emergence of new individuals

Only a limited number \hat{N}_{seed} of potential seedlings N_{seed} (cf. Sec. 3.3.1) can germinate successfully within the same patch:

$$\hat{N}_{seed} = N_{seed} \cdot germ_{\%}, \quad (3.8)$$

where $germ_{\%}$ denotes the germination rate [1/day]. Environmental conditions are not considered for the germination process, so the germination rate can be interpreted as a constant success rate. Those of the potential seedlings, which cannot germinate successfully, i.e. $N_{seed} \cdot (1 - germ_{\%})$, are assumed to die immediately. The successfully germinated seedlings have an initial height h_{min} . Further geometrical properties can be derived from h_{min} (cf. Sec. 3.2).

3.3.3 Mortality

Crowding mortality

On a patch, only a finite number of individuals is able to survive due to limited space. Typically, the so-called self-thinning law of a community regulates the number of individuals. Numerous studies promote a power-law describing the number of surviving individuals according to their mean weight (Lonsdale & Watkinson 1982, 1983; Matthew *et al.* 1995).

Based on an indicator M_C (cf. Sec. 3.3.5), crowding mortality is either triggered or not. If space is limited, that means $M_C < 1$, a certain number of individuals N_{crowd} are removed stochastically so that the factor M_C exceeds the threshold of one:

$$N_{crowd} = N \cdot (1 - M_C). \quad (3.9)$$

Base mortality

Besides crowding, mortality is modelled using a rate m_b [1/day]. The value of this rate depends on the *age* of an individual:

$$m_b = \begin{cases} 0 & , age = 0 \\ m_{seed} & , 0 < age < age_{rep} \\ m_{basic} & , age_{rep} \leq age < life \\ 1 & , age \geq life \end{cases} \quad (3.10)$$

A basic mortality rate m_{basic} [1/day] is used for reproductive individuals, whereas a special mortality rate is used for seedlings. Individuals in the seedling state, which are not yet reproducing, have a higher mortality m_{seed} [1/day]. The time, at which individuals start to reproduce, is modelled by reaching a certain age (i.e. the parameter age_{rep}). Further, based on the species-specific lifespan $life$ [years] of a reproductive individual, the rate m_b can be set to one. For example, annual species die after one year. Thus, m_b is set to one, if the age [years] of an annual individual exceeds one year. Analogously, for bi-annuals and perennials m_b is set in a similar way, as bi-annuals die after two consecutive years, and perennial species may persist for several years.

3.3.4 Light climate

An increasing number of individuals on a patch differing in height, results in shading among the individuals. Therefore, the global radiation I_0 [$\mu\text{mol}(\text{photons})/\text{m}^2/\text{s}$] coming in above the highest individuals is increasingly attenuated down the bottom of the patch. To calculate light conditions in different heights on a patch, the aboveground space is divided into layers of constant width Δh [cm]. For each individual, its height h determines the highest layer l_{max} it covers completely by its shoot:

$$l_{max} = \left\lfloor \frac{h}{\Delta h} \right\rfloor. \quad (3.11)$$

Since the leaf area L is uniformly distributed in vertical direction within an individual's encasing cylinder (cf. Sec. 3.2), the individual's leaf area index contribution \hat{L}_i [$\text{cm}^2(\text{leaves})/\text{cm}^2(\text{area})$] is also assumed to be uniformly distributed among the covered height layers $i = 1, \dots, l_{max}$:

$$\hat{L}_i = \begin{cases} \frac{L \cdot cov}{h} \cdot \Delta h & , 0 \leq i \leq l_{max} \\ 0 & , i > l_{max} \end{cases}, \quad (3.12)$$

where cov is the ground area of the individual's encasing shoot cylinder. Summing up these leaf area contributions for all individuals on a patch results in the patch-based community leaf area index LAI_i [$\text{cm}^2(\text{leaves})/\text{cm}^2(\text{area})$] for each height layer i :

$$LAI_i = \frac{1}{area} \cdot \sum_{all\ individuals} k \cdot \hat{L}_i, \quad (3.13)$$

where k denotes the species-specific light extinction coefficient and $area$ is the area expansion of the patch (cf. Sec. 3.1). The light extinction coefficient is a species-specific constant parameter and thus, includes the assumption of constant leaf angles along the stem of an individual's shoot.

To determine the irradiance I_s [$\mu\text{mol}(\text{photon})/\text{m}^2/\text{s}$] at the top of an individual, the patch-based leaf area indices LAI_i of all height layers above the individual's height are summed up. Light attenuation through these height layers is then calculated using the approach of Monsi & Saeki (1953):

$$I_s = I_0 \cdot e^{-\left(\sum_{i>I_{\max}} LAI_i \right)}, \quad (3.14)$$

where I_0 [$\mu\text{mol}(\text{photon})/\text{m}^2/\text{s}$] is the non-attenuated incoming photosynthetic active radiation (PAR) modelled as the daily average photosynthetic active radiation from sunrise to sunset. Photosynthetic active radiation can be derived from the global radiation (cf. Sec. 3.4.1). Thus, competition for light between individuals is considered. Species growing higher receive more light and reduce the light received by smaller individuals via shading (Fig. 3.4). Noteworthy, not only green but also standing senescent shoot leaves contribute to shading. To reduce the effect of shading we weight the patch-based leaf area indices LAI_i each by a factor of $1/9$, which equals a subdivision of a 1 m^2 patch into 9 sub-patches of homogeneous leaf area distribution.

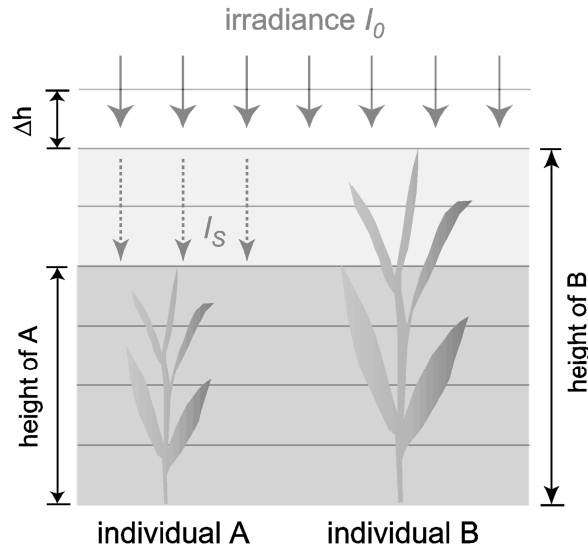


Figure 3.4: Illustration of light competition between individual species of different heights. Aboveground space is divided into height layers of width Δh . Here, B is higher than A (cf. vertical black arrows) and receives the unreduced incoming irradiance I_0 . A is shaded by those parts of B's leaf area that are higher than A, hence receiving the reduced irradiance I_s (Eq. 3.14). The height layers marked in light grey are shaded by B only, whereas those in dark grey are shaded by A and B. Each individual's leaf area is uniformly distributed among the respective height layers covered.

3.3.5 Space conditions

The indicator M_c triggering crowding mortality is calculated as the reciprocal of the coverage of the community CC on a patch:

$$M_c = CC^{-1}. \quad (3.15)$$

Noteworthy, the coverage of the community CC includes species-specific overlapping factors, thus influencing also the process of crowding on a patch. Crowding mortality is then triggered earliest in the subsequent time step (cf. Sec. 3.3.3).

3.3.6 Gross primary production

Gross biomass production of an individual is modelled via photosynthesis. Following the approach of Thornley & Johnson (1990), we calculate the gross photosynthetic rate for a single leaf using a saturation function:

$$P_{Leaf} = \frac{\alpha \cdot I_{Leaf} \cdot p_{max}}{\alpha \cdot I_{Leaf} + p_{max}}. \quad (3.16)$$

Here, α is the species-specific initial slope of the light response curve [$\mu\text{mol}(\text{CO}_2)/\mu\text{mol}(\text{photon})$], p_{max} is the species-specific maximum gross photosynthetic rate [$\mu\text{mol}(\text{CO}_2)/\text{m}^2/\text{s}$], and I_{Leaf} is the incoming irradiance on the leaf surface [$\mu\text{mol}(\text{photon})/\text{m}^2/\text{s}$]. The latter is derived by correcting the incoming irradiance I_s at the top of an individual (cf. Sec. 3.3.4):

$$I_{Leaf} = \frac{k}{1-m} \cdot I_s, \quad (3.17)$$

where k is the species-specific light extinction coefficient and m the transmission coefficient. To obtain the gross photosynthetic rate P_{shoot} [$\mu\text{mol}(\text{CO}_2)/\text{m}^2/\text{s}$] of an entire individual shoot, the single-leaf photosynthesis (Eq. 3.16) is integrated over the individual's green leaf area index L_{green} (cf. Sec. 3.2.1):

$$P_{Shoot} = \int_0^{L_{green}} P_{Leaf}(\tilde{L}) d\tilde{L} \quad (3.18)$$

leading to:

$$P_{Shoot}(I_{Leaf}) = \frac{p_{max}}{k} \cdot \ln \left(\frac{\alpha \cdot k \cdot I_{Leaf} + p_{max} \cdot (1-m)}{\alpha \cdot k \cdot I_{Leaf} \cdot e^{-k \cdot L_{green}} + p_{max} \cdot (1-m)} \right). \quad (3.19)$$

Multiplying the gross photosynthetic rate (Eq. 3.19) by three conversion factors leads to the potential gross primary production GPP_{pot} [g(DM)/day] of an individual shoot per day:

$$GPP_{pot} = P_{Shoot}(I_{Leaf}) \cdot \varphi_{ODM} \cdot \varphi_{day} \cdot \varphi_{area}, \quad (3.20)$$

where $\varphi_{ODM} = 0.63 \cdot 44 \cdot 10^{-6}$ [g(DM)/ $\mu\text{mol}(\text{CO}_2)$], $\varphi_{day} = 60 \cdot 60 \cdot length_{day}$ [s/day] with $length_{day}$ as the number of hours per day from sunrise to sunset, and $\varphi_{area} = cov$ [cm²].

3.3.7 Temperature effects

Photosynthesis and respiration are sensitive to temperature changes (Larcher 2001). Gross primary production (Eq. 3.20) is reduced for air temperatures T [°C] below a threshold of 10 °C according to Schippers & Kropff (2001; cf. also Larcher 1976):

$$R_T = \begin{cases} 0 & T \leq -5^\circ\text{C} \\ 0.02857 \cdot T + 0.142 & -5^\circ\text{C} < T \leq 2^\circ\text{C} \\ 0.1 \cdot T & 2^\circ\text{C} < T \leq 10^\circ\text{C} \\ 1 & 10^\circ\text{C} < T \end{cases} \quad (3.21)$$

Maintenance respiration r_m increases with air temperature according to Schippers & Kropff (2001, cf. Larcher 1976):

$$f_T = \begin{cases} 0 & T \leq 0^\circ\text{C} \\ 0.033 \cdot T & 0^\circ\text{C} < T \leq 15^\circ\text{C} \\ 2^{\frac{(T-25)}{10}} & 15^\circ\text{C} < T \end{cases} \quad (3.22)$$

3.3.8 Water competition

The individual's uptake of water resources from soil is modelled taking into account its demand on the one hand and the soil water available on the other hand. The individual's water demand θ_{demand} [mm/day], which is equal to its potential transpiration, is modelled using the water-use efficiency concept:

$$\theta_{demand} = \frac{GPP_{pot}}{WUE}, \quad (3.23)$$

where GPP_{pot} is the gross primary productivity (cf. Sec. 3.3.6) and WUE [g(DM)/kg(H₂O)] the water-use-efficiency parameter. By coupling Grassmind with the soil model Candy (Franko *et al.* 1995), the soil is divided into layers of constant width $\Delta s = 10$ cm down to a soil depth of 2 m.

Required water demands of all individuals can be restricted either by (a) the sum of interception and potential evapotranspiration or (b) by the difference of soil water content and permanent wilting point (Fischer *et al.* 2013, *accepted*). We assume an interception of zero for grasslands. In the first case, if the required water demands of all individuals on a patch exceed the potential evapotranspiration (PET), the water demands are reduced linearly by the reciprocal of PET to the required water demands. In the second case, if the difference of soil water content and permanent wilting point is lower than the required water demands, these water demands are set either to zero (if soil water content is below permanent wilting point) or reduced linearly by the reciprocal value of the respective difference to the required water demands (Fischer *et al.* 2013, *accepted*).

After the restriction of the water demands by the potential evapotranspiration and permanent wilting point, we calculate on the individual-level how much soil water an individual can take up by competing with other individuals on a patch. Using the vertical soil discretization of the soil model Candy, we calculate for each individual the soil layer s_{\max} , the individual roots into dependent on its rooting depths:

$$s_{\max} = \left\lceil \frac{\text{depth}_{\text{root}}}{\Delta s} \right\rceil. \quad (3.24)$$

Soil water uptake is also dependent on the individual's vertical root distribution within soil (Gerwitz & Page 1974) besides its rooting depth. For simplicity, roots are assumed to be equalled vertically distributed among the soil layers the individual is rooting into. Thus, we divide the demand of the individual θ_{demand} by number of soil layers s_{\max} :

$$\theta_{\text{demand}}^j = \frac{\theta_{\text{demand}}}{s_{\max}}, \quad (3.25)$$

where θ_{demand}^j [mm/layer/day] denotes the individual's demand per soil layer j . Using the individual's demand per soil layer θ_{demand}^j , we can calculate the patch-based total water demand θ_{total}^j [mm/layer/day] of all individuals for a specific soil layer j :

$$\theta_{\text{total}}^j = \sum_{\substack{\text{all individuals} \\ \text{on a patch} \\ \text{with } j < s_{\max}}} (\theta_{\text{demand}}^j). \quad (3.26)$$

To determine the fraction of demanded water an individual can take up from soil while competing with other individuals, the calculations of Granier *et al.* (1999) are used. Therefore, a *rooting zone* is determined for each individual. It represents the composition of the respective soil layers $j = 1, \dots, s_{\max}$ the individual is rooting in (Fig. 3.5).

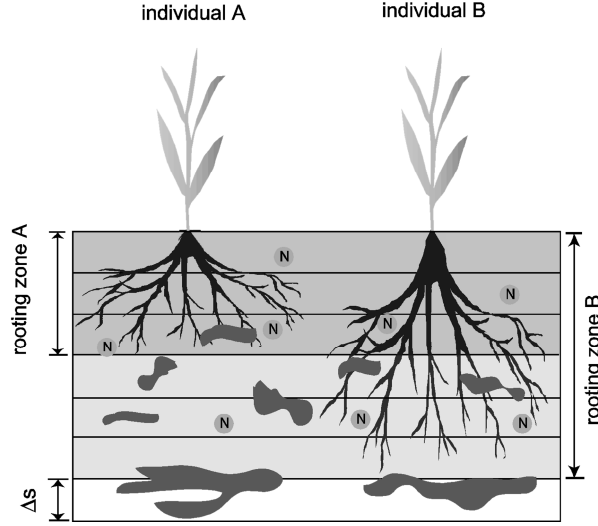


Figure 3.5: Illustration of the rooting zones of two different individuals. Horizontal light grey shadow marking the first three soil layers indicates the rooting zone A of individual A. In this example, the rooting zone of individual B covers the entire soil. Vertical dark grey shadows around the roots indicate the division of root branches equally among the soil layers in the respective rooting zone.

For an individual's *rooting zone*, the fraction of demanded water, which can be taken up, is determined individually based on the *remaining soil water content* θ_{rem} [mm(H₂O)/day], which would remain if the patch-based total demands per soil layer θ_{total}^j would be subtracted from the available soil water content:

$$\theta_{rem} = \sum_{j < s_{max}} (\theta_{soil}^j - \theta_{total}^j), \quad (3.27)$$

where θ_{soil}^j [mm/layer/day] is the volumetric soil water content in layer j . The remaining soil water content θ_{rem} represents that content, which would remain in an individual's rooting zone, if the total potential water demands of all individuals also rooting into these layers would be taken up. Using the potentially remaining soil water content, the fraction of an individual's demanded water, which can actually be taken up, is then determined by:

$$R_w = \begin{cases} 0 & , \theta_{rem} < \theta_{PWP} \\ (\theta_{rem} - \theta_{PWP}) / (\theta_{MSW} - \theta_{PWP}) & , \theta_{PWP} \leq \theta_{rem} \leq \theta_{MSW} \\ 1 & , \theta_{MSW} \leq \theta_{rem} \end{cases}, \quad (3.28)$$

where the dimensionless factor R_w increases from 0 to 1 (Granier *et al.*, 1999). If water demands exceed accessible soil water resources, demands cannot be fulfilled and the fraction R_w is less than one. For example, if the remaining soil water content would fall below the permanent wilting point θ_{PWP} [mm/d], the fraction R_w is set to zero. If available soil water resources would merely last for fulfilling partial water demands, uptake is linearly reduced.

The threshold defining the exceedance of accessible water resources is determined by the so-called *minimal soil water content* θ_{MSW} [mm/day]:

$$\theta_{MSW} = \theta_{PWP} + \frac{1}{3} \cdot (\theta_{FC} - \theta_{PWP}), \quad (3.29)$$

where θ_{FC} [mm/day] denotes the field capacity. The actual water uptake θ_{uptake} [mm/day] of an individual is calculated using the calculated fraction R_W :

$$\theta_{uptake} = R_W \cdot \theta_{demand}. \quad (3.30)$$

The consumption of soil water by the individuals influences the soil water content and thus, the availability of resources in the next time steps.

3.3.9 Nitrogen competition

Nitrogen non-fixing species

Similar to the water uptake, nitrogen uptake is dependent on the available nitrogen content, the individual's availability to take it up and its demand. To calculate the demand N_{demand} [kg(NO₃N)/cm²] (i.e. mineral nitrogen NO₃N), an approach based on the nitrogen-use efficiency concept is used comparable to water demands (cf. Sec. 3.3.8). The amount of nitrogen demands cannot always be met by the soil. Soil nitrogen $N_{available}$ [kg(NO₃N)/cm²], which is potentially available for absorption by an individual, is calculated by:

$$N_{available} = \sum_{j < s_{max}} F_j \cdot (N_j - N_{min}), \quad (3.31)$$

where $N_{available}$ [kg(NO₃N)/cm²] denotes the available nitrogen resources in soil, the individual has access to, N_{min} [kg(NO₃N)/cm²] represents a minimum amount of inaccessible soil nitrogen and F_j represents a competition factor. The factor F_j regulates the amount of nitrogen an individual can access by competing with other individuals. F_j is defined as the percentage of root branch lengths of the individual in relation to all other individuals per soil layer j :

$$F_j = \left(\frac{length_{root}}{s_{max}} \right) / \left(\sum_{\substack{\text{all individuals} \\ \text{on a patch} \\ \text{with } j < s_{max}}} \left(\frac{length_{root}}{s_{max}} \right) \right). \quad (3.32)$$

By this, it is assumed, that the individual's total root branches $length_{root}$ are divided equally among the soil layers in its *rooting zone* composed of the soil layers $j = 1, \dots, s_{max}$, the individual is rooting in (Fig. 3.5). The potential nitrogen uptake N_{uptake} [kg(NO₃N)/cm²] is then defined as:

$$N_{uptake} = \min(N_{demand}; N_{available}). \quad (3.33)$$

A nitrogen reduction factor $R_N \in [0;1]$ can then be calculated by:

$$R_N = \frac{N_{uptake}}{N_{demand}} = \min\left(1; \frac{N_{available}}{N_{demand}}\right). \quad (3.34)$$

Similar to soil water, soil nitrogen resources are also influenced by consumption of all individuals. As water is a means of transport for nitrogen uptake, actual soil nitrogen uptake \hat{N}_{uptake} of an individual is modelled proportionally to its soil water uptake:

$$\hat{N}_{uptake} = R_W \cdot R_N \cdot N_{demand}. \quad (3.35)$$

Nitrogen fixing species

Symbiotic nitrogen fixation, e.g. by legumes, is modelled using the following two assumptions:

- Species able to be in symbiosis with rhizobia, which fixes atmospheric nitrogen, never compete for nitrogen with other individuals. Thus, they never experience nitrogen limitation (reduction factor R_N always equals one).
- Receiving unlimited nitrogen, individuals have to pay for with carbon. A specific fraction $rhiz_{\%}$ of their net primary production NPP is given away to rhizobia. This amount of carbon is in turn missing for structural growth or recruitment, but productivity is not reduced due to nitrogen limitation.

Both aspects are considered for nitrogen-fixing species throughout the entire simulation. Positive effects of nitrogen-fixing species within a mixture appear as the nitrogen-fixing species do not take place in the nitrogen competition process and thus, more nitrogen resources in soil are available for other individuals. Further, nitrogen-fixing species release their nitrogen amount to soil by death. This results in an extra supply of available nitrogen in soil (Liu *et al.* 2011).

3.3.10 Respiration

We consider respiratory costs for maintenance of structural tissue (i.e. shoot and root biomass) and for growth of new biomass. Maintenance costs r_{main} [g(DM)/day] are modelled proportionally to the green shoot biomass B_{shoot}^{green} [g(DM)] and living root biomass B_{root} [g(DM)]:

$$r_{main} = r_m \cdot f_T \cdot (B_{shoot}^{green} + B_{root}), \quad (3.36)$$

where r_m is a constant maintenance respiration rate [1/day] and the factor f_T accounts for changing demands for maintenance respiration with varying air temperature (cf. Sec. 3.3.7). Growth respiratory costs are modelled by a constant parameter r_g [].

3.3.11 Net primary production

An individual's produced gross primary production GPP_{pot} is used for (a) respiratory costs, (b) growth of an individual's shoot as well as root and (c) reproduction. Losses due to maintenance and growth respiration (cf. Sec. 3.3.10) lead to the individual's net primary production NPP [g(DM)/day]:

$$NPP = (1 - r_g) \cdot (GPP_{act} - r_{main}), \quad (3.37)$$

where GPP_{act} [g(DM)/day] represents the actual gross primary production. The potential gross primary production (Eq. 3.20) can be reduced according to environmental limitations leading to the actual gross primary production:

$$GPP_{act} = R_W \cdot R_N \cdot R_T \cdot GPP_{pot}, \quad (3.38)$$

where R_W , R_N , and R_T (all $\in [0;1]$) account for reductions due to soil water limitations (R_W ; Eq. 3.28), soil nitrogen limitations (R_N ; Eq. 3.34), and temperature influences (R_T ; Eq. 3.21), respectively.

3.3.12 Senescence of leaves and root branches

All individual (i.e. seedlings and reproductive individuals) are subject to tissue turnover by partly yellowing of leaves and dying of root branches. The transformation rate

from green to yellow (senescent) shoot biomass B_{shoot}^{sen} [g(DM)] is set to the reciprocal value of the leaf life span LLS [days]. Senescent shoot leaves may not photosynthesize any longer (cf. Sec. 3.3.6), but may still shade other leaves (cf. Sec. 3.3.4) as they are maintained within an individual's shoot geometry. The transfer of senescent shoot biomass into the litter pool only occurs if an entire individual is dying due to mortality (cf. sec. 3.3.3).

Equivalent to leave senescence, the transformation rate of root branches into dead root biomass is set to the reciprocal value of the root life span RLS [days]. Dead parts are not maintained within an individual's root system and geometry, as they are transferred directly to the belowground litter pool.

3.3.13 Allocation of net primary production

For reproductive individuals, the net primary production NPP (Eq. 3.37) is allocated to the structural growth of shoot biomass and root biomass and to reproduction as follows:

- The fraction allocated to shoot growth $alloc_{shoot}$ is a species-specific parameter.
- The fraction allocated to root growth $alloc_{root}$ is derived from the fixed species-specific shoot-root ratio s_1 (Eq. 3.4):

$$alloc_{root} = \frac{alloc_{shoot}}{s_1} \quad (3.39)$$

- The remaining fraction is allocated to reproduction:

$$B_{rep} = (1 - alloc_{shoot} - alloc_{root}) \cdot NPP. \quad (3.40)$$

For seedlings, the fraction allocated to reproduction is zero. Hence, the fraction allocated to shoot growth is set such that the total net production NPP is used (i.e. $alloc_{shoot} + alloc_{root} = 1$). This modifies the allocation rates as follows:

$$alloc_{shoot} = \frac{s_1}{1 + s_1}. \quad (3.41)$$

The fraction allocated to root growth is then derived as in Eq. (3.39). As soon as an individual leaves the seedling's stage (i.e. its age exceeds age_{rep} ; cf. Sec. 3.3.3), the above-described allocation scheme including reproduction is used.

3.3.14 Growth of an individual

The described allocations of net primary production and the senescence transformations result in the following changes in the individual's biomass pools:

$$\frac{\Delta B_{shoot}^{sen}}{\Delta t} = \frac{1}{LLS} \cdot B_{shoot}^{green} \quad (3.42)$$

$$\frac{\Delta B_{shoot}^{green}}{\Delta t} = alloc_{shoot} \cdot NPP - \frac{1}{LLS} \cdot B_{shoot}^{green} \quad (3.43)$$

$$\frac{\Delta B_{root}}{\Delta t} = alloc_{root} \cdot NPP - \frac{1}{RLS} \cdot B_{root} \quad (3.44)$$

Based on the change of the biomass pools B_{shoot} and B_{root} , the geometrical state variable of an individual are updated (cf. Sec. 3.2).

3.3.15 Management

Management currently comprises only mowing. If mowing is planned on a specific date, the height of all individuals on a patch greater than the cutting height, for example 10 cm, is decreased leading to a modified *height:width ratio*. Based on the changed height of an individual, its aboveground biomass is also changed accordingly. For the consecutive time steps, growth of aboveground biomass only attributes to height growth until the time step at which the *original height:width ratio* is reached again.

3.4 Model inputs and outputs

3.4.1 Input parameter

The grassland model Grassmind has 37 parameters in total, whereby five of which attribute to technical adjustments. Of the remaining 32 parameters, only nine are not species-specific. Technical parameters are listed in Table 3.1. In Table 3.2 the geometrical parameters and in Table 3.3 all other process parameters of Grassmind are shown.

Table 3.1: Technical parameters of the grassland model Grassmind.

Parameter	Unit	Description	value
Δt	days	time step of Grassmind	1
Δh	cm	discretization of aboveground space	1
<i>area</i>	cm x cm	area expansion of a patch	100 x 100
Δs	cm	discretization of belowground space	10
$depth_{soil}$	cm	soil depth	200

Table 3.2: Geometrical parameters of the grassland model Grassmind.

Parameter	Unit	Description
h_{max}	cm	maximum height of an individual
hw	cm/cm	height:width ratio of an individual's encasing cylinder
f_s	g (DM)/cm ³	shoot correction factor
f_o	-	overlapping factor
<i>SLA</i>	cm ² /g (DM)	specific leaf area
<i>SRL</i>	cm/g (DM)	specific root length
r_1, r_2	-	parameters of the rooting depth power-law relationship
s_1	g (DM)/g (DM)	shoot:root ratio of biomass parts

Table 3.3: Process parameters of the grassland model Grassmind. Parameters, which are not species-specific, are written in bold.

Process	Parameter	Unit	Description
Recruitment and emergence of new seedlings	B_{seed}	g (DM)	seed biomass
	t_{em}	days	time until emergence of a seedling since sowing
	$germ\%$	-	germination rate of seeds
	age_{rep}	years	age at which recruitment starts
	h_{min}	cm	minimum height of a seedling at establishment
	t_{sow}	Date	initial sowing date
Mortality	<i>LLS</i>	days	leaf life span (start of yellowing leaves)
	<i>RLS</i>	days	root life span
	<i>life</i>	years	life span of the individual
	m_{basic}	1/year	basic mortality rate of mature individuals
	m_{seed}	1/year	mortality rate of established seedlings

Photosynthesis	p_{max}	$\mu\text{mol (CO}_2\text{)}/\text{m}^2/\text{s}$	maximum gross leaf photosynthesis
	α	$\mu\text{mol (CO}_2\text{)}/\mu\text{mol (photons)}$	initial slope of light response curve
Photosynthesis	k	-	light extinction coefficient
Competition	m	-	transmission coefficient
	WUE	g (DM)/ kg (H₂O)	water-use-efficiency coefficient
	NUE	g (DM)/ kg (N)	nitrogen-use-efficiency coefficient
Competition	N_{min}	kg(N)/cm²	minimum remaining soil nitrogen content per soil layer
Respiration	n_{fix}	yes/no	ability for symbiotic nitrogen fixation
	$rhiz_{\%}$	-	fraction of <i>NPP</i> given away to rhizobia (symbiosis)
	r_m	1/day	maintenance respiration rate
	r_g	-	growth respiration factor
Growth	$alloc_{shoot}$	-	allocation rate of <i>NPP</i> to shoot growth

External climatic data are needed on a daily basis. For the coupling interface of the grassland model Grassmind and the soil model, global radiation should be provided in [J/cm²/d], precipitation in [mm/d] and daily air temperature in [°C]. The grassland model itself needs a modification of the global radiation as photosynthesis is calculated based on the photosynthetic active radiation (*PAR*) in [$\mu\text{mol (photons)}/\text{m}^2/\text{s}$]. Therefore, global radiation is converted into *PAR* by assuming that *PAR* is approximately half of the global radiation. Day length and potential evapotranspiration are calculated based on external climatic data (Forsythe *et al.* 1995; Franko *et al.* 1995).

Further input parameters comprise management data and soil parameters (for an overview of soil parameters cf. Sec. 3.5.1). Management input parameters currently comprise only those concerned with mowing like the date of the event and the height, to which the sward is cut down. Further management options comprise, for example fertilization (with date, amount and type, i.e. organic or inorganic), irrigations (date and amount), ploughing and others.

3.4.2 Output variables

Typical output variables of the grassland model Grassmind comprise state variables like the number of individuals, the aboveground green and senescent shoot biomass, the belowground root biomass, the leaf area index, as well as geometrical characteristics like height and coverage. Rates like productivity, carbon sequestration in soil or soil resource consumption can also be observed. Different variables can be calculated (a) on the individual-level, (b) on the population-level as the sum of all individuals per species and (c) on the community-level as the sum of all individuals.

3.5 Coupling Grassmind with a soil model

We coupled the grassland model Grassmind with an already existing soil model. We choose the extensively studied model Candy (Franko *et al.* 1995). For both models, a dynamic link library (DLL) was created. Via an interface, the exchange of dynamic variables between both models is scheduled.

3.5.1 A brief summary of the soil model

The simulation model Candy is a one-dimensional soil model simulating the daily dynamics of nitrogen and carbon in soil (Franko *et al.* 1995). Besides, the water and heat balance in soil is calculated. It covers different horizons down to a soil depth of 2 m. Calculations are based on the division of soil in layers of 10 cm. Soil horizons group soil layers of homogenous properties like texture. Table 3.4 gives an overview of the soil parameters needed for the parameterization of each soil horizon. The ones marked in grey can be derived from others (Maidment 1993).

Table 3.4: Soil parameters of the soil model Candy.

Description	Unit
Sand content	%
Silt content	%
Clay content	%
Bulk density	g/cm ³
Particle density	g/cm ³
Field capacity	Vol%

Permanent wilting point	Vol%
Saturated water conductivity	mm/day

Soil water dynamics are calculated using a capacity approach, whereby soil temperature is simulated using a one-dimensional heat conduction equation (Franko *et al.* 1995). For the simulation of the dynamics of carbon in soil, a differentiation between soil organic matter (SOM) and primary organic matter (e.g. root tissue, litter or organic fertilizer) is made. Soil organic matter (SOM) is in turn divided into active SOM and stabilized SOM, which are both included in the carbon turnover process. Soil nitrogen is divided into the inorganic compounds nitrate and ammonium.

Within the soil model Candy, carbon (C) turnover is prioritized before nitrogen (N) turnover. Carbon turnover processes are described by first-order kinetics dependent on soil moisture, soil temperature and aeration. Nitrogen turnover is derived from carbon turnover and C/N ratios of the specific carbon pools resulting in nitrogen-immobilization, nitrogen-mineralization or no change of the specific nitrogen pools (Franko *et al.* 1995).

3.5.2 An interface for linking both models

The interface for scheduling the exchange of important dynamic variables between the grassland and soil model is designed and implemented in Delphi using Embarcadero 2010. Input parameters for both models as well as climate and management data are organized in a Microsoft Access database. The following flow diagram shows the schedule of exchange of the dynamic variables of each model via the interface (Fig. 3.6).

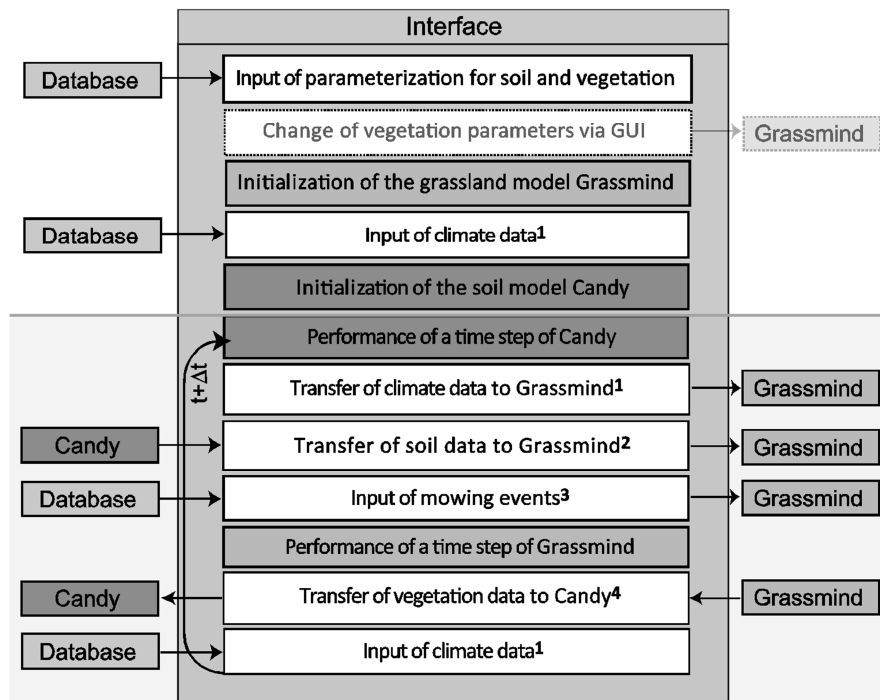


Figure 3.6: Flow diagram of the interface program showing the scheduled exchange between the grassland model Grassmind and the soil model Candy as well as input by the database. Within the second box the abbreviation GUI stands for graphical user interface. ¹climate data from the external database and exported to Grassmind: global radiation, precipitation, air temperature, potential evapotranspiration. ²soil data exported to Grassmind: permanent wilting point, field capacity, soil water content, mineral and ammonium nitrogen content, each per soil layer. ³mowing information exported to Grassmind: date of mowing and height, to which the grassland is mown. ⁴vegetation data exported to Candy: maximum grassland height, mean rooting depth, coverage on the patch, uptake of soil water and mineral nitrogen per soil layer, litterfall of green, senescent leaves and dead root branches. The lower horizontal grey shadow marks the steps executed in a daily time loop ($t + \Delta t$). Boxes above are processes, which are run only once at the beginning of the program.

**Simulating the Structure and Dynamics of Temperate Grasslands
in the Context of Diversity-Productivity Relationships****Abstract**

The role of species diversity on ecosystem functions like productivity is an important field in current research. Several field experiments show positive effects of increasing species-richness on the productivity of grasslands. However, simulation studies on these relationships are rarely performed. We use the individual-based grassland model Grassmind to simulate mixtures of temperate herbaceous species. We parameterize and calibrate the model for a selected Central European grass species using published field data. This species acts as a reference type for additionally defined species groups. These differ in their characteristics in acquiring resources individuals compete for, e.g. light, soil water and soil nitrogen. We analyse the role of these species types in 2-species-mixtures under extensive management in the context of diversity-productivity relationships. We can reproduce the monoculture structure and dynamics of the parameterized grass species well according to density of individuals, percentage of ground area covered by the community, maximum height and leaf area index of the community. The simulated monocultures and 2-species-mixtures of the defined species types show in the mean no effect of diversity on productivity, but for selected 2-species-mixtures slight positive or even negative effects can be observed. We conclude that the individual-based and process-oriented grassland model Grassmind is able to reproduce the monoculture structure and dynamics well. Further investigations on the role of certain species and their traits in shaping the diversity-productivity relationship are required.

4.1 Introduction

Semi-natural grasslands are rich in species diversity. On a local scale the number of vascular species can exceed those of tropical forests (Wilson *et al.* 2012). For resolutions smaller than 50 m², semi-natural temperate grasslands of Central Europe, Baltic and Argentina under chronic mowing or grazing, provide the highest richness of all vegetation types across

the world (Wilson *et al.* 2012). For example, dry sandy grasslands in Germany show on 1 cm² 5 species (Wilson *et al.* 2012; Dengler *et al.* 2004). In 2007 in Europe about 13.2 % of the land surface area has been covered by grasslands (Eurostat Yearbook 2012). Among all grasslands mostly semi-dry and dry grasslands or those in the higher mountains provide a high species-richness in Central Europe (Ellenberg & Leuschner 2010; Wilson *et al.* 2012).

The diversity of grasslands has received increasing interest in the last decades by the setup of large biodiversity experiments, for example in the United States of America, Europe and Germany (Tilman *et al.* 2001; Hector *et al.* 1999; Spehn *et al.* 2005; Weigelt *et al.* 2010). Those experimental studies show commonly a positive effect of species-richness or functional group richness on the aboveground productivity of grasslands (Reich *et al.* 2012; Spehn *et al.* 2005; Loreau & Hector 2001). Even under different management regimes, ranging from no fertilization and one cut per year to 200 kg/ha/yr fertilization and four cuts per year, a positive effect increasing with species-richness remains (Weigelt *et al.* 2009). Moreover, those experiments with no fertilization show equal or even higher productivity values than those with high fertilizer input and frequent mowing (Weigelt *et al.* 2009). Further benefits of species diversity are also demonstrated on other ecosystem functions like carbon sequestration in soil and roots (Tilman *et al.* 2006b).

Hypotheses have been developed for understanding the underlying mechanisms, which induce these effects (Loreau *et al.* 2001; Loreau & Hector 2001; Kinzig *et al.* 2002). In general, these comprise stochastic selective mechanisms (e.g. sampling; Tilman 1988; Loreau & Hector 2001; Loreau *et al.* 2001; Kinzig *et al.* 2002) and deterministic complementarity mechanisms (e.g. niche differentiation and facilitation; Tilman 1988; Loreau & Hector 2001; Loreau *et al.* 2001; Kinzig *et al.* 2002). By using the additive partitioning approach as proposed by Loreau & Hector (2001), the selection and complementarity effect can be investigated independently. A selection effect would be observed if no multi-species-mixture exceeds the highest monoculture productivity, thus promoting the relevance of intraspecific interactions (Loreau *et al.* 2001, Loreau & Hector 2001; Kinzig *et al.* 2002). In contrast, a complementarity effect would be observed if the productivity of species exceeds that expected from the monoculture performance, thus promoting the relevance of interspecific interactions (Loreau *et al.* 2001; Loreau & Hector 2001; Kinzig *et al.* 2002). In biodiversity experiment, generally both effects are observed. In most experimental studies, a positive complementarity effect increasing with species-richness and time (Reich *et al.* 2012; Spehn *et al.* 2005; Loreau *et al.* 2001; Loreau & Hector 2001) and a neutral selection effect mainly remaining constant over diversity levels and time reveal (Reich *et al.* 2012; Spehn *et al.* 2005; Loreau *et al.* 2001; Loreau & Hector 2001). For the BioCON and BioDIV experiments, for example, results can be explained by accumulated complementarity in resource use due to increasing functional diversity and feedback effects, especially concerning soil nitrogen (Reich *et al.* 2012).

In this study, the individual-based and process-oriented grassland model Grassmind (Taubert *et al.* 2012) is used, which is designed for simulating species-rich temperate grasslands including management. It is coupled with the soil model Candy simulating the daily dynamics of carbon-, nitrogen- and water-dynamics in soil (Franko *et al.* 1995). The model framework allows investigating the structure and dynamics of temperate grasslands. Using published field data of the *Jena biodiversity experiment* in Germany, we parameterize the model for a typical Central European grass species. This species serves as a reference type, from which we derive additional species types. We simulate different combinations of 2-species-mixtures from monocultures. Our analyses focus on the following questions:

- Can we reproduce the structure and dynamics observed in grassland field experiments by using the individual-based simulation model Grassmind?
- How does aboveground productivity change from monocultures to 2-species-mixtures?

4.2 Material and methods

4.2.1 The grassland model Grassmind

We use the individual-based grassland model Grassmind for simulating species-rich temperate grasslands (Taubert *et al.* 2012). The grassland model follows the principles of the gap-approach typically applied in forest modelling (Köhler & Huth 2004; Bugmann 2001). Within a gap, here called patch, individuals do not have a spatially explicit position, but compete for resources equally (Shugart 1998). Resources considered in the model comprise light, space, soil water and soil nitrogen. A full description of the grassland model is presented in chapter 3.

To account for the importance of soil resources and dynamics, we couple the grassland model with the soil model Candy (Franko *et al.* 1995). The soil model simulates the daily dynamics of water, carbon and nitrogen (Franko *et al.* 1995) and provides the grassland model each day with information on available soil resources. Exchange between the below-ground resource availabilities and above-ground vegetation characteristics are managed by an interface written in Delphi including both models as dynamic link libraries.

4.2.2 Field data and site-specific conditions

We parameterize the grassland model for the grass species *Festuca pratensis*, which occurs typically in Central Europe (Ellenberg & Leuschner 2010). We choose site characteristics like climate, soil properties and management based on a biodiversity grassland experiment in Central Germany (*Jena Experiment*; Jena, Germany, 50°55'N, 11°35'E), for which field measurements are published (Weigelt *et al.* 2010, Heisse *et al.* 2007, Roscher *et al.* 2004). In the following paragraphs, we present detailed information used for the parameterization similar to the field experiments.

Field observations

In the field, seeds of the monoculture *Festuca pratensis* had been sown between 11 and 16 May 2002 and have been observed for six consecutive years (Heisse *et al.* 2007; Weigelt *et al.* 2010). From the published field measurements, we use the monthly estimated coverage of the community on the ground area and number of individual shoots (Heisse *et al.* 2007) as well as twice a year measured aboveground biomass, community leaf area index, maximum height and community coverage (Weigelt *et al.* 2010). Repeated measurements are only available for aboveground biomass and sward height (Weigelt *et al.* 2010). Although field measurements are available until the year 2008, we exclude data from 2008 because the coverage of weeds on the monoculture plot of *Festuca pratensis* exceeds 70% (Weigelt *et al.* 2010). For the years 2002 to 2007, the coverage of weeds had been below 20 % (Weigelt *et al.* 2010).

Climatic conditions

Precipitation, global radiation and air temperature have been measured by two weather stations located near the experimental plots of the biodiversity experiment. Data from November of 2003 onwards are available from the weather station of the Max-Planck-Institute (MPI) for Biogeochemistry (MPI for Biogeochemistry, Jena, Germany). As our simulation starts on 16 May 2002, the missing climate data from 1 January 2002 onwards are substituted by data from the weather station of the Ernst-Abbe-Fachhochschule Jena (FH Jena), also located near the experimental plots (Ernst-Abbe-Fachhochschule, Jena, Germany). For consistency, we use weather data from the FH Jena for the years 2002 and 2003 and from 1 January 2004 onwards those of the MPI for Biogeochemistry. Within the measurements from the MPI of Biogeochemistry, there are missing values from 17 to 21 May 2007, which we also substitute using measurements from the FH Jena.

Soil properties

In general, the soil of the Jena Experiment is classified as *Eutric Fluvisol* (Oelmann *et al.* 2007). Although the area had been agriculturally managed intensively in the last decades, an influence of former fertilization is not assumed (Oelmann *et al.* 2007). From Steinbeiss *et al.* (2008) detailed information on the soil texture in the upper horizon (down to 30 cm) is available. Based on this and some assumptions, we estimate soil properties for the experimental monoculture plot of *Festuca pratensis* (Appendix A2). The estimated soil attributes of the experimental plots seem to be similar to soil attributes of an experimental site in Eastern Germany (Bad Lauchstädt, Saxony-Anhalt, Germany; Franko *et al.* 1995), for which a parameterization of the soil model Candy is already available (Franko *et al.* 1995).

Management

The management activities in our simulations are similar to those of the *Jena biodiversity experiment* (Weigelt *et al.* 2010). In the experimental plots, mowing of the grassland to a height of 10 cm and weeding each twice a year has been performed (Roscher *et al.* 2004, Heisse *et al.* 2007). Within our model, we do not consider weeding. For the first year, mowing was done eight weeks and 15 weeks after sowing (assumed exact dates: 11 July, 24 September; Roscher *et al.* 2004, Heisse *et al.* 2007). For the consecutive years (2003 to 2007), we assume mowing to occur on the fifth of the months, for which mowing has been planned (as in some publication mowing is stated as done in early June or early September; Weigelt *et al.* 2010, Roscher *et al.* 2004).

4.2.3 Simulation studies

Monoculture of *Festuca pratensis*

In our simulation experiments, we sow seeds on 16 May 2002 and simulate in total 100 m² of the monoculture of *Festuca pratensis* until the end of year 2007. We chose this grass species because much information is available from literature. The grassland model Grassmind requires in total 39 parameter values, whereby five of them attribute to technical adjustments. From the remaining 34 parameter values, 17 of them are available from literature for the grass species *Festuca pratensis* (Appendix A2). The unknown parameter values have been estimated by inverse parameterization using (a) information from literature (Hauck *et al.* 1997) and (b) field data from the *Jena biodiversity experiment* as described in section 2.2.1 (Appendix A2). Thereby, we estimate in a first step maximum leaf photosynthetic rate by

reproducing the photosynthetic curve of a single leaf under increasing light conditions (Hauck *et al.* 1997) using the functional approach of Thornley & Johnson (1990). Afterwards, we calibrate the remaining parameters of geometry (four parameters), growth (six parameters), reproduction (two parameters) and mortality (two parameters) processes stepwise by hand, trying to reach the data points of the field measurements. An initial value for the parameter estimation and calibration of water-use-efficiency (*WUE*) was used (mean value for legumes 1.4, available from Larcher 2001).

Two-species mixtures

Using the reference of the grass species *Festuca pratensis* (the species *Festuca pratensis* acts as a reference type) we define additional species groups by changing specific physical attributes of the reference type. We investigate on the change of productivity values from monocultures to 2-species-mixtures.

We choose the reference type *Festuca pratensis* as the first species group and derive three additional groups differing in their characteristics to acquire resources (Fig. 4.1). The defined species groups show different attributes for rooting depth, total root branch length and specific leaf area. Rooting depth of group 2 is increased (by 100 %), so this species group receives an advantage compared to the other ones by accessing deeper soil water resources. In contrast, the third defined species group has higher *specific root length* compared to the other groups (700 % increase), which increases its ability to take up nitrogen resources. At least, the fourth species group is characterized by an increased *specific leaf area* (10 % increase), which advantages this group in absorbing light resources compared to the other species groups. Trade-offs within the change of the specific parameters for the groups are not considered.

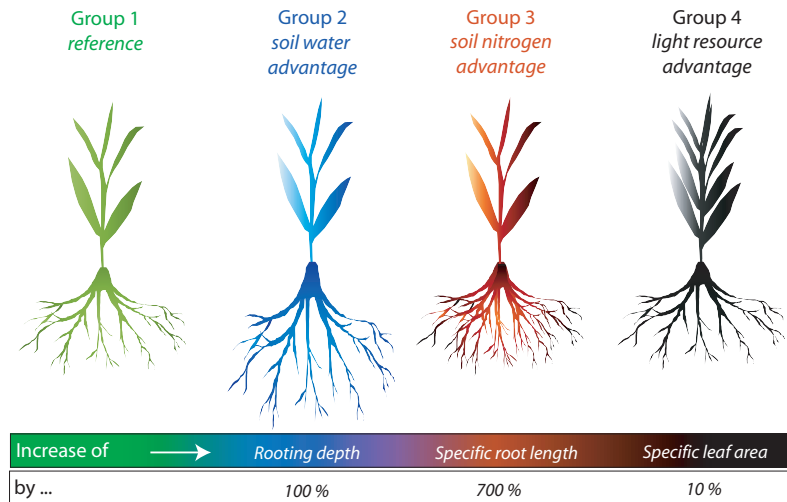


Figure 4.1: Summary of the defined species groups and their change according to the reference species *Festuca pratensis* (“Increase of ... by ...”). ¹Parameter r_1 is adjusted for deeper rooting depths to twice as high as the reference species. ²Parameter *SRL* is changed eight times higher than the reference species, which can be interpreted as an increase in root surface area, i.e. longer root branches. ³The parameter *SLA* is increased by 10% compared to the reference species.

We simulate monocultures and all combinations of 2-species mixtures using the defined species groups on 50 m² in total. For each simulation of a mixture the initial number of seeds to be sown of the respective species group is calculated based on the germination rate and the number of species sown as done in the field experiments in year 2002 (Roscher *et al.* 2004, Heisse *et al.* 2007). By this, a total number of 1000 individuals per patch (1 m²) germinating at the beginning of the simulation are ensured with equal abundances of the respective species groups at seedlings emergence. Simulations have been performed for the period starting at the sowing date in May 2002 until the end of year 2005. Site-specific conditions according to climate, soil properties and management activities are chosen as explained in section 4.2.2.

The effects of diversity on productivity

We investigate on the increase of productivity from monocultures to 2-species-mixtures. Net productivity is taken only from the last simulated year. We calculate aboveground net productivity from the simulations similar to observations in the field experiments (Weigelt *et al.* 2010). That means, aboveground biomass is observed twice a year directly before a mowing event (assumed exact date: 25 of the respective month). Both observations are summed up for the annual aboveground biomass in [g(DM)/m²/yr] to estimate the annual net productivity rate.

4.3 Results

4.3.1 Can we simulate the observed structure and dynamics of experimental grasslands using the model Grassmind?

In year 2002, individual seedlings emerge two weeks after sowing with a cover of approximately 20 % of the ground area (Fig. 4.2). As seedlings are exposed to a higher mortality than a mature individual, within the next two weeks the seedling density and community coverage decrease down to approximately 150 individuals per m² and 10 %. The remaining individuals reach the stage of reproductive ability at about mid of June (not distinguished between vegetative and generative type). During this period, the density of individuals and the community coverage are rapidly increasing up to approximately 2700 individuals per m² and 100 % until the end of August (Fig. 4.2). With an increasing fraction of yellowed leaves per individual, reproduction decreases, which results in a decrease of density down to 1500 individuals per m² but a constantly remaining community coverage at 100 %. By the start of winter (when daily temperatures, day length and daily radiation have been decreased), the photosynthetic production of an individual is lowered down and no significant changes in the density of individuals and community coverage can be observed anymore. In general, we can observe for both simulated dynamics a good match to the field data (Fig. 4.2).

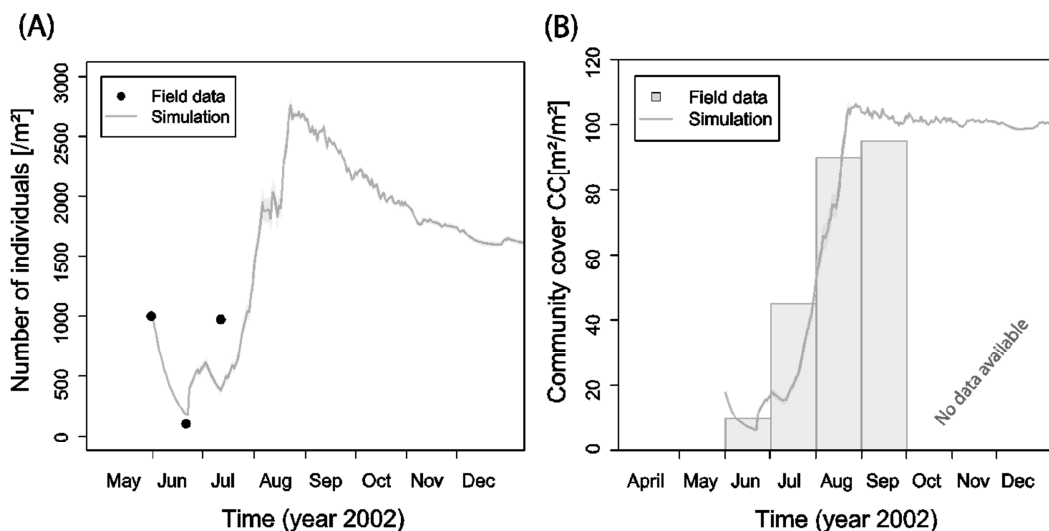


Figure 4.2: Simulation of the parameterized species *Festuca pratensis* using the grassland model Grassmind compared to observation data for (A) density of individuals and (B) community cover of individuals. Simulations are run 100 times. Solid green line represents the average of 100 m² and light green shadows behind indicate their standard deviation. For the community cover no data from October to December are available.

For the following years 2003 to 2007, the leaf area index and grassland's maximum height increase during the vegetation period of favourable climatic conditions and decrease according to mowing events (Fig. 4.3). Few field data values cannot be reached entirely, but the general trend of the simulated leaf area index of approximately 2 and the dynamics of the grassland height ranging between 60 and 10 cm match well the field measurements. Community cover of total aboveground biomass, including green and yellowed leaves, in general increases in the first year of establishing to 100 % coverage of the ground area and remains at that level (Fig. A7.1). Within the growing periods in spring and summer, higher variations in total community cover can be observed (Fig. A7.1). As leaves get senescent by starting yellowing in late summer, the community cover is decreasing in late summer down to approximately 20 % and again increasing in spring (here community cover includes only green leaves; Fig. A7.1). Community cover of green leaves reaches maximum values of about 70 to 80 % (Fig. A7.1). In general, we can also observe good matches between simulated and observed community cover despite some small discrepancies, especially in the year 2007 (Fig. A7.1).

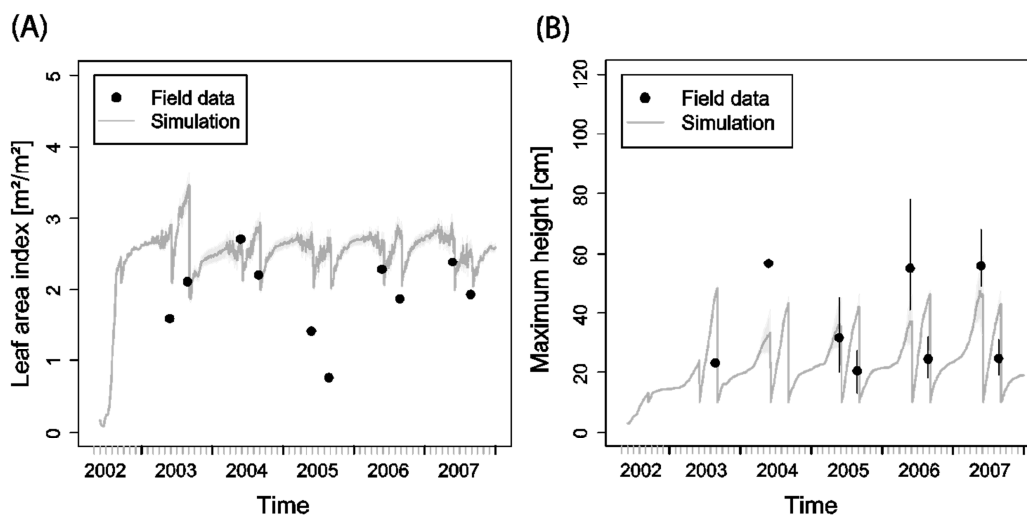


Figure 4.3: Comparison of the simulated and measured community leaf area index and maximum height of the sward for the parameterized species *Festuca pratensis*. Black points represent the field observations and vertical black lines denote the range from the minimum to the maximum value. Solid green line shows the average of 100 m^2 simulation and the light green shadow behind denotes the standard deviation.

Simulations of aboveground biomass, including green and yellowed leaves, increase since emergence of seedlings up to approximately 200 g dry matter per m^2 (Fig. A7.2). Mowing events rapidly reduce aboveground biomass by approximately 20 to 50 g dry matter per m^2 (Fig. A7.2). During spring and summer biomass is accumulated quickly again, reaching around 200 g dry matter per m^2 with ± 50 g dry matter per m^2 (Fig. A7.2). Observed

and simulated aboveground biomass differ for the years 2003 and 2004, for which extreme values of 600 to 800 g dry matter per m² have been measured (Fig. A7.2; Weigelt *et al.* 2010).

4.3.2 How does aboveground productivity change from monocultures to 2-species-mixtures?

By looking into detail in the species-mixture combinations, we can compare the annual productivity of monocultures with the respective combinations of the 2-species-mixtures (Fig. 4.4). Some of the simulated 2-species-mixtures show a higher or lower productivity compared to the best or worst monoculture productivity of the respective species groups included in the mixture. Nevertheless, the change of productivity from a specific monoculture to its corresponding 2-species-mixture is on average below 10 g(DM) per m² and year.

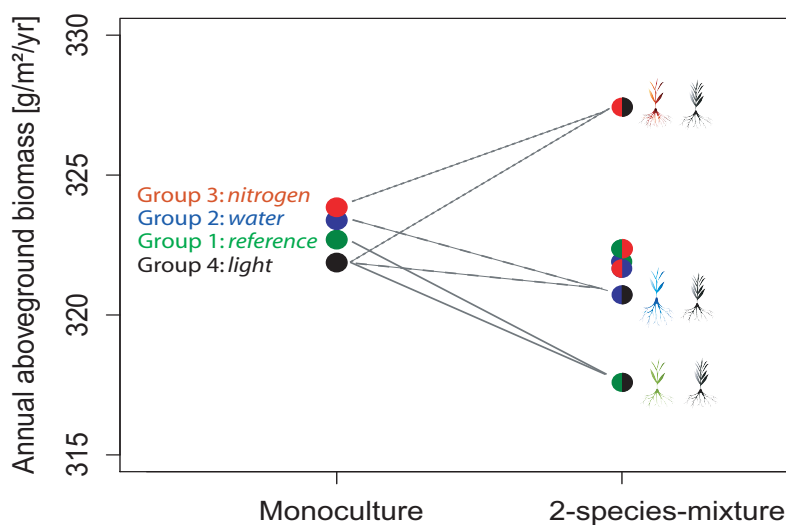


Figure 4.4: Comparison of the monocultures with the 2-species-mixtures of the defined species groups for 50 m². For the monocultures, each species group is represented by a point. For the 2-species-mixtures, each combination of the respective two simulated species groups is represented by two semicircles filled with the corresponding colours. We indicate three examples of species-mixtures by solid lines (group 1 and 4), dotted lines (group 3 and 4) and dashed lines (group 2 and 4).

We select three examples of the 2-species-mixture, for which the mean annual aboveground productivity on 50 m² changes compared to both respective monoculture productivities (Fig. 4.4). The first selected species-mixture includes the nitrogen favourable

group 3 and the light favourable species group 4, which shows an annual productivity 5 g(DM)/m²/yr higher than the monocultures of group 3 and 10 g(DM)/m²/yr higher than the monoculture of group 4 (Fig. 4.4). The second selected species-mixture shows in contrast an annual productivity lower than those of the monocultures of the reference species group 1 and the light favourable group 4 (Fig. 4.4). This 2-species-mixture is on average 10 g(DM)/m²/yr lower than both monoculture productivities (Fig. 4.4). The third selected species-mixture includes the deep rooting species group 2 and the light favourable species group 4. The mixture shows an annual productivity approximately as high as the monoculture of species group 4 (Fig. 4.4).

4.4 Discussion

We use the individual-based grassland model Grassmind for simulating monocultures and 2-species mixtures. Simulations concerning a monoculture of a typical Central European grass species *Festuca pratensis* as reference type show a good match in comparison with field measurements. Based on the reference species, we defined additionally species types and carry out investigations concerning the change of annual aboveground productivity from monocultures to 2-species-mixtures.

When parameterizing the grassland model for the reference grass species *Festuca pratensis* some field observations are not exactly reached. Several factors may influence the results like (a) uncertainties in the field observations and (b) assumptions of the model. Field measurements of the biodiversity experiment are collected in different ways and sub-areas of the plots for the consecutive years (Weigelt *et al.* 2010). For example, different investigators contributed measurements of the years 2002 to 2008 working at different temporal and spatial scales. Measurement and mowing dates are not documented exactly and thus, only could approximately be assumed for the parameterization of Grassmind. Although weeding was performed twice a year, the coverage of weeds increased with increasing years of the experiment (Weigelt *et al.* 2010). This aspect, i.e. the invasion of weeds or weeding as a management activity, is not included in the grassland model Grassmind, which can cause some mismatches with our simulation results.

Further, not for all input parameters of our simulation model is field data available. A number of parameter values are found in literature, but can be based on experiments, which differ in design and environmental constraints. Despite this, some plant attributes like the *specific leaf area* or *specific root length* may change during the lifetime of an individual (Schippers & Olf 2000), which we assume to remain constant over time in our grassland model. Such variations in input parameters may have an additional influence on the simulation results. By performing a local sensitivity analysis of the grassland model

Grassmind based on the parameterization of *Festuca pratensis*, we observe a high sensitivity of the shoot allocation rate and geometrical parameters (Appendix A3). Especially, the allocation rate of productivity attributed to the growth of aboveground biomass shows a high sensitivity for all measurement dates from 2002 to 2007 (Fig. A7.4). Trying to reach the few extreme measured biomass values in year 2003 and 2004 would also induce a change of other well reproduced values in the years 2005 onwards. Further, increasing the accumulation of biomass, e.g. by adjusting the fraction of net productivity allocated to shoot growth, induces an increase in leaf area index (Fig. A7.8). This in turn would result in mismatches with field data of leaf area (Fig. 4.3 A). Thus, we have not included measurements of the years 2003 and 2004 for calibration. Inverse parameterization algorithms could be helpful in such cases (Grimm & Railsback 2012; Hartig *et al.* 2011).

Based on the monoculture simulation of the grass species *Festuca pratensis*, we carry out a simulation study of 2-species-mixtures. In contrast to field observations of the planted biodiversity experiments (Loreau & Hector 2001; Reich *et al.* 2012; Spehn *et al.* 2005; Fargione *et al.* 2006), our simulations show in the mean no positive effect on productivity from monocultures to 2-species-mixtures, but an increased variability of productivity values for the 2-species-mixtures. These discrepancies may be caused by the attributes we have changed compared to the reference species *Festuca pratensis*. In measurements of Marquard *et al.* (2009b), it is revealed that the grass species *Festuca pratensis* is on average underyielding in diverse mixtures. That means, the reference species we used for our analysis as a basis shows in highly diverse mixtures less productivity than expected from its monoculture performance (Marquard *et al.* 2009b). Marquard *et al.* (2009b) revealed that the positive effect in diversity-productivity relationships is mainly driven by the increasing density of overyielding species in mixtures. In contrast to the underyielding species *Festuca pratensis*, which we used, predominantly herbs and legumes turned out to be overyielding species (Marquard *et al.* 2009b). So, our findings of the species-mixtures simulations using the defined species groups could suffer from attributes similar to those of *Festuca pratensis*. Those traits we have changed for the defined species groups, cannot explain positive effects in diversity-productivity relationships alone. Considering a higher density of additionally parameterized herbs and legumes in future analysis may yield positive effects in productivity with increasing diversity as more attributes will be presumably different compared to *Festuca pratensis*. Further, we created these types without considering trade-offs explicitly. Trade-offs are usually considered within such studies, so that no supercompetitive species is included (Kinzig *et al.* 2002). For example, species with higher specific leaf area may have shorter lifespans (Reich *et al.* 1998). In pursuing future theoretical simulation studies using the grassland model Grassmind, such trade-offs should be included.

We can conclude that our developed individual-based and process-oriented grassland model Grassmind is able to reproduce the monoculture structure and dynamics of the grass

species *Festuca pratensis* well. Further parameterization of additional species, especially herbs and legumes, substantiate either the modelling approaches of Grassmind or lead to required modifications of modelling parts in Grassmind. Concerning our simulation study of defined species types, we can conclude that different trends (e.g. positive, negative and neutral) in simulated monocultures compared to their corresponding 2-species-mixtures can be observed, but in the mean we got no trend for all species combinations. This might indicate that observed diversity-productivity relationships cannot be explained entirely by three physical functionalities in acquiring resources, species compete for. Future analyses on the role of certain species traits in shaping the diversity-productivity relationship in grasslands are required.

On the Challenge of Fitting Tree Size Distributions in Ecology³

Abstract

Patterns that resemble strongly skewed size distributions are frequently observed in ecology. A typical example represents tree size distributions of stem diameters. Empirical tests of ecological theories predicting their parameters have been conducted, but the results are difficult to interpret because the statistical methods that are applied to fit such decaying size distributions vary. In addition, binning of field data as well as measurement errors might potentially bias parameter estimates. Here, we compare three different methods for parameter estimation – the common maximum likelihood estimation (*MLE*) and two modified types of *MLE* correcting for binning of observations or random measurement errors. We test whether three typical frequency distributions, namely the power-law, negative exponential and Weibull distribution can be precisely identified, and how parameter estimates are biased when observations are additionally either binned or contain measurement error. We show that uncorrected *MLE* already loses the ability to discern functional form and parameters at relatively small levels of uncertainties. The modified *MLE* methods that consider such uncertainties (either binning or measurement error) are comparatively much more robust. We conclude that it is important to reduce binning of observations, if possible, and to quantify observation accuracy in empirical studies for fitting strongly skewed size distributions. In general, modified *MLE* methods that correct binning or measurement errors can be applied to ensure reliable results.

³ A research paper with analogous content has already been published (Taubert *et al.* 2013).

5.1 Introduction

Strongly skewed size distributions occur in a wide range of natural systems. Examples include search patterns in animals known as Lévy flights (Edwards *et al.* 2007; Edwards 2008; Sims *et al.* 2008; Reynolds *et al.* 2009; Reynolds *et al.* 2012), frequency distribution of earthquake magnitudes (Gutenberg & Richter 1954) and fire sizes (Clar *et al.* 1996; Reed & McKelvey 2002), and the relation of species abundances to their individual body size (White *et al.* 2007; Enquist *et al.* 2009; West *et al.* 2009), in particular, stem size distributions of trees (Shinozaki *et al.* 1964; Shimano 2000; Enquist & Niklas 2001; Muller-Landau *et al.* 2006; Wang *et al.* 2009). Several studies, for example the self-organized criticality (e.g. applied to forest fires), or metabolic theories, focus on the nature of the processes that underlie such size distributions and make specific predictions about the functional form and associated parameters (Enquist *et al.* 2009; West *et al.* 2009; Drossel & Schwabl 1992; Turcotte & Malamud 2004; Stegen & White 2008). For example, Enquist & Niklas (2001) propose a power-law distribution with a scaling parameter $\alpha = 2$ for the stem size frequency distribution of natural forests (Enquist *et al.* 2009).

When testing theoretical predictions, we have to consider that field data contain uncertainties. For example, in forest science field data on tree size are typically analysed by constructing a stem size frequency distribution which summarizes the number of trees in different measured stem diameter classes (Fig. 5.1 a). Such a classification of the measured data into diameter classes of a certain width is also called binning of data. Thus, results of analyses depend on the class width, whereby in forestry widths of 5 cm or 10 cm are often used. Besides the influence of binning, uncertainties in field data can also arise from irregularities or errors that occur during the measurement process (Chave *et al.* 2004). Such measurement errors typically lead to a symmetric variation around the true value. Both binning and measurement errors change the functional shape of the analysed frequency distribution (Fig. 5.1 b, 5.1 c).

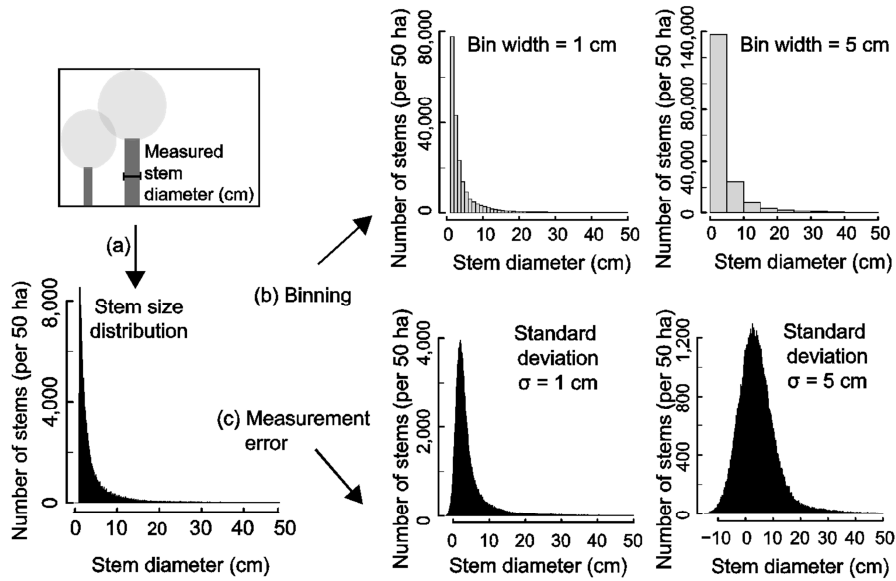


Figure 5.1: Outline of tree size measurements in forests. (a) In general, the stem diameter of a tree is measured at breast height (1.3 m). Each tree in the area of interest is tagged, recorded and measured. Using a specific class width (here 1 mm) each measured stem diameter is classified in its corresponding class. This results in a number of stems per class and is summarized in a stem size distribution. (b)-(c) Change of the functional form of the stem size distribution of stem diameters under binning or including measurement errors. (b) Change of the stem size distribution using binning of measured stem diameters with bin widths of 1 cm and 5 cm. (c) Change of the stem size distribution adding random measurement errors of standard deviations $\sigma = 1$ cm and $\sigma = 5$ cm to the recorded stem diameters.

Two methods are mainly used to estimate the parameters of size distributions - maximum likelihood estimation (*MLE*) and linear regression. Linear regression can only be applied to pre-binned data and thus, leads to serious complications not only in assessing parameters (Edwards 2008; White *et al.* 2008), but also in determining the correct corresponding distribution as the best fit using the coefficient of determination r^2 (Franziska Taubert, unpublished data). Instead, *MLE* is known to be the most accurate approach to date as it does not require pre-binned data and thus, shows numerous advantages, for example, low bias and low variance of parameter estimates (Edwards 2008; White *et al.* 2008; Clauset *et al.* 2009). Nevertheless, linear regression is still used (Sims *et al.* 2008; Enquist *et al.* 2009). However, even when *MLE* is applied, difficulties may also arise when there are observation uncertainties in the data.

In this study we analyse how parameter estimation and the selection of the true corresponding frequency distribution are affected by (a) binning and (b) random measurement errors. As far as we know, no previous study has systematically examined the effect of binning and random measurement errors on *MLE* parameter estimates and distribution selection results for decaying size distributions in ecology. To account for binning and to correct random measurement errors, we propose modified *MLE* methods. Using large virtual

data sets produced from three distributions (power-law, negative exponential and Weibull distribution) we also test whether potential effects can be corrected by these modified methods. We investigate the following questions:

- Which effects do observation uncertainties have on parameter estimates and on determining the underlying frequency distribution when uncertainties are not considered in the *MLE* method?
- To what extent do the two modified *MLE* methods reduce potential effects in parameter estimation?
- Which advantages do the two modified *MLE* methods show in determining the frequency distribution that underlies the observations?

Finally, we demonstrate the application of the investigated methods on a large field data set of measured stem diameters for a tropical forest.

5.2 Materials and methods

5.2.1 Maximum likelihood estimation

In this study, we use maximum likelihood estimation (*MLE*) for inferring parameters of frequency distributions. Given a sample $x = \{x_i\}_{i=1}^n$ of observations, the likelihood L is defined as the probability of obtaining these measured field data. Assuming that the data points are independent, L can also be written as the product of the single probabilities $p(x; \theta)$ of each data point depending on unknown parameters θ :

$$L(x; \theta) = \prod_{i=1}^n p(x_i; \theta), \quad (5.1)$$

where i is indexing the corresponding observation points. To estimate the unknown parameters θ , the likelihood $L(x; \theta)$ is maximized.

Different types of assumptions can be made for the probability $p(x; \theta)$ of a measured data point. Most simple is the presumption that this probability is given by an assumed frequency distribution $f(x; \theta)$ without observation uncertainties. Therefore, $p(x; \theta)$ is simply replaced by the assumed frequency distribution $f(x; \theta)$:

$$p(x; \theta) = f(x; \theta). \quad (5.2)$$

In the following, we call this method *standard MLE*.

Generally, *standard MLE* is applied to continuous data. But, field data often show inaccuracies. Such data inaccuracies occur either as binning (e.g. rounding measured data) or as random measurement errors (e.g. non-systematic uncertainties). Binning ε_{bin} equals a classification of data into half-open intervals of width $b \geq 0$ cm. Measurement stochasticity ε_{meas} is typically assumed to be Gaussian distributed with mean $\mu = 0$ cm and standard deviation $\sigma > 0$ cm.

To account for binning of data, the multinomial approach is used to describe the expected probability of observing a single data point within a class of a certain width b (cm). This probability depends on the assumed frequency distribution $f(x; \theta)$:

$$p(x; \theta) = \frac{n!}{N_1! \dots N_q!} \cdot \left[\int_{B_j}^{B_j+b} f(x; \theta) dx \right]^{N_j}, \quad (5.3)$$

with the j^{th} bin denoted as $[B_j, B_j + b)$ and N_j as the number of observations falling in the corresponding bin. Altogether there are q classes, where $\sum_{j=1}^q N_j = n$ is the total number of observations. A few studies have already followed this approach (Edwards *et al.* 2007; Muller-Landau *et al.* 2006). Here, we call this *MLE* which considers binning uncertainties the *multinomial MLE*.

For correcting measurement errors we use a hierarchical fitting function: first it is assumed that the data points originate from the presumed frequency distribution $f(x; \theta)$ and are then perturbed by a random measurement error ε_{meas} :

$$p(x; \theta) = \int_{lower}^{upper} \left[\frac{f(x; \theta)}{\sigma \cdot erf(1/\sqrt{2}) \cdot \sqrt{2} \cdot \pi} \cdot \exp\left(-\frac{(x_i - x)^2}{2 \cdot \sigma^2}\right) \right] dx, \quad (5.4)$$

where x_i stands for the i^{th} observation value, x_{min} and x_{max} correspond to their minimum and maximum and $erf()$ refers to the Gauss error function. In detail, we assume for the measurement error a truncated Gaussian distribution with mean $\mu = 0$ cm and constant standard deviation $\sigma > 0$ cm. We set the truncation at $3 \cdot \sigma$, which results in limits of the integral (cf. Eq. 5.4) of $upper = \min(x_{max}; x_i + 3 \cdot \sigma)$ and $lower = \max(x_{min}; x_i - 3 \cdot \sigma)$. As before, for the purpose of this paper we refer to this *MLE*, which amends measurement errors, as the *Gaussian MLE*.

5.2.2 Virtual data sets

A power-law distribution is mostly used to fit strongly skewed frequency distributions (Edwards *et al.* 2007; Sims *et al.* 2008; Newman 2005). However, a typical question is whether a given empirical distribution is really best described by a power-law distribution, or whether similar frequency distributions such as a negative exponential distribution also provide a good fit. Therefore we concentrate here not only on the power-law, but also on the negative exponential distribution and the Weibull distribution. We include the Weibull distribution because some studies take it into account to possibly describe a size distribution, for example, of tree diameters (Muller-Landau *et al.* 2006; Bailey & Dell 1973; Rennolls *et al.* 1985). In general, our results will qualitatively apply to most functions that depict strongly skewed distributions.

To test the *MLE* methods, we generate 1,000 virtual data sets of sample size n from each assumed frequency distribution $f(x;\theta)$ using the inverse transformation method (Appendix A4). Parameters of these distributions are set as follows:

- scaling parameter $\alpha = 2$ for the power-law distribution,
- parameter $\lambda = 0.5$ for the negative exponential distribution and
- parameters $\beta = 0.5$ and $\gamma = 0.5$ for the Weibull distribution.

We choose an exponent of $\alpha = 2$ for the power-law distribution because this value is suggested by Enquist & Niklas (2001) for the stem size frequency distribution of natural forests. Parameters of the other distributions are chosen in a way that the shape of the probability density function is comparable to those of the power-law distribution. We assume that these three distributions are truncated in the range of $[x_{\min}; x_{\max}]$ (Table 5.1). We set $x_{\min} = 1$ cm and $x_{\max} = 1,000$ cm throughout the evaluations (typical values for tree size distributions).

Table 5.1: Presentation of the three assumed truncated frequency distributions $f(x; \theta)$ used in our investigations.

frequency distribution	$f(x; \theta)$
power-law distribution ($\theta = \alpha$)	$c \cdot x^{-\alpha}$ with $c = (\alpha - 1) / (x_{\min}^{-(\alpha-1)} - x_{\max}^{-(\alpha-1)})$
exponential distribution ($\theta = \lambda$)	$c \cdot \exp\{-\lambda \cdot x\}$ with $c = \lambda / (\exp\{-\lambda \cdot x_{\min}\} - \exp\{-\lambda \cdot x_{\max}\})$
Weibull distribution ($\theta = (\beta; \gamma)$)	$c \cdot x^{(\gamma-1)} \cdot \exp\{-\beta \cdot x^\gamma\}$ with $c = (\beta \cdot \gamma) / (\exp\{-\beta \cdot x_{\min}^\gamma\} - \exp\{-\beta \cdot x_{\max}^\gamma\})$

To assess the accuracy of *MLE* for imprecise data, we either apply binning to the virtual samples or overlay them with a measurement error. Concerning binning, we increase the width b from $b_{\min} = 0.1$ cm to $b_{\max} = 50$ cm with a step size of 0.1 cm. For measurement errors we randomly generate values from a Gaussian distribution with $\mu = 0$ cm and $\sigma > 0$ cm and add them to the produced virtual data. The parameter σ of ε_{meas} we use in our investigations ranges from $\sigma_{\min} = 0.1$ cm to $\sigma_{\max} = 14$ cm increasing with a step size of 0.1 cm. For the example of stem diameter distributions in forestry, a standard deviation $\sigma = 1$ cm results in an expected average deviation of 20 % for stem diameters of 5 cm. Finally, we evaluate each sample applying the three *MLE* methods (cf. Eq. 5.2, Eq. 5.3, Eq. 5.4). We also vary the sample size n of the produced virtual data ($n = 100; 500; 1,000; 5,000; 10,000; 50,000$) to check for an effect of sample size on estimation. Due to computational limitations, we reduce repetitions and sample size for the *Gaussian MLE*, for which we only analyse 250 samples (of sample size $n = 100; 500$).

The calculations result in parameter values for each distribution dependent on ε_{bin} or ε_{meas} . We fit the raw and modified virtual data sets by applying *standard MLE* as well as *multinomial MLE* or *Gaussian MLE*. This allows us to compare the estimation bias for each type of observation uncertainty and offers the opportunity to evaluate the capability of error correction (Fig. 5.2). For the binned virtual data we use the centre of the bins as data values when evaluated with the *standard MLE*.

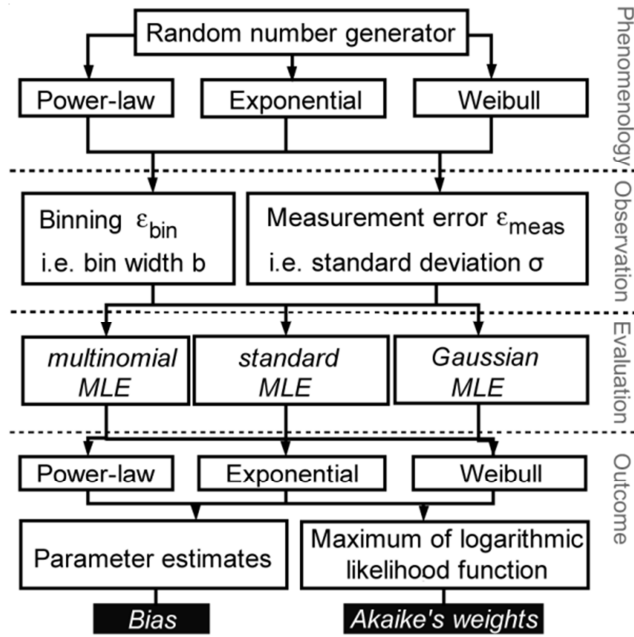


Figure 5.2: Scheme of the evaluation procedure of virtual data sets.

To evaluate which of the supposed distributions $f(x; \theta)$ best represents a specific data sample, we choose *Akaike weights* (Burnham & Anderson 2002). The distribution with the highest *Akaike weight* expresses the data best according to the set of the supposed distributions.

To apply our methods to real-world data, we use data from a forest inventory on Barro Colorado Island (BCI) from the year 2000 (Condit 1998; Hubbell *et al.* 1999; Hubbell *et al.* 2005⁴). Stem diameter measurements are recorded as integers (in mm) at breast height (1.3 m). Here, we report data values in (cm). We only take into account those measured trees that are declared as ‘alive’ and as ‘main stems’. We exclude measurements of the smallest possible recorded diameter value (1 cm) to avoid distortions due to uncertainty about rounding for the smallest values (Muller-Landau *et al.* 2006). Minimum and maximum measurements are set to x_{\min} and x_{\max} , encompassing in total 207,105 observations. Bin width is documented as $b = 0.1$ cm. The measurement error has been estimated by repeated measurements of 1,715 trees (Chave *et al.* 2004; Condit 1998). The corresponding deviations have been fitted with a sum of two Gaussian distributions. The first Gaussian distribution depicts small deviations increasing with stem diameter in (cm) (mean $\mu = 0$ cm; \square standard deviation

⁴ The BCI forest dynamics research project was made possible by National Science Foundation grants to Stephen P. Hubbell: DEB-0640386, DEB-0425651, DEB-0346488, DEB-0129874, DEB-00753102, DEB-9909347, DEB-9615226, DEB-9615226, DEB-9405933, DEB-9221033, DEB-9100058, DEB-8906869, DEB-8605042, DEB-8206992, DEB-7922197, support from the Center for Tropical Forest Science, the Smithsonian Tropical Research Institute, the John D. and Catherine T. MacArthur Foundation, the Mellon Foundation, the Small World Institute Fund, and numerous private individuals, and through the hard work of over 100 people from 10 countries over the past two decades. The plot project is part the Center for Tropical Forest Science, a global network of large-scale demographic tree plots.

$sd_1 = 0.0062 \cdot diameter + 0.0904$ cm), according to 95 % of the observed trees. The second Gaussian distribution describes larger ones (mean $\mu = 0$ cm; standard deviation $sd_2 = 4.64$ cm), associated with the remaining 5 % of trees (Chave *et al.* 2004).

All evaluations of the virtual and BCI data are performed with R-2.10.0 (R Development Core Team 2009). For *MLE* optimization of the power-law or exponential distribution, we employ a combination of *golden section search* and *successive parabolic interpolation* (Kiefer 1953; Heath 2002); for the Weibull distribution, we choose the *Nelder-Mead algorithm* (Nelder & Mead 1965; Nocedal & Wright 2006). In cases of convergence difficulties for Weibull distributed data, we change the optimization technique to the *L-BFGS-B algorithm* (Nocedal & Wright 2006; Byrd *et al.* 1995). All optimization algorithms used are already implemented in R-2.10.0.

5.3 Results

5.3.1 Effect of binning and measurement errors

Increasing bin widths generally affects the parameter estimates of all three considered distributions, thus creating remarkable biases (Fig. 5.3 a). Based on representative virtual data of sample size $n = 500$, only small bin widths of approximately $b < 1$ cm ensure a mean bias of less than 5 % of the true parameter of the corresponding distributions (Appendix A5). With incrementing widths of $b > 1$ cm, nearly all parameters are on average underestimated, except the parameter γ of the Weibull distribution, which is highly overestimated (Fig. 5.3 a). Maximum absolute values of the mean bias range from 48 % (α -estimates) to 280 % (γ -estimates) (Appendix A5). Standard deviations of α -, λ - and β -parameter estimates decrease with bin width, whereas the standard deviation of γ -values increases (Fig. 5.3 a).

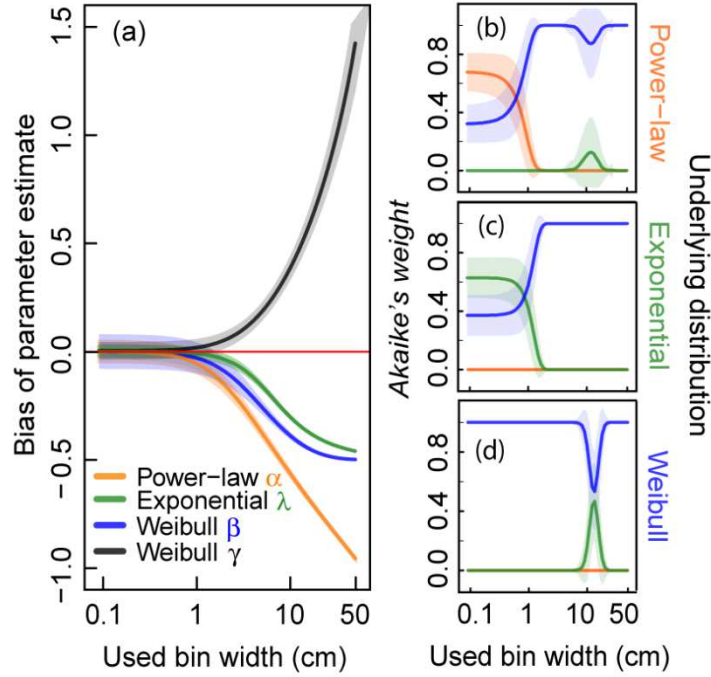


Figure 5.3: Analyses of binned virtual data using different bin widths. We evaluate 1,000 virtual data sets of sample size $n = 500$ from a truncated power-law, a truncated negative exponential and a truncated Weibull distribution. Virtual data are classified into classes of certain bin width (x-axis in cm) before applying *standard MLE*. (a) Effect of binning on parameter estimates of the three investigated distributions. (b)-(d) Effect of binning on *Akaike weights* supposing three distributions (power-law, negative exponential and Weibull distribution) for (b) power-law distributed virtual data, (c) negative exponentially distributed virtual data and (d) Weibull distributed virtual data. The highest *Akaike weight* determines the best fit of a frequency distribution to the data. Solid lines represent the mean values and shaded areas show the standard deviation (of 1,000 calculated values).

Random measurement errors included in the virtual data sets with 500 values also have substantial effects on parameter estimates (Fig. 5.4 a). For α -, λ - and β -estimates the mean parameter value is underestimated (again, except for the parameter γ). Significant effects already start at a small measurement error of $\sigma \approx 0.1$ cm with a mean bias of approximately 5 % of the true parameter value (Fig. 5.4 a, Appendix A5). Absolute mean biases reach their maximum in the range between 37 % (α -estimates) and 110 % (γ -estimates) (Appendix A5). Standard deviations of parameter estimates show similar trends as was observed for binned data.

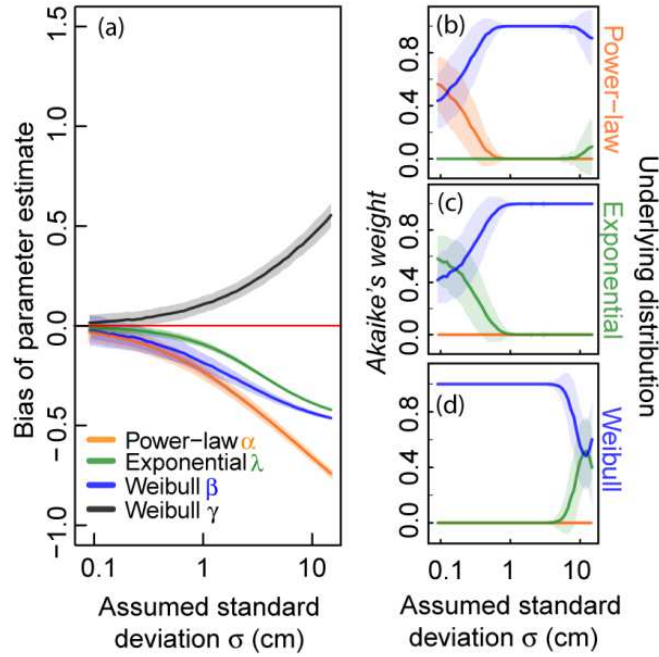


Figure 5.4: Analyses of virtual data including different levels of measurement errors. We evaluate 1,000 virtual data sets of sample size $n = 500$ from a truncated power-law, a truncated negative exponential and a truncated Weibull distribution. An error value generated from a Gaussian distribution with mean $\mu = 0$ cm and an assumed standard deviation σ (x-axis in cm) is added to each virtual data point before applying *standard MLE*. (a) Effect of random measurement errors on parameter estimates of the three investigated distributions. (b)-(d) Effect of random measurement errors on *Akaike weights* supposing three distributions (power-law, negative exponential and Weibull distribution) for (b) power-law distributed virtual data, (c) negative exponentially distributed virtual data and (d) Weibull distributed virtual data. The highest *Akaike weight* determines the best fit of a frequency distribution to the data. Solid lines represent the mean values and shaded areas show the standard deviation (of 1,000 calculated values).

Binning strongly affects the correct determination of a power-law distribution. Only for small bin widths (< 0.67 cm) can the correct distribution be identified using *Akaike weights* (Fig. 5.3 b, Appendix A5). Thereby, the distribution with the highest weight best represents the data with regard to the set of the three supposed distributions. For widths above this threshold, an increasing chance of selecting a Weibull distribution occurs instead (Fig. 5.3 b). Surprisingly, this effect is not improved by increasing the sample size (Appendix A6). Looking at exponentially distributed data, the true distribution cannot be distinguished from the Weibull distribution with high certainty even when the data are not binned. For bin widths below approximately 0.91 cm the probability of correct identification is on average higher than 50 % (Fig. 5.3 c, Appendix A5). Above this threshold, the probability of selecting a Weibull distribution instead increases strongly. Again, this problem is not solved by increasing the sample size (Appendix A6). Binning of Weibull distributed data does not influence the determination of the correct distribution over a large range of bin widths (Fig. 5.3 d, Appendix A5). But, for bin widths between approximately 11 cm and 15 cm there is a small chance of

wrongly selecting an exponential distribution. With increasing sample size, this small probability of false selection decreases (Appendix A6). Note that the Weibull distribution is more flexible than the other two as it includes one additional parameter.

If we include measurement errors in the raw data, the determination of the correct distribution using *Akaike weights* based on the *standard MLE* method shows different results than for binning (Fig. 5.3.1.2 b, c, d). Only for small measurement errors of $\sigma < 0.14$ cm can a power-law be identified correctly by looking at the mean *Akaike weights* (Fig. 5.4 b, Appendix A5). For assumed standard deviations σ greater than this threshold, a steeply increasing probability of determining a Weibull distribution is observed. An exponential distribution can only be detected for a small measurement error of $\sigma < 0.18$ cm (Fig. 5.4 c, Appendix A5). Weibull distributions are in most cases correctly identified, except for very large measurement errors ($\sigma \approx 12$ cm) (Fig. 5.4 d, Appendix A5). At this value, the chance of selecting an exponential distribution increases. Similar effects can be observed for the data sets with higher sample size (Appendix A6).

5.3.2 Performance of modified MLE methods

Using *multinomial MLE*, the negative effects can be reduced to a large extent (Fig. 5.5 a, Appendix A5). For the entire range of investigated bin widths, a significantly lower mean bias of α -, β - and γ -parameter estimates can be observed not exceeding a mean bias of 9 % of the corresponding true parameter value (Appendix A5). For λ -estimates binning correction fails only for high widths (> 11 cm, Fig. 5.5 a). However, it reaches a maximum absolute mean bias of 59 % of the true λ -value, which is still smaller than for employing *standard MLE* (Appendix A5). Standard deviations of the parameter estimates increase with increasing bin width for nearly all parameters, except for λ , which decreases (Fig. 5.5 a).

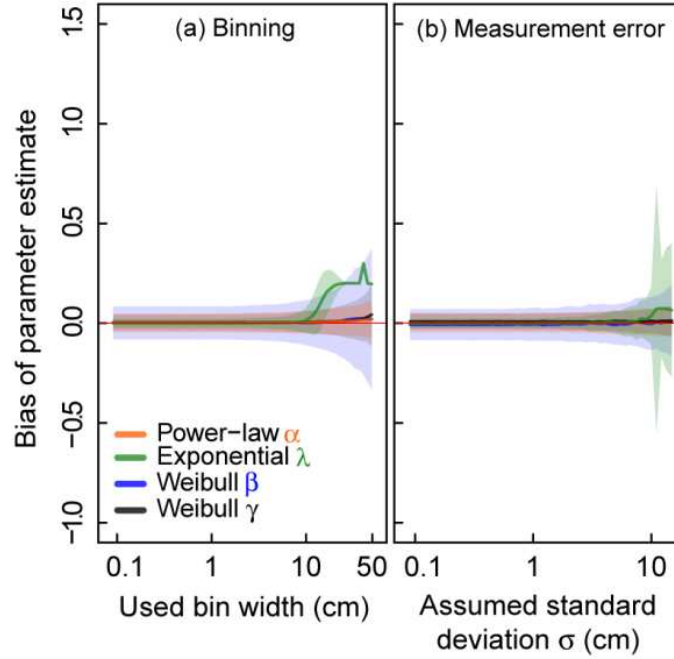


Figure 5.5: Effects of binning and random measurement errors on parameter estimation using different MLE methods. (a) MLE including binning (*multinomial MLE*) and (b) MLE accounting for measurement errors (*Gaussian MLE*). We evaluate virtual data sets of sample size $n = 500$ from a truncated power-law, a truncated negative exponential and a truncated Weibull distribution. Solid lines represent the mean estimates and shaded areas show the standard deviation (of (a) 1000 values and (b) 250 values). (a) Effect of binning on parameter estimates. Virtual data are classified into classes of certain bin width (x-axis in cm). (b) Effect of random measurement errors on parameter estimates. An error value generated from a Gaussian distribution with mean $\mu = 0$ cm and an assumed standard deviation σ (x-axis in cm) is added to each virtual data value.

For data overlaid with a measurement error, the *Gaussian MLE* provides significantly better results than the *standard MLE* (Fig. 5.5 b). The mean bias remains below 3 % of the true α -, β - and γ -parameter (Appendix A5). For a large range of measurement errors ($\sigma < 9.9$ cm), λ -estimates are within the 5 % mean bias threshold. But for increasing errors of $\sigma > 9.9$ cm, also the *Gaussian MLE* produces a higher mean bias, reaching up to 14 % of the true λ -parameter value (Appendix A5).

5.3.3 Determination of the correct frequency distribution

The identification of the underlying distribution with *MLE* including observation uncertainties (*multinomial MLE* and *Gaussian MLE*) shows a significant improvement compared to *standard MLE* (Fig. 5.6). An underlying power-law or Weibull distribution is always correctly determined (Fig. 5.6 a, c, d, f). For exponentially distributed data, the correct distribution is identified with at least 50 % probability for a large range of bin widths ($b < 27$

cm, Appendix A5). Above this threshold, *Akaike weights* favour a power-law distribution (Fig. 5.6 b). Concerning measurement errors, the exponential distribution is identified for all measurement errors ($0.1 \leq \sigma \leq 14$) in the range of our investigations (Fig. 5.6 e). An increment in sample size has considerable positive effects for both modified *MLE* methods (Appendix A6).

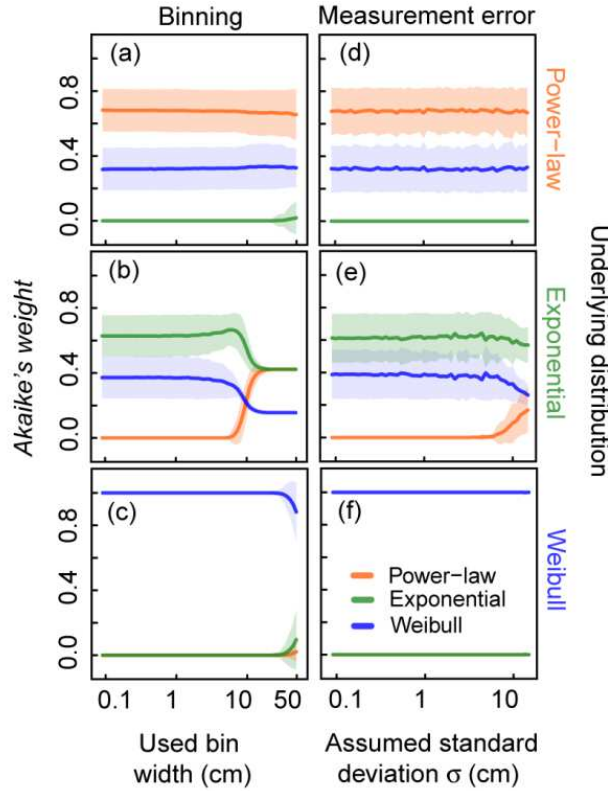


Figure 5.6: Effect of errors on *Akaike weights* for the correct determination of the underlying distribution. In each row virtual data sets of sample size $n = 500$ which originate from the three truncated distributions (power-law, negative exponential and Weibull distribution) are evaluated. Weights are calculated supposing these distributions (power-law, negative exponential and Weibull distribution) with (a)-(c) *multinomial MLE* and (d)-(f) *Gaussian MLE*. The highest *Akaike weight* determines the best fit of a frequency distribution to the data. (a)-(c) Effect of binning of virtual data sets with used bin width (x-axis in cm) on *Akaike weights*. (d)-(f) Effect of random measurement errors added to the virtual data sets on *Akaike weights*, whereby errors are Gaussian distributed with mean $\mu = 0$ cm and assumed standard deviation σ (x-axis in cm). Solid lines represent the mean of *Akaike weights* and shaded areas show the standard deviation (of (a)-(c) 1000 values and (d)-(f) 250 values).

5.3.4 Application: Stem size distribution of a tropical forest

We now employ the investigated fitting methods on forest inventory data, here on measured stem diameters of a tropical rainforest (207,105 observations). We apply *standard*, *multinomial* and *Gaussian MLE* to the field data supposing a truncated power-law, a negative exponential and a Weibull distribution (Table 5.1). For comparison, we also estimated (using algorithms implemented in R-2.10.0) the parameters of (a) a truncated power-law distribution with linear regression on log-log axes, (b) a truncated negative exponential distribution with linear regression on a logarithmic y-axis of stem frequencies, and (c) a truncated Weibull distribution with nonlinear regression on log-log axes.

MLE parameter estimates do not differ significantly according to the different methods used (whether observation uncertainty was accounted for or not). For each supposed distribution according to the different methods (in brackets from left to right *standard MLE*, *multinomial MLE*, *Gaussian MLE*) estimates are $\underline{\alpha} = (1.92; 1.92; 1.93)$, $\underline{\lambda} = (0.247; 0.247; 0.247)$, $\underline{\beta} = (2.48; 2.49; 2.51)$ and $\underline{\gamma} = (0.285; 0.284; 0.283)$. These results fit well to our findings where we showed that for a width of $b = 0.1$ cm no significant difference in the mean estimates using standard or *multinomial MLE* is expected. Additionally, we showed that for small measurement errors of $\sigma = 0.1$ cm only small biases are expected using *standard MLE* compared to *Gaussian MLE*. The stem diameter of 80 % of the BCI data is less than or equal to 5.8 cm and thus, a small estimated measurement error of less than $\sigma \approx 0.1$ (with 95 % probability) is expected.

Results of regression methods differ significantly from those of the *MLE* methods (Appendix A6). Regression provides the following estimates of parameters compared to *standard MLE* (in brackets from left to right regression, *standard MLE*): $\underline{\alpha} = (2.14; 1.92)$, $\underline{\lambda} = (0.037; 0.247)$, $\underline{\beta} = (1.08; 2.48)$ and $\underline{\gamma} = (0.352; 0.285)$. Additionally, linear regression favours the truncated power-law distribution and *standard MLE* the truncated Weibull distribution. The residual standard error or determination coefficient r^2 used within regression does not always reliably determine the underlying distribution (Franziska Taubert, unpublished data).

5.4 Discussion

Maximum likelihood estimation (*MLE*) has been recommended for fitting size distributions by several authors (Edwards 2008; White *et al.* 2008; Clauset *et al.* 2009). In this study, we investigated the effects of different types of uncertainties on the estimation

procedure using *MLE*. We focused on the bias of parameter estimates and on the reliability to determine the underlying frequency distribution using *Akaike weights*. Our results show that using *MLE* without correcting uncertainties does not solve the main problems arising when estimating parameters of strongly skewed size distributions. This method is appropriate as long as uncertainties in the observations do not have a great influence. However, even when the underlying ecological process can be described well by a strongly skewed frequency distribution, random errors and rounding in the data acquisition process can lead to biased parameter estimates and falsely selected distributions. In these cases, we recommend the use of modified *MLE* methods for including observation uncertainty.

A problem that arises in practical applications that we have not addressed in this study is the estimation of the truncation parameters $[x_{\min}; x_{\max}]$. In particular, it is known that the definition of x_{\min} influences the fitting results (Clauset *et al.* 2009). Also the upper truncation parameter x_{\max} has an effect on the fitting. One could estimate both parameters in such a way that the interval $[x_{\min}; x_{\max}]$ covers only a section of the entire empirical size distribution. Fitting only such a section would lead to high biases in the estimation of parameters and in the selection of the best fitting frequency distribution. Fitting segments of size distributions caused either by estimating a narrow interval $[x_{\min}; x_{\max}]$ or by assuming a composite function to describe the size distribution, are not further discussed here. Related investigations concerning binning can be found elsewhere (Virkar & Clauset 2012).

In our investigations we used *Akaike weights*, based on the *Akaike Information Criteria (AIC)*, to select the best fitting frequency distribution from our three assumed skewed, decaying distributions. The *AIC* may cause some difficulties, for example, when data values are not independent of each other (Kieseppä 1997). Additionally, the *AIC* does not consider sample size in its calculation. Nevertheless, the *AIC* is an often used criterion for model selection in ecological studies. Please notice also, the *AIC* is only a criterion for model selection, but does not ensure that the best fitting frequency distribution is in fact the true underlying one. For this purpose, hypothesis tests are recommended.

Regarding the types of uncertainties and their strength (i.e. bin width b and measurement error σ) we assume them to be known in our study. However, in practice this may often not be the case. Random measurement errors can be detected in the field by repeated measurements (Chave *et al.* 2004; Condit 1998). However, errors may also be hidden in such repeated measurements, similar or different to those in the first observations. For example, similar errors might occur due to irregularities in the observation object. In general, it cannot be guaranteed that all possible sources of random errors are captured correctly or that each can be assumed to be Gaussian distributed.

In practice, both systematic and stochastic observation uncertainties will often appear together, also with differing relative importance. For example, field measurements of tree diameter with high measurement precision may be more affected by stochastic measurement errors. On the other hand, if field observations are measured using pre-defined bins with a width of, for example, 5 cm or 10 cm, the effects of binning are expected to be greater than those of random measurement errors. If equally great effects of these two observation uncertainties are present, it might be necessary to consider both. Therefore, another modified *MLE* method should be created to include both uncertainties. Further investigations are needed to determine whether such an *MLE* method would show an advantage over those *MLEs* that correct only one type of observation uncertainty.

Nevertheless, these limitations do not alter our general findings, namely, that uncertainties in the observation process lead to serious difficulties in the correct determination of the underlying frequency distribution and in the estimation of its parameters. This makes comparing inferred parameters across data sets or with ecological theory difficult. Modified *MLE* methods that are discussed in this paper lead to significantly better parameter estimates and more reliable identifications of frequency distributions underlying size distributions.

Discussion and future perspectives

In the following, we discuss the presented results in this thesis. We address three main aspects: (i) developed approaches and performed analyses, (ii) the main results of the thesis with respect to our main research objectives and (iii) future perspectives and research questions.

6.1 The approach developed in this thesis

6.1.1 The developed grassland model Grassmind

Based on the review of grassland models, we developed a new individual-based and process-oriented grassland model for temperate herbaceous communities. Several simplified components of our model allow extensions, which could in turn suffer from increased complexity.

One main concept of the developed individual-based grassland model Grassmind is the assumption that competition acts spatially implicit on a patch. This approach is extensively applied in forest modelling, but represents a novelty for grasslands. In forest models, for which radiation is the predominant resource to compete for, the patch size corresponds to the projected crown area of the largest tree (Shugart 1998; Köhler & Huth 2004). In contrast, temperate grasslands are prioritized more on belowground resource competition like for soil water and soil nutrients rather than aboveground for light (Ellenberg & Leuschner 2010; Coffin & Urban 1993). The area of the influence aboveground can differ from that belowground. By choosing too small patch sizes, light competition may be modelled correctly, but overestimate belowground resource competition. In contrast, too large patch sizes would overestimate competition for light resources in grasslands. Integrating the different spatial resolutions for above- and belowground competition in the current Grassmind model version is possible by weighting the cumulative community leaf area index in the light climate calculations in Eq. (3.14) of the model description in chapter 3. In the current version of the grassland model Grassmind, we do so by using a weighting factor of 1/9, which can be

interpreted as subdividing a 1 m x 1 m patch into nine smaller sub-patches of homogenous leaf area distribution, only affecting aboveground light competition.

Another characteristic of our new model is the inclusion of competition for light, soil water and soil nutrients on the individual-level and for space on the community-level. For each individual, reduction factor for light, water and nitrogen could be calculated as the ratio between actual uptake and potential demands. These individual-based reduction factors in combination with the size structure of the community can be used to estimate the relative strength of intra- and interspecific competition for light, water and nitrogen. For example, in a two-species-mixture, one species consisting of many seedlings, which shows low reduction factors (that means, strong reduction of potential photosynthesis), can be expected to grow in biomass less than a monoculture. This would indicate suppression by a dominating species, if the second species consists of a higher fraction of mature individuals with high reduction factors (that means, less reduction of potential photosynthesis). In this situation, individuals of the second species in turn, will have a higher biomass growth than a monoculture. In this case, intraspecific interactions are more intense than interspecific ones (Kinzig *et al.* 2002). However, the above-mentioned example is time dependent. The strength of intra- and interspecific interactions can change within time, thus resulting in different shapes of the diversity-productivity relationships.

We built our model as simple as possible in relation to our research questions. Nevertheless, we believe that some simplified model parts can be extended. One potential extension includes the relationship between the height and width of an individual. We use in our grassland model a simple ratio between height and width remaining constant over time. Instead, height allometry of herbaceous species can be described using a power-law, for which plant height scale with stem diameter to the power of 1.53 (Niklas 1995). Another example comprises the allometric relationship between aboveground shoot biomass and belowground root biomass, which we simplified by using only a ratio (*shoot-root ratio*). However, using an allometric relation, with an exponent different from one, includes dynamic changes in allocation rates according to the individual's growth. In addition, environmental conditions could also cause changes in allocation patterns (Müller *et al.* 2000; Reich *et al.* 2003) or other species traits (Schippers & Olf 2000). Increased allocation of net productivity to the belowground root system can be favoured in times of drought or low nutrient availability to ensure sufficient growth (Müller *et al.* 2000; Reich *et al.* 2003). This aligns with aspects of adaptive plant strategies, for which currently no general rules are available. Another aspect comprises simplified assumption concerning recruitment of new individuals. In our current model version of Grassmind, we do not distinguish between generative and vegetative reproduction. Further, dispersal of seeds to neighbouring patches is not included. We currently consider new individuals to germinate on the same patch as their mother plant. Additionally, we do not include a persistent seed bank. Seeds, which do not germinate are assumed not to

be viable to germinate ever. However, for simulation studies on a regional scale or including disturbances like wildfire, the integration of dispersal kernels as well as a persistent seed bank would be required.

Adaptive behaviour of human actions, i.e. flexible management strategies, is another interesting possibility for an extension. Currently, dates of management actions have to be planned before the start of the simulation. However, for example mowing may be planned dependent on the further processing of the harvested material. For example, mowing grasslands, which are needed for combustion, would not be planned for rainy days. Management strategies could be timed dynamically based on structural characteristics of the vegetation (e.g. ratio of green to dead leaves) or on environmental conditions (e.g. days of low precipitation probabilities).

6.1.2 Simulation studies using Grassmind

We simulated multi-species-mixtures using the developed grassland model Grassmind and defined species groups. The creation of these types is based on the parameterized grass species *Festuca pratensis*.

During the process of parameterization and calibration of *Festuca pratensis*, we had difficulties in matching all field observations with simulation results. These mismatches can be traced back either to (a) simplified modelling approaches in Grassmind or to (b) inconsistencies in the field observations. For example, field data of aboveground biomass of years 2003 and 2004 are three to four times higher than in the other years. The attempt to reach these extreme biomass values results in mismatches of other well reproduced data points, especially concerning community leaf area index. Techniques like pattern-oriented modelling or inverse parameterization tools can be helpful in such cases (Grimm & Railsback 2012, Hartig *et al.* 2011). Their use could reveal whether current modelling approaches in Grassmind have to be modified or whether field observations may include uncertainties.

The species types we defined for our simulation studies in chapter 4 are based on our selection of specific traits concerning different strategies in acquiring resources and compete for them with other individuals. For example, we only changed the parameters of rooting depth, specific root length and specific leaf area, which are important for the groups to acquire soil water, nutrient and light resources. All other parameters remain constant for all functional groups based on the species *Festuca pratensis*. However, this grass species performs in field experiments of multi-species-mixtures worse than expected from their monoculture performance – denoted as *underyielding* (Marquard *et al.* 2009b). Parameterizing other

species like herbs or legumes and using them as reference type could result in different shapes and effects in the diversity-productivity relationship. Besides this aspect, no trade-offs between physiological attributes of the competing species are considered in these investigations. Nevertheless, species show in experimental observations trade-offs, for example between seed size and lifespan or between specific leaf area and lifespan (Ryser & Urbas 2000).

6.1.3 Methods for analysing stem size distributions of forests

We explored the maximum likelihood approach for estimating unknown parameters of distributions, which describe stem size distributions of natural forests. Virtually produced data of three decaying distributions, i.e. the power-law, the negative exponential and the Weibull distribution, were analysed including binning and random measurement errors.

During the analyses, we had to make some assumptions concerning characteristics of the chosen distributions. For example, we assumed that the minimum and maximum stem diameter values, i.e. x_{min} and x_{max} , are known before the analysis. However, in practice these values can only be estimated from the minimum and maximum measurement values. Further, the extent of the measurement error is also assumed to be known during the analyses. The width of stem diameter classes of binning can usually be estimated quite easily from the measurements. However, uncertainties in the measurements (here the measurement of stem diameters) can only be estimated by repeated measurements (Chave *et al.* 2004). In our analyses, we modelled measurement uncertainties by a Gaussian distribution with a mean of zero. In practice, differences in repeated measurements are often fitted by Gaussian distributions (using regression analysis or maximum likelihood estimation). Biased estimations occurring within the analyses of errors could then propagate in the analyses of stem size distributions (Chave *et al.* 2004). For example, estimating a lower standard deviation of a Gaussian distributed error from repeated measurements could lead again to biased estimates in the analysed stem size distribution (i.e. in case of applying *Gaussian MLE*).

Another issue for discussion comprises the separate consideration of the systematic and random errors. In practice, both errors can occur to different extents. For example, when a diameter class width of 20 cm is chosen, an estimated random measurement error of ± 0.1 cm is less influencing. In this case, maximum likelihood estimation considering binning in the analyses would reduce the bias in the estimates to a greater extent. However, the independence of both uncertainties cannot be excluded.

6.2 Main results

From our review, we have concluded that the already existing grassland models are only partly suitable for investigating and understanding diversity-productivity relationships in grasslands. Some modelling approaches within the existing grassland and vegetation models provide good representation of specific processes. Some of these modelling approaches have been followed within our newly developed grassland model Grassmind.

Parameterization of the grassland model Grassmind for a typical Central European grass species shows good matches with density of individuals, community coverage, maximum sward height and community leaf area index. Some discrepancies between observed and simulated aboveground biomass values in the year 2003 and 2004 are present. Further investigations have to be carried out on whether either modification in Grassmind is required or field data include measurement uncertainties.

A simulation study of 2-species-mixtures based on the parameterized species has been performed in the context of observed diversity-productivity relationships of large biodiversity experiments. The study has been carried out for four defined species types, which differ only in the main characteristics defining their competitive strength in resource acquisition and competition. Simulating the aboveground productivity for monocultures and 2-species-mixtures show in the mean no significant trend, but can reveal increases for selected 2-species-mixtures.

Regarding the analysis of stem size distributions in tropical forests using maximum likelihood estimation, we found by using virtually created field data set that the bias of the estimated parameter increases more than linear with increasing uncertainties. That means, for binning we observed a significant bias of the estimated parameter for diameter class widths greater than 1 cm, whereby for random measurement errors bias of the estimated parameter is already present for random errors of 0.1 cm. Moreover, we noticed that both uncertainties-either binning or random errors, complicate the detection of the true underlying distribution using *Akaike weights* and lead towards the detecting a wrong distribution. By including such uncertainties in the maximum likelihood method, we can show that negative effects can be reduced to a large extent for both – parameter estimation and detection of the underlying distribution. An exemplarily application of the developed and examined methods to field measurements of a 50 ha Panamanian forest on Barro Colorado Island underpin our findings.

6.3 Outlook

6.3.1 Future investigations using the grassland model Grassmind

The developed model offers the possibility of important theoretical investigations. It would be important to know how a species mixture (and the species' trait mixture) influences the shape of the diversity-productivity relationships. The question raises whether negative or neutral diversity-productivity relationships are possible and which species traits, species compositions, climatic conditions, soil properties or management activities are responsible for corresponding results. Further, by applying pattern-oriented analyses, we can narrow the range of species traits, which are able to create observed diversity-productivity relationships. We can link calculated biodiversity effects (complementarity and selection using the additive partitioning method) with the structure and dynamics, observable for the whole year rather than only two measurement days per year. By this, detailed examinations on the underlying mechanisms responsible for experimentally observed findings can be carried out.

Besides such theoretical analyses using defined species types, a transfer to practice is of main relevance. As already proposed in the work of Tilman *et al.* (2006b), mixtures of perennial grass species have the potential to substitute fossil energy resources (or monocultures of annual crops). In this context models like Grassmind can be a useful tool. Within the 'Energiewende' debate, policy claims that energy demands in Germany have to be fulfilled predominantly by renewable energy sources until 2050 (BMU). This entails also challenges in the reliable and steady supply. Soil is differential across the German landscape and climate shows intra- and inter-annual fluctuations. The appropriate selection of species composition for the planted mixtures as well as management options applied for cultivation play an important role for the achievable potentials for biomass production. Using the grassland model Grassmind, the spatial and temporal potentials of biomass production by multi-species-mixtures can be explored. Possible questions would be:

- Which species should be selected for planted grassland mixtures to obtain high annual productivity at a specific site?
- Are productivity potentials of these species mixtures temporally stable concerning changing climatic conditions?
- Can we select species mixture, which even can profit from climate change?
- Which management options are best for achieving highest harvest yield?

Besides the assessment of productivity of various multi-species-mixtures, other aspects like availability of land, conflicts with food production, technics for the conversion of herbaceous biomass to energy products, cultivation and transportation costs are influencing the use of bioenergy. Ecological functions (e.g. soil formation or nutrient cycling) represent

ecosystem services, which can either (a) influence productivity of the planted grassland mixture positively later in time or (b) provide a buffer mechanism on a regional scale. Serving as a buffer can be considered, for example, either (a) spatially as part of a regional landscapes composed of different cultivations (e.g. together with wheat or rapeseed) or (b) temporally on a local scale as part of a crop rotation.

Besides selecting herbaceous species typically occurring in Central European grasslands, new substrates or different forms of cultivation systems could be included. For example, perennial energy crop like switchgrass or miscanthus become increasingly relevant in the context of biomass production for energy supply (McKendry 2002; Tilman *et al.* 2006b). Monocultures of miscanthus are in terms of productivity similar to maize and can provide up to 30 t dry matter per hectare and year, but they show also positive environmental effects as semi-natural grasslands show (low input of fertilizers and pesticides; FNR). In addition to such new plants, different forms of cultivations can possibly provide new perspectives. Using monocultures of annual or perennial crops like maize or miscanthus undersown by highly diverse mixtures of herbaceous grassland species offers new options (e.g. intercropping), which deserves further investigation. Questions rise like:

- Which energy crops perform best undersown with particular herbaceous species mixtures under given site conditions?
- Which crops and herbaceous species sown together complement or even facilitate each other?
- In which system do crops and herbs interfere physically with each other?

6.3.2 Maximum likelihood estimations of size distributions

Possible applications of *MLE* for analysing size distributions to the ecosystem structure of grasslands raise at first the question whether functional relationships of size structures as assumed for tropical forests can also be observed in grasslands. In contrast to forests, measurements in species-rich grasslands are often restricted to aggregated attributes on the population- or community-level recorded once or twice per year. For example, to estimate the aboveground biomass of the community, the entire vegetation is cutted, dried and weighted. Conversely, observations on the individual-level are difficult as a clear definition of an 'individual' for species of various growth forms can differ. Nevertheless, a few studies recorded the growth of individuals in a grass sward, for example by measures of individual

height or shoot biomass (Nagashima & Terashima 1995; Turner & Rabinowitz 1983; Marquard *et al.* 2009b).

Histograms similar to the stem size distribution of forests can be created for individual-based measurements of height, aboveground biomass or even diameter of a plant's stem in grasslands (Nagashima & Terashima 1995; Turner & Rabinowitz 1983). Factors influencing the individual growth characteristics have been tested in small-scale grassland experiments. Experiments comprise different initial sowing density, specific crowding conditions and fertilization (Nagashima & Terashima 1995; Turner & Rabinowitz 1983). These demonstrate results of significant differences in the shape of histograms. For example, height distribution shifted from bimodal shapes at sowing densities of 400 plants per m² to L-shaped distributions at sowing densities of 800 to 1200 plants per m² (Nagashima & Terashima 1995). Currently, analyses comprise only summary statistics like skewness and kurtosis of the respective histogram (Nagashima & Terashima 1995; Turner & Rabinowitz 1983). Regression analyses or maximum likelihood estimation, as they are applied to stem size distributions of forests, are not yet common practice for grasslands. By using simulations of the grassland model Grassmind, we can have easily access to the height and aboveground biomass of individuals. Applying our developed methods of stem size distributions in forest to height and biomass distributions in temperate grasslands can reveal interesting findings, which could in turn also be linked to simulated diversity-productivity relationships.

Appendices

Appendix A1 List of reviewed vegetation models

Grassland Models

GEM

Hunt HW, Trlica MJ, Redente EF, Moore JC, Detling JK, Kittel TGF *et al.* Simulation model for the effects of climate change on temperate grassland ecosystems. *Ecol Model* 1991; 53:205-46.

HURLEY PASTURE MODEL

Thornley JHM, Verberne ELJ. A model of nitrogen flows in grassland. *Plant Cell Environ* 1989; 12:863-86.

Thornley JHM, Cannell MGR. Temperate Grassland Responses to Climate Change: an Analysis using the Hurley Pasture Model. *Ann Bot* 2000; 80:205-21.

Thornley JHM. Grassland dynamics: an ecosystem simulation model. *CAB International*; 1998.

LINGRA

Schapendonk AHCM, Stol W, van Kraalingen DWG, Bouman BAM. (1998) LINGRA, a sink/source model to simulate grassland productivity in Europe *Eur J Agron* 9:87-100.

PaSim

Riedo M, Grub A, Rosset M, Fuhrer J. A pasture simulation model for dry matter production, and fluxes of carbon, nitrogen, water and energy. *Ecol Model* 1998; 105:141-83.

Riedo M, Gyalistras D, Fuhrer J. Net primary production and carbon stocks in differently

managed grasslands: simulation of site-specific sensitivity to an increase in atmospheric CO₂ and to climate change. *Ecol Model* 2000; 134:207-27.

GREENLAB

Yan HP, Kang MZ, de Reffye P, Dingkuhn M. A Dynamic, Architectural Plant Model Simulating Resource-dependent Growth. *Ann Bot* 2004; 93:591-602.

Other Grassland Models

Acevedo MF, Raventós J. Growth dynamics of three tropical savanna grass species: an individual-module model. *Ecol Model* 2002; 154:45-60.

Coffin DP, Lauenroth WK. A gap dynamics simulation model of succession in a semiarid grassland. *Ecol Model* 1990; 49:229-66.

Coughenour MB, McNaughton SJ, Wallace LL. Modelling primary production of perennial graminoids – uniting physiological processes and morphometric traits. *Ecol Model* 1984; 23:101-34.

Detling JK, Parton WJ, Hunt HW. A Simulation Model of *Bouteloua gracilis* Biomass Dynamics on the North American Shortgrass Prairie. *Oecologia* 1979; 38:167-91.

Duru M, Adam M, Cruz P, Martin G, Ansquer P, Ducourtieux C et al. Modelling above-ground herbage mass for a wide range of grassland community types. *Ecol Model* 2009; 220:209-25.

Reuss JO, Innis GS. A Grassland Nitrogen Simulation Model. *Ecology* 1977; 58:379-88.

Schippers P, Kropff MJ. Competition for Light and Nitrogen among Grassland Species: A Simulation Analysis. *Functional Ecol* 2001; 15:155-64.

Siehoff S, Lennartz G, Heilburg IC, Roß-Nickoll M, Ratte HT, Preuss TG. Process-based modeling of grassland dynamics built on ecological indicator values for land use. *Ecol Model* 2011; 222:3854-68.

Global Vegetation Models

SEIB-DGVM

Sato H, Itoh A, Kohyama T. SEIB-DGVM: A new Dynamic Global Vegetation Model using a

spatially explicit individual-based approach. *Ecol Model* 2007; 200:279-307.

LPJ-DGVM

Sitch S, Smith B, Prentice C, Arneth A, Bondeau A, Cramer W et al. Evaluation of ecosystem dynamics, plant geography and terrestrial carbon cycling in the LPJ dynamic global vegetation model. *Glob Change Biol* 2003; 9:161-85.

LPJ-GUESS

Smith B, Prentice IC, Sykes MT. Representation of vegetation dynamics in the modelling of terrestrial ecosystems: comparing two contrasting approaches within European climate space. *Glob Ecol Biogeogr* 2001; 10:621–37.

Forest models

FOREST-BGC

Running SW, Gower ST. FOREST-BGC, A general model of forest ecosystem processes for regional applications. II. Dynamic carbon allocation and nitrogen budgets. *Tree Physiol* 1991; 9:147-60.

FORMIND

Köhler P, Huth A. Simulating growth dynamics in a south-east Asian rainforest threatened by recruitment shortage and tree harvesting. *Clim Change* 2004; 67:95–117.

SILVA

Pretzsch H, Biber P, Dursky J. The single tree-based stand simulator SILVA: construction, application and evaluation. *For Ecol Manage* 2002; 162:3-21.

Appendix A2 Details for the parameterization of *Festuca pratensis*

Table A7.1: List of geometrical parameters found in literature and estimated for the species *Festuca pratensis*. Given is the description of the parameter, its denotation in the grassland model Grassmind, its unit and the value found in literature or estimated (for the latter the reference is at last).

Parameter	Unit	Description	Value	Reference
h_{max}	cm	maximum height of an individual	120	Estimated
hw	cm/cm	height:width ratio of an individual's encasing cylinder	2	Estimated
f_s	g (DM)/cm ³	shoot correction factor	0.002	Estimated
f_o	-	overlapping factor	1	Estimated
SLA	cm ² /g (DM)	specific leaf area	160	Heisse <i>et al.</i> 2007
SRL	cm/g (DM)	specific root length	38000	Elberse <i>et al.</i> 1993
r_1, r_2	-	parameters of the rooting depth power-law relationship	5.48/0.301	Estimated (Schenk & Jackson 2002)
s_1	g (DM)/g (DM)	shoot:root ratio of biomass parts	2.2	Heisse <i>et al.</i> 2007

Table A7.2: List of process parameters found in literature and estimated for the species *Festuca pratensis*. Given is the description of the parameter, its denotation in the grassland model Grassmind, its unit and the value found in literature or estimated (for the latter the reference is at last).

Process	Parameter	Unit	Description	Value	Reference
Recruitment and emergence of new seedlings	B_{seed}	g (DM)	seed biomass	0.0018	Elberse <i>et al.</i> 1993
	t_{em}	days	time until emergence of a seedling since sowing	14	Heisse <i>et al.</i> 2007
	$germ_{\%}$	-	germination rate of seeds	0.3	Roscher <i>et al.</i> 2004
	age_{rep}	years	age at which recruitment starts	0.055	Estimated
	h_{min}	cm	minimum height of a seedling at establishment	3	Estimated
Mortality	t_{sow}	Date	initial sowing date	16.5.2002	Estimated (Roscher <i>et al.</i> 2004)
	LLS	days	leaf life span (start of yellowing leaves)	42	Ryser & Urbas 2000
	RLS	days	root life span	709	Used from <i>Poa pratensis</i> (Tjoelker <i>et al.</i> 2005)
	$life$	years	life span of the individual	> 2	Estimated (Biolflor; Kühn <i>et al.</i> 2004)
	m_{basic}	1/year	basic mortality rate of	0.02	Estimated

	m_{seed}	1/year	mature individuals mortality rate of established seedlings	30	Estimated
Photosynthesis	p_{max}	$\mu\text{mol (CO}_2\text{)}/\text{m}^2\text{/s}$	maximum gross leaf photosynthesis	25	Estimated (Hauck <i>et al.</i> 1997)
	a	$\mu\text{mol (CO}_2\text{)}/\mu\text{mol (photons)}$	initial slope of light response curve	0.06	Hauck <i>et al.</i> 1997
	k	-	light extinction coefficient	0.4	Thornley & France 2007
	m	-	transmission coefficient	0.1	Thornley & France 2007
Competition	WUE	$\text{g (DM)}/\text{kg (H}_2\text{O)}$	water-use-efficiency coefficient	4	Estimated
	NUE	$\text{g (DM)}/\text{kg (N)}$	nitrogen-use-efficiency coefficient	350000	Estimated
	N_{min}	$\text{kg(N)}/\text{cm}^2$	minimum remaining soil nitrogen content per soil layer	10^{-8}	Estimated
	n_{fix}	yes/no	ability for symbiotic nitrogen fixation	no	Estimated
	$rhiz\%$	-	fraction of <i>NPP</i> given away to rhizobia (symbiosis)	-	Estimated
Respiration	r_m	1/day	maintenance respiration rate	0.02	Amthor 1984
	r_g	-	growth respiration factor	0.25	Amthor 1984
Growth	$alloc_{shoot}$	-	allocation rate of <i>NPP</i> to shoot growth	0.54	Estimated

Additional simulation graphics

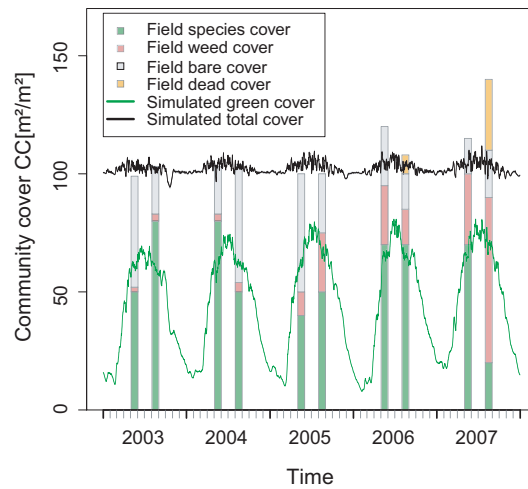


Figure A7.1: Comparison of observed and simulated community coverage. Visually estimated field data on cover are available for the respective species *Festuca pratensis* (green), weeds (red), bare ground (grey) and dead material (orange). The green line denotes the mean simulated community cover of green leaves of *Festuca pratensis* and the black line represents the mean total community cover (green and yellowed leaves) of the grass species *Festuca pratensis* for 100 simulation runs. Shadows behind the displayed lines represent the standard deviation of 100 simulation runs.

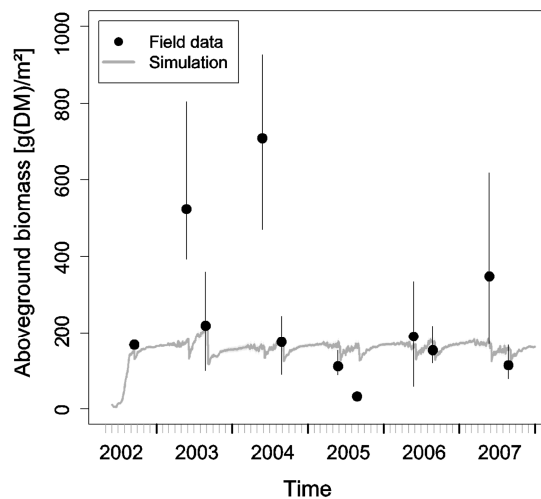


Figure A7.2: Comparison of observed and simulated aboveground biomass. Field data on aboveground biomass is represented as black points. Repeated field measurements for each field data point are available for the respective species *Festuca pratensis*. Vertical black lines denote the range between the minimum and maximum value of the repeated field measurements. The green line denotes the mean simulated aboveground biomass (green and yellowed leaves) of *Festuca pratensis* and the shadow behind the displayed line represents the standard deviation of 100 simulation runs.

Additional information on the site conditions used for the simulation

Field observations

In the experimental fields different plots were established. Besides others, we use published data of (a) small establishment plots (3.5 x 3.5 m) and (b) larger monoculture plots (20 x 20 m). On the small establishment plots monocultures were sown between the 11th and 16th of May 2002 and observed for the first year of emergence only (Heisse *et al.* 2007). From the recorded observation data we use the monthly estimated coverage and the tiller numbers (Heisse *et al.* 2007). Seeds on the larger monoculture plots were also sown between the 11th and 16th of May 2002 and observed from autumn 2002 on for six consecutive years (Weigelt *et al.* 2010). Measurements were done twice a year. Dates are only given in months since the 1st May of the year of sowing. We assume them to be on the 25th of each month documented as in some publication observations are stated as done in late May or late August (Weigelt *et al.* 2010, Roscher *et al.* 2004, Heisse *et al.* 2007). Observations comprise the above-ground biomass, community leaf area index, maximum height and community coverage (Weigelt *et al.* 2010). For both experimental plots, the small and large one, measurements are given for 1 m² resolution. Only within the large monoculture plots repeated measurements for biomass and height were done. Biomass was measured in three to four sub-samples of an area of 0.1 m² randomly selected in the sub-area of 15 m x 5 m inside the large plot (Weigelt *et al.* 2010). Maximum sward height was measured in 2003 for 30 individuals along a transect of 5 m (with 10 cm distance in-between), in 2004 three times within a selected sub-area and from 2005 on at ten spots along a transect of 10 m (with 1 m distance between each) within the core sub-area of 15 m x 5 m inside the large plot (Weigelt *et al.* 2010). Individuals were stretched in year 2003 before measurement, but not in year 2004. From 2005 on, the appearance of the highest leaf was measured (Weigelt *et al.* 2010). Measurement areas or transects differ between the measurement years 2003, 2004 and 2005-2008. For all other observations no replications are available.

Soil properties

The experimental plots of the Jena Experiment are grouped into four blocks, whereby within each block soil conditions are assumed to be homogeneous. The first block is located beside the river Saale and the fourth block is furthest from the river. The blocks are arranged in parallel to the river. From Steinbeiss *et al.* (2008) information on the soil texture in the upper horizon (down to 30 cm soil) is available. In general, soil is classified as a *Eutric Fluvisol* (Oelmann *et al.* 2007). In particular, soil types range from sandy soil near the soil river to silty soil furthest from the river Saale (Steinbeiss *et al.* 2008).

The large monoculture plot of *Festuca pratensis*, which we use for parameterization, is located in the second block. We estimated the soil texture in block two by assuming a linear increase or decrease of the corresponding sand, silt, and clay contents from locations near the river to those furthest from the river. From soil texture, the other soil parameters can be derived (Maidment 1993). Table A7.3 shows the soil parameters in the upper horizon (0 – 30 cm) used in the simulation and derived from field measurements (Steinbeiss *et al.* 2008).

Table A7.3: Summary of the important soil parameters used for the parameterization of the soil type in the model Candy (Franko *et al.* 1995). Given is a description of the parameter, its unit, and the estimated values for the soil of the Jena Experiment found in literature and the comparison to the corresponding values of the soil type from Bad Lauchstädt used for parameterization.

Description	Unit	Estimated value in Jena Experiment	Value in Candy
Sand content	%	29	approx. 25 – 40
Silt content	%	52.33	approx. 30 – 65
Clay content	%	18.67	approx. 10 – 30
Bulk density	g/cm ³	1.32	1.37
Particle density	g/cm ³	2.56	2.56
Field capacity	V%	33	29.9
Permanent wilting point	V%	13.3	17.7
Saturated soil conductivity	mm/d	163.2	260

Details on the inverse parameterization steps

We estimate the geometrical parameter (p_{\max}) by reproducing the leaf photosynthetic rate of a single individual under various light conditions (comparison of Fig. A7.3 (b) with Fig. A7.3 (a) of Hauck *et al.* 1997). In contrast to Hauck *et al.* (1997), which fitted an exponential function $P_{Leaf} = p_{\max} - k \cdot r^I$ to the measured leaf photosynthetic rates P_{Leaf} [$\mu\text{mol}/\text{m}^2/\text{s}$], we reproduced their functional curve using the functional approach of Thornley & Johnson (1990) of $P_{Leaf} = (\alpha \cdot p_{\max} \cdot I) / (\alpha \cdot I + p_{\max})$ with I as the photon flux density PPF in [$\mu\text{mol}/\text{m}^2/\text{s}$], p_{\max} the maximum photosynthetic rate [$\mu\text{mol}/\text{m}^2/\text{s}$], α the initial slope of the light response curve [$\mu\text{mol}/\mu\text{mol}$], k and r specific parameters.

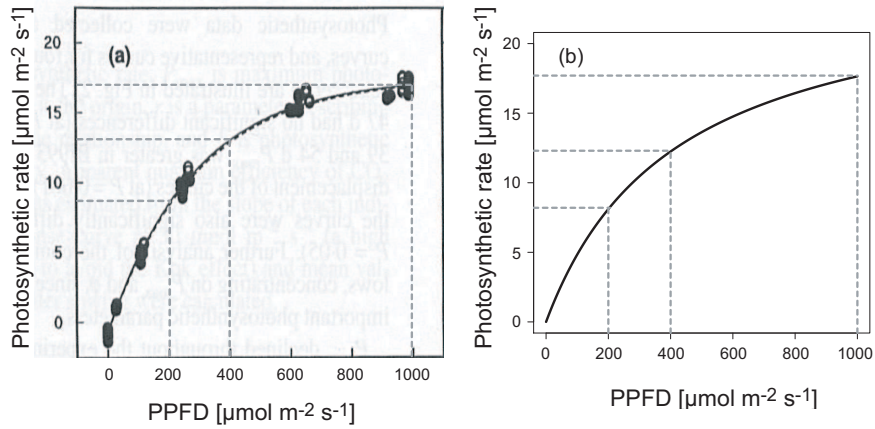


Figure A7.3: Curves of leaf photosynthetic rate for different conditions of photosynthetic photon flux density PPFD. (a) Figure copied and modified from Hauck *et al.* (1997). Hauck *et al.* (1997) measured rates at different PPFDs on leaves of the grass species *Festuca pratensis* (open circles: wild-type *Rossa*; closed circles: stay-green mutant *Bf993*). Their measurements are fitted to an exponential function dependent on PPFD (Hauck *et al.* 1997). Grey dotted vertical and horizontal lines should help to compare the results of Hauck *et al.* (1997) with (b) our fit of the functional approach for leaf photosynthetic rate of Thornley & Johnson (1990).

Appendix A3 Local sensitivity analyses

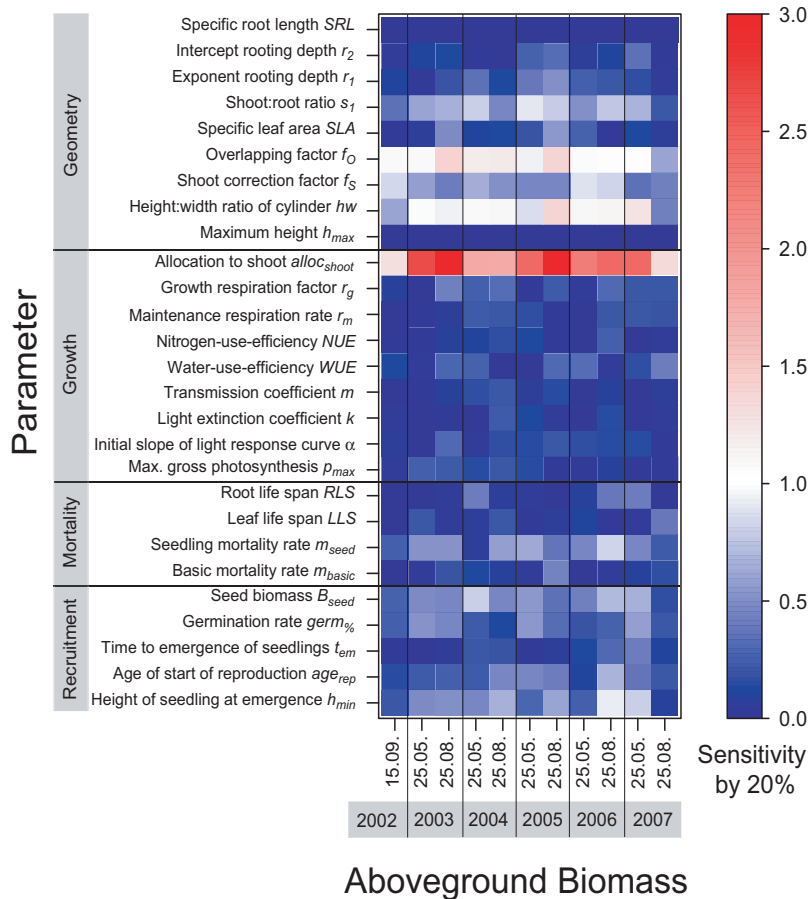


Figure A7.4: Local sensitivity analysis for the response variable *aboveground biomass* of the specific measurement dates of the Jena biodiversity experiment. Different parameters categorized into geometry, growth, mortality and recruitment are one at a time varied by $\pm 20\%$. From the resulting response of aboveground biomass at a specific date, a sensitivity index is calculated. This index ranges between 0 and 3. A value of 1 indicates that an increase of a parameter by 20 % results in a similar increase of aboveground biomass by 20 %. Those indices smaller than one indicate a smaller change and those higher than one a greater increase. This means, a value of 0.5 indicates that an increase of a parameter by 20 % only results in an increase of aboveground biomass by 10 %. In contrast, a value of 2 indicates that an increase of a parameter by 20 % results in a higher increase of aboveground biomass by 40 %. Here, aboveground biomass is mostly sensitive to geometrical parameters and a growth parameter, i.e. the fraction of net productivity allocated to the growth of aboveground shoot biomass $alloc_{shoot}$.

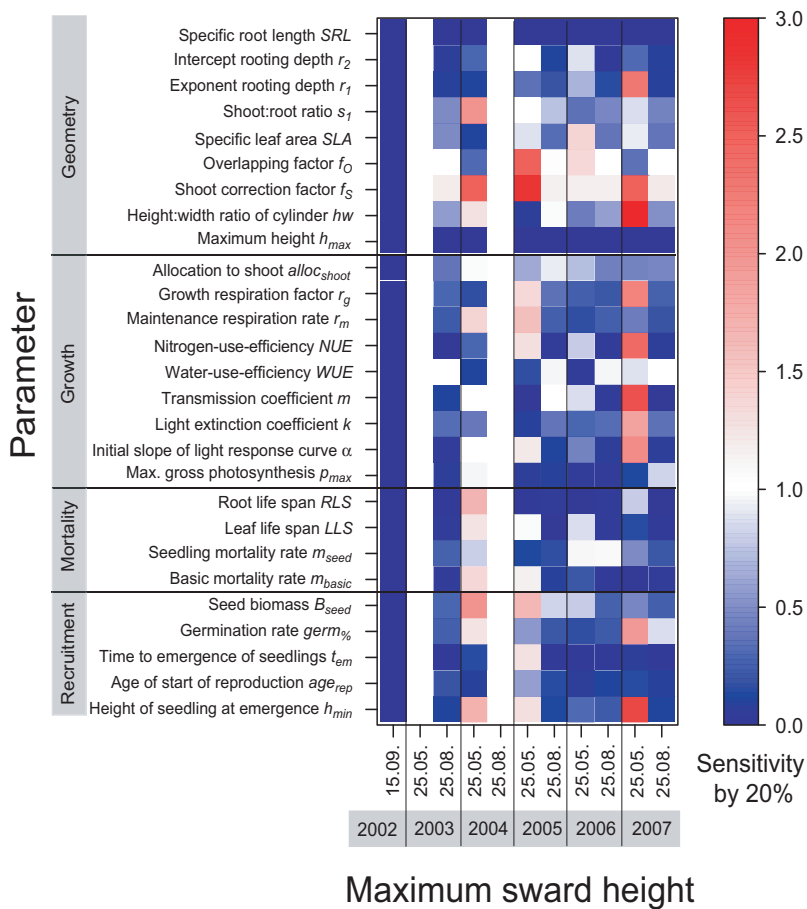


Figure A7.5: Local sensitivity analysis for the response variable *maximum sward height* of the specific measurement dates of the Jena biodiversity experiment. Different parameters categorized into geometry, growth, mortality and recruitment are one at a time varied by $\pm 20\%$. From the resulting response of maximum height at a specific date, a sensitivity index is calculated. This index ranges between 0 and 3. A value of 1 indicates that an increase of a parameter by 20 % results in a similar increase of maximum height by 20 %. Those indices smaller than one indicate a smaller change and those higher than one a greater increase. This means, a value of 0.5 indicates that an increase of a parameter by 20 % only results in an increase of maximum height by 10 %. In contrast, a value of 2 indicates that an increase of a parameter by 20 % results in a higher increase of maximum sward height by 40 %. Here, maximum sward height can be sensitive to most of the parameters. However, only the 25th of May for the years 2004, 2005 and 2007 seems to be sensitive to the parameters.

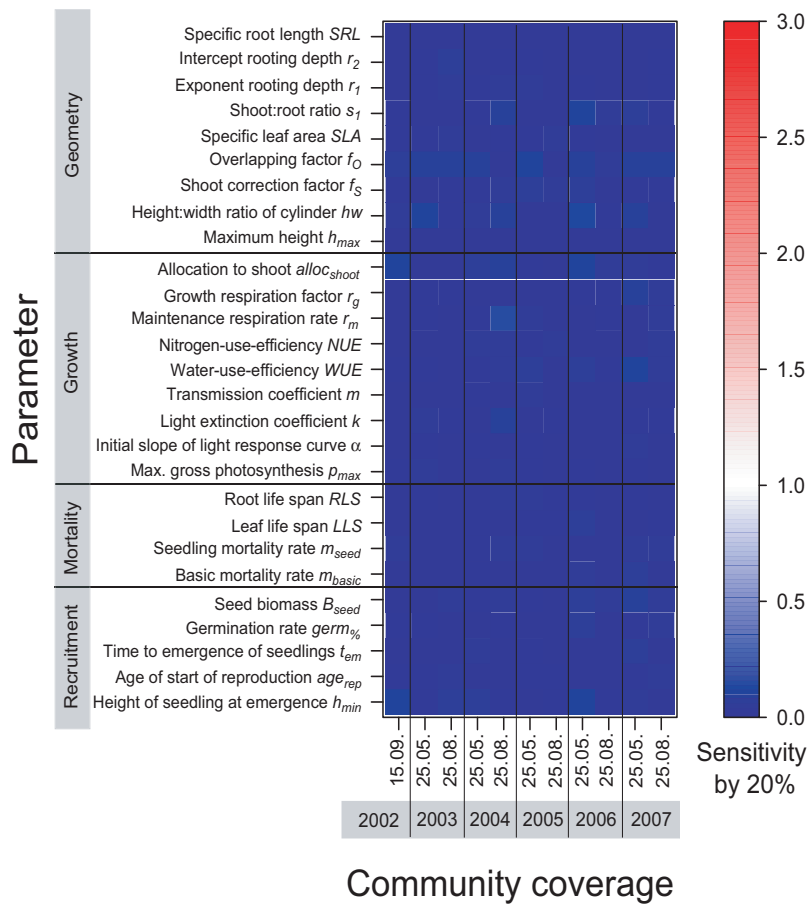


Figure A7.6: Local sensitivity analysis for the response variable *community coverage* of the specific measurement dates of the Jena biodiversity experiment. Different parameters categorized into geometry, growth, mortality and recruitment are one at a time varied by $\pm 20\%$. From the resulting response of community cover at a specific date, a sensitivity index is calculated. This index ranges between 0 and 3. A value of 1 indicates that an increase of a parameter by 20 % results in a similar increase of community coverage by 20 %. Those indices smaller than one indicate a smaller change and those higher than one a greater increase. This means, a value of 0.5 indicates that an increase of a parameter by 20 % only results in an increase of community cover by 10 %. In contrast, a value of 2 indicates that an increase of a parameter by 20 % results in a higher increase of community cover by 40 %. Here, community cover seems to be insensitive to almost all parameters.

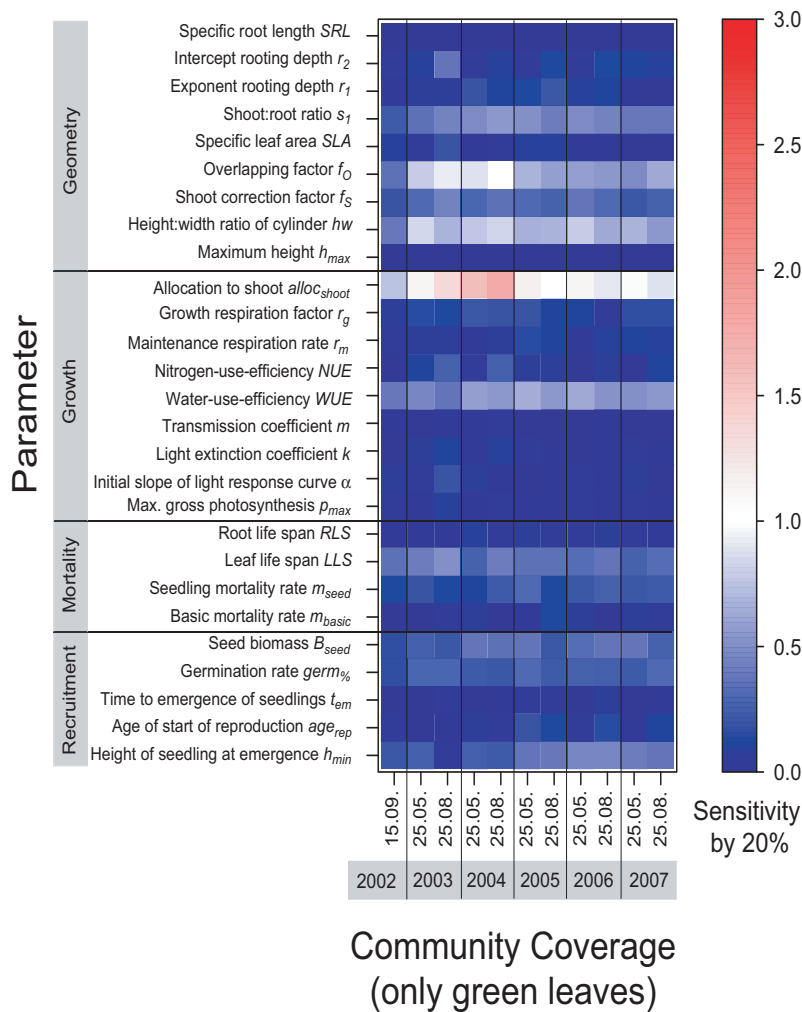


Figure A7.7: Local sensitivity analysis for the response variable *community coverage of green leaves* of the specific measurement dates of the Jena biodiversity experiment. Different parameters categorized into geometry, growth, mortality and recruitment are one at a time varied by $\pm 20\%$. From the resulting response of community coverage of green leaves at a specific date, a sensitivity index is calculated. This index ranges between 0 and 3. A value of 1 indicates that an increase of a parameter by 20 % results in a similar increase of community coverage of green leaves by 20 %. Those indices smaller than one indicate a smaller change and those higher than one a greater increase. This means, a value of 0.5 indicates that an increase of a parameter by 20 % only results in an increase of community coverage of green leaves by 10 %. In contrast, a value of 2 indicates that an increase of a parameter by 20 % results in a higher increase of community coverage of green leaves by 40 %. Here, community coverage of green leaves seems to be only sensitive to geometrical parameters and a growth parameter, i.e. the fraction of net productivity that is allocated to the growth of aboveground shoot biomass.

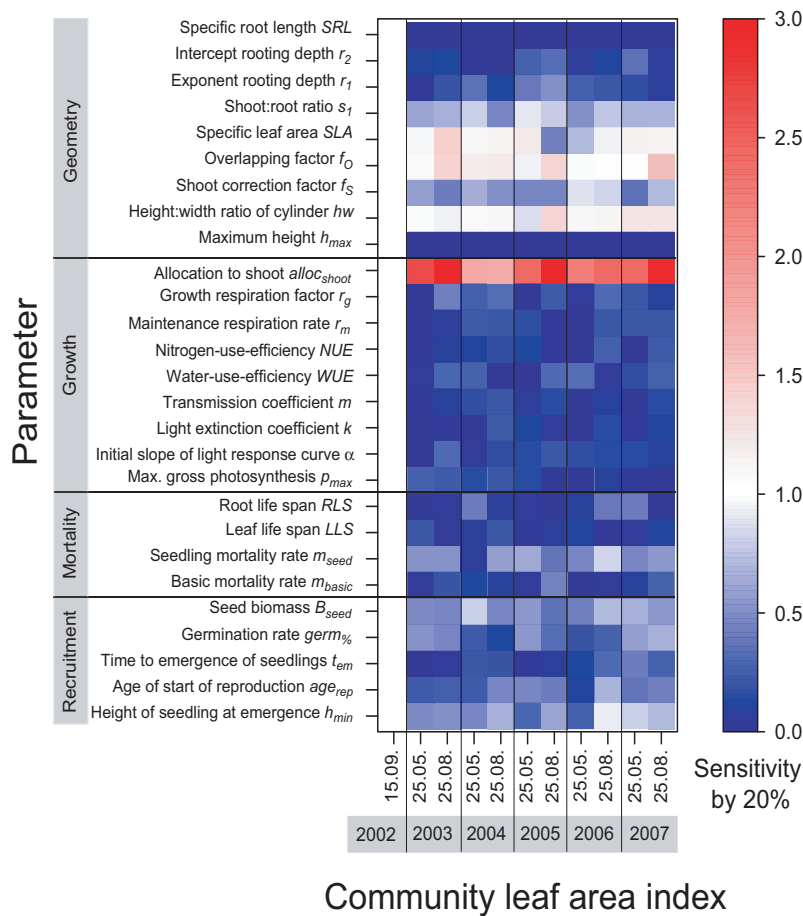


Figure A7.8: Local sensitivity analysis for the response variable *community leaf area index* of the specific measurement dates of the Jena biodiversity experiment. Different parameters categorized into geometry, growth, mortality and recruitment are one at a time varied by $\pm 20\%$. From the resulting response of community leaf area index at a specific date, a sensitivity index is calculated. This index ranges between 0 and 3. A value of 1 indicates that an increase of a parameter by 20 % results in a similar increase of community leaf area index by 20 %. Those indices smaller than one indicate a smaller change and those higher than one a greater increase. This means, a value of 0.5 indicates that an increase of a parameter by 20 % only results in an increase of community leaf area index by 10 %. In contrast, a value of 2 indicates that an increase of a parameter by 20 % results in a higher increase of community leaf area index by 40 %. Here, community leaf area index seems to be only sensitive to geometrical parameters and a growth parameter, i.e. the fraction of net productivity that is allocated to the growth of aboveground shoot biomass.

Appendix A4 Details on the evaluation procedure and formulas

Standard MLE

As perfect observation values of the sample $x = (x_1, \dots, x_n)$ are assumed, we maximize the likelihood (cf. Eq. 5.1). Thereby, for MLE that do not consider observation uncertainties the probability $p(x; \theta)$ is merely replaced by the corresponding density function $f(x; \theta)$ for each frequency distribution (Table 5.1):

$$(a) \quad \ln(L(x; \theta)) = \sum_{i=1}^n \ln((\alpha - 1) \cdot [x_{\min}^{-(\alpha-1)} - x_{\max}^{-(\alpha-1)}]^{-1} \cdot x_i^{-\alpha})$$

$$(b) \quad \ln(L(x; \theta)) = \sum_{i=1}^n \ln(\lambda \cdot [\exp(-\lambda \cdot x_{\min}) - \exp(-\lambda \cdot x_{\max})]^{-1} \cdot \exp(-\lambda \cdot x_i))$$

$$(c) \quad \ln(L(x; \theta)) = \sum_{i=1}^n \ln(\beta \cdot \gamma \cdot [\exp(-\beta \cdot x_{\min}^\gamma) - \exp(-\beta \cdot x_{\max}^\gamma)]^{-1} \cdot \exp(-\beta \cdot x_i^\gamma) \cdot x_i^{(\gamma-1)})$$

Transforming these likelihoods leads to:

$$(a) \quad \ln(L(x; \theta)) = n \cdot \ln(\alpha - 1) - n \cdot \ln(x_{\min}^{-(\alpha-1)} - x_{\max}^{-(\alpha-1)}) - \alpha \cdot \sum_{i=1}^n \ln(x_i)$$

$$(b) \quad \ln(L(x; \lambda)) = n \cdot \ln(\lambda) - n \cdot \ln(\exp(-\lambda \cdot x_{\min}) - \exp(-\lambda \cdot x_{\max})) - \lambda \cdot \sum_{i=1}^n x_i$$

$$(c) \quad \ln(L(x; \beta, \gamma)) = n \cdot \ln(\beta \cdot \gamma) - n \cdot \ln(\exp(-\beta \cdot x_{\min}^\gamma) - \exp(-\beta \cdot x_{\max}^\gamma)) + (\gamma - 1) \cdot \sum_{i=1}^n \ln(x_i) - \beta \cdot \sum_{i=1}^n x_i^\gamma$$

Multinomial MLE

Following Eq. (5.1) we also maximize the likelihood, but the probability $p(x; \theta)$ accounting for binning of data is now expressed by the multinomial distribution including the corresponding density function $f(x; \theta)$ of the assumed frequency distributions. Thereby n denotes the sample size, N_j the number of observations falling in the bin j with $j = 1, \dots, q$ and q the total number of bins. Bins are half-open intervals $[B_j; B_j + b)$ of width b (cm) and start at $B_1 = x_{\min}$ (cm). For each bin a theoretical probability, describing an observation value to fall within that bin, is calculated based on the assumed distribution with its density function $f(x; \theta)$:

$$(a) \quad \tilde{f}(x; \alpha) := \int_{B_j}^{B_j+b} f(x; \alpha) dx = \frac{B_j^{-(\alpha-1)} - (B_j + b)^{-(\alpha-1)}}{x_{\min}^{-(\alpha-1)} - x_{\max}^{-(\alpha-1)}}$$

$$(b) \quad \tilde{f}(x; \lambda) := \int_{B_j}^{B_j+b} f(x; \lambda) dx = \frac{\exp(-\lambda \cdot B_j) - \exp(-\lambda \cdot (B_j + b))}{\exp(-\lambda \cdot x_{\min}) - \exp(-\lambda \cdot x_{\max})}$$

$$(c) \quad \tilde{f}(x; \beta, \gamma) := \int_{B_j}^{B_j+b} f(x; \beta, \gamma) dx = \frac{\exp(-\beta \cdot B_j^\gamma) - \exp(-\beta \cdot (B_j + b)^\gamma)}{\exp(-\beta \cdot x_{\min}^\gamma) - \exp(-\beta \cdot x_{\max}^\gamma)}$$

For each density function of the three distributions we then get the following specific likelihood:

$$\ln(L(x; \theta)) = \ln(n!) - \sum_{j=1}^q [\ln(N_j!) + N_j \cdot \ln(\tilde{f}(x; \theta))]$$

Gaussian MLE

Following Eq. (5.1) we maximize the likelihood according to the probability $p(x; \theta)$, which is expressed by the convolution of an assumed truncated Gaussian distribution for measurement errors $\varepsilon_{meas} \sim N(\mu = 0; \sigma > 0)$ and the corresponding density function $f(x; \theta)$ of the assumed frequency distribution (Table 5.1):

$$\ln(L(x; \theta)) = \sum_{i=1}^n \ln \left(\int_{\max(x_{\min}; x_i - 3 \cdot \sigma)}^{\min(x_{\max}; x_i + 3 \cdot \sigma)} \frac{f(x; \theta)}{\sigma \cdot \operatorname{erf}\left(\frac{3}{\sqrt{2}}\right) \cdot \sqrt{2} \cdot \pi} \cdot \exp\left(-\frac{(x_i - x)^2}{2 \cdot \sigma^2}\right) dx \right),$$

where $\operatorname{erf}()$ represents the Gauss error function.

Random number generators for the considered frequency distributions

Using the inverse transformation method to generate virtual data values from an assumed frequency distribution $f(x; \theta)$, the inverse of the cumulative distribution function $F^{-1}(r; \theta)$, also known as the r -quantile, is calculated. On the basis of a randomly produced number $r \in [0; 1]$ drawn from a uniform distribution, we calculated the inverse of the cumulative distribution function in the following manner, so that it is easier to solve them afterwards according to x :

$$1 - F(x; \theta) = 1 - r \quad \rightarrow \quad [1 - F]^{-1}(1 - r; \theta) = x$$

This results in the following random number generator (or r -quantiles) for each distribution:

$$(a) \quad x_{Power-law} = \left[(1-r) \cdot (x_{\min}^{-(\alpha-1)} - x_{\max}^{-(\alpha-1)}) + x_{\max}^{-(\alpha-1)} \right]^{-1/(\alpha-1)}$$

$$(b) \quad x_{Exponential} = -\frac{1}{\lambda} \cdot \ln\left((1-r) \cdot (\exp(-\lambda \cdot x_{\min}) - \exp(-\lambda \cdot x_{\max})) + \exp(-\lambda \cdot x_{\max}) \right)$$

$$(c) \quad x_{Weibull} = \left[-\frac{1}{\beta} \cdot \ln\left((1-r) \cdot (\exp(-\beta \cdot x_{\min}^\gamma) - \exp(-\beta \cdot x_{\max}^\gamma)) + \exp(-\beta \cdot x_{\max}^\gamma) \right) \right]^{1/\gamma}$$

Appendix A5 Specific key points of the evaluation of the virtual data samples

Table A7.4: Display of specific key points evaluated during the assessment of maximum likelihood methods.

distribution $f(x; \theta)$	Specific key points	Binning		Measurement error	
		<i>Standard</i>	<i>Multinomial</i>	<i>Standard</i>	<i>Gaussian</i>
Power-law	Mean bias greater than or equal to 5% of true parameter for a bin width b or σ (cm) of:	$b > 1.5$	none	$\sigma > 0.33$	none
	Max. absolute value of mean bias (% of true parameter)	48 %	0.95 %	37 %	0.55 %
	Next best distribution having the same or a higher mean weight for a bin width b or σ (cm) of:	$b > 0.67$	none	$\sigma > 0.14$	none
Negative exponential distribution	Mean bias greater than or equal to 5% of true parameter for a bin width b or σ (cm) of:	$b > 1.6$	$b > 11$	$\sigma > 0.27$	$\sigma > 9.9$
	Max. absolute value of mean bias (% of true parameter)	92 %	59 %	84 %	14 %
	Next best distribution having the same or a higher mean weight for a bin width b or σ (cm) of:	$b > 0.91$	$b > 27$	$\sigma > 0.18$	none
Weibull distribution	Mean bias greater than or equal to 5% of true parameter for a bin width b or σ (cm) of:	$b > 1$	none	$\sigma > 0.08$	none
	Max. absolute value of mean bias (% of true parameter)	$b > 1.2$	$b > 44$	$\sigma > 0.17$	none
	Mean bias greater than or equal to 5% of true parameter for a bin width b or σ (cm) of:	100 %	4.8 %	92 %	2.8 %
	Max. absolute value of mean bias (% of true parameter)	280 %	8.6 %	110 %	2.4 %
	Next best distribution having the same or a higher mean weight for a bin width b or σ (cm) of:	none	none	$\sigma > 12.0$	none

Appendix A6 Further graphics on the Akaike weights

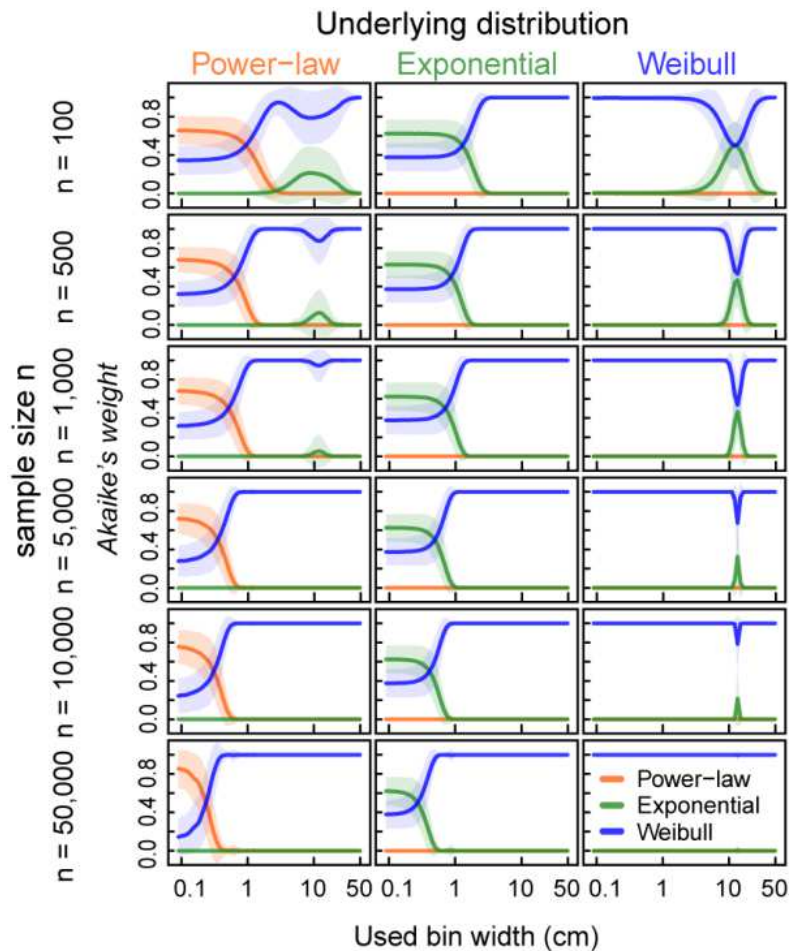


Figure A7.9: Effect of binning on Akaike weights with increasing sample size using *standard MLE*. Weights are calculated with MLE assuming perfect observations (*standard MLE*) dependent on the used bin width b (x-axis in cm). The highest Akaike weight determines the best fit of a frequency distribution to the data. The evaluated virtual data sets originate from the three truncated distributions (per column from left to right: power-law, negative exponential and Weibull distribution) which underlie them. Rows from top to bottom: Effect of binning on the identification of the correct distribution based on virtual data of sample size $n = 100$; 500; 1,000; 5,000; 10,000 and 50,000. Solid lines represent the mean Akaike weights and shaded areas show the standard deviation (of 1,000 calculated values).

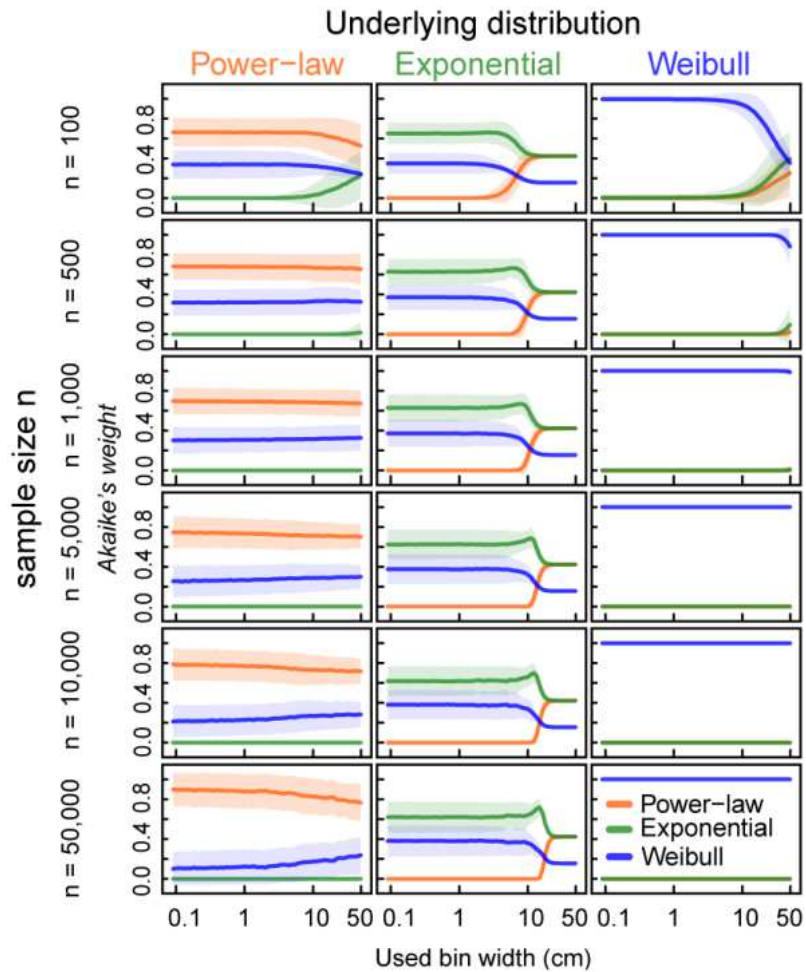


Figure A7.10: Effect of binning on Akaike weights with increasing sample size using multinomial MLE. Weights are calculated with MLE accounting for binning (multinomial MLE) dependent on the used bin width b (x-axis). The highest Akaike weight determines the best fit of a frequency distribution to the data. The evaluated virtual data sets originate from the three truncated distributions (per column from left to right: power-law, negative exponential and Weibull distribution) which underlie them. Rows from top to bottom: Effect of binning on the identification of the correct distribution based on virtual data of sample size $n = 100; 500; 1,000; 5,000; 10,000$ and $50,000$. Solid lines represent the mean Akaike weights and shaded areas show the standard deviation (of 1,000 calculated values).

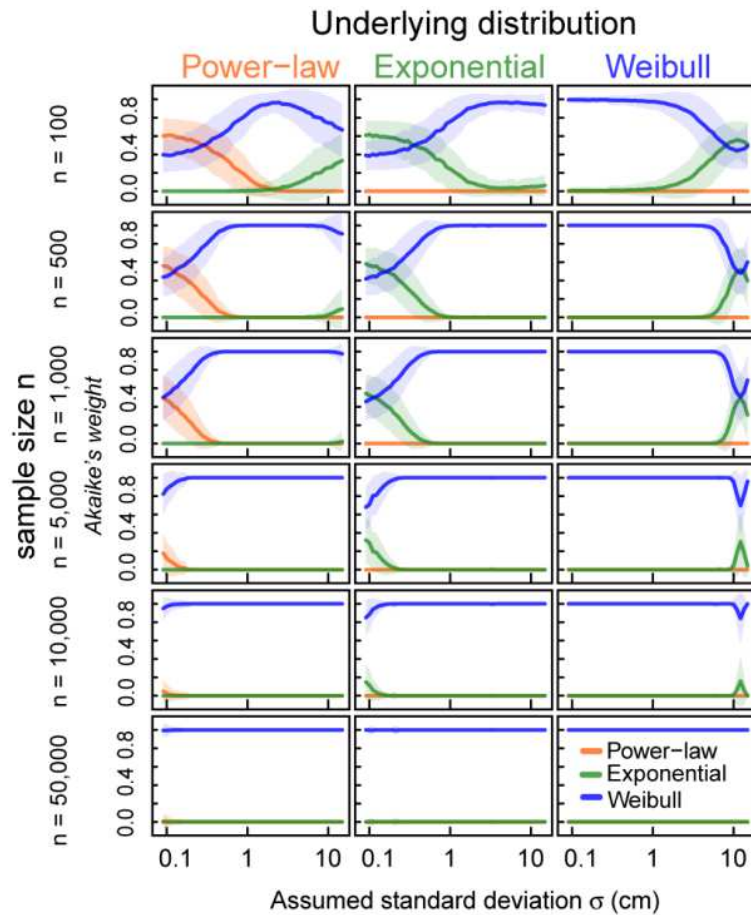


Figure A7.11: Effect of random measurement errors on *Akaike weights* with increasing sample size using *standard MLE*. Weights are calculated with MLE assuming perfect observations (*standard MLE*) dependent on the Gaussian distributed errors with mean $\mu = 0$ cm and assumed standard deviation σ (x-axis in cm). The highest *Akaike weight* determines the best fit of a frequency distribution to the data. The evaluated virtual data sets originate from the three truncated distributions (per column from left to right: power-law, negative exponential and Weibull distribution) which underlie them. Rows from top to bottom: Effect of measurement errors on the identification of the correct distribution based on virtual data of sample size $n = 100$; 500; 1,000; 5,000; 10,000 and 50,000. Solid lines represent the mean *Akaike weights* and shaded areas show the standard deviation (of 1,000 calculated values).

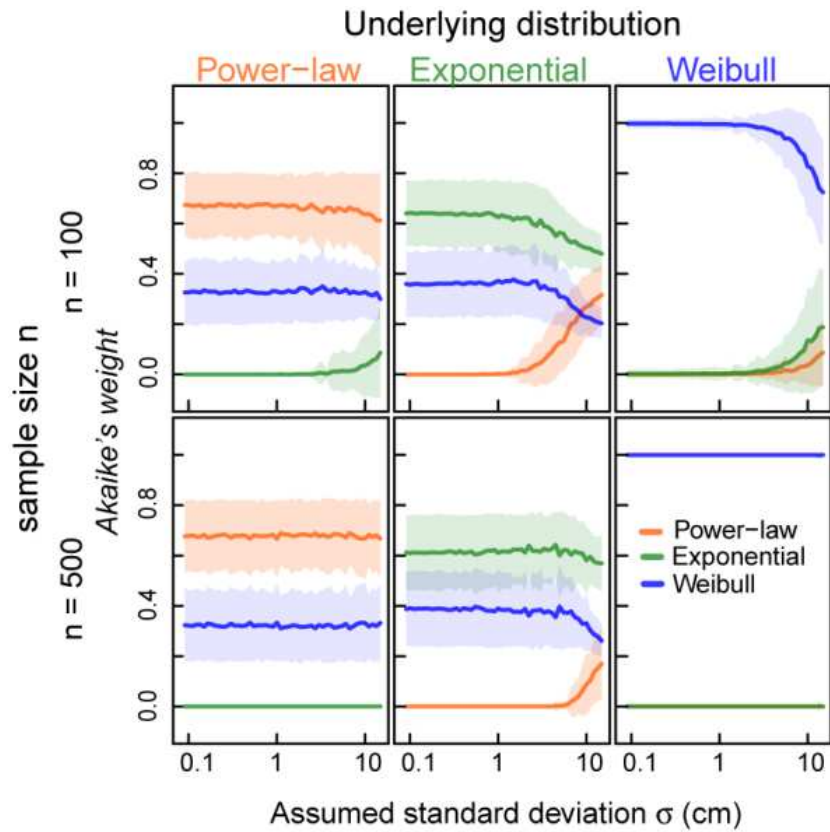


Figure A7.12: Effect of random measurement errors on *Akaike weights* with increasing sample size using *Gaussian MLE*. Weights are calculated with MLE assuming measurement errors (*Gaussian MLE*) dependent on the Gaussian distributed errors with mean $\mu = 0$ cm and assumed standard deviation σ (x-axis in cm). The highest *Akaike weight* determines the best fit of a frequency distribution to the data. The evaluated virtual data sets originate from the three truncated distributions (per column from left to right: power-law, negative exponential and Weibull distribution) which underlie them. Top: Effect of measurement errors on the identification of the correct distribution based on virtual data of sample size $n = 100$. Bottom: Effect of measurement errors on the identification of the correct distribution based on virtual data of sample size $n = 500$. Solid lines represent the mean *Akaike weights* and shaded areas show the standard deviation (of 250 calculated values).

Barro Colorado Island 2000

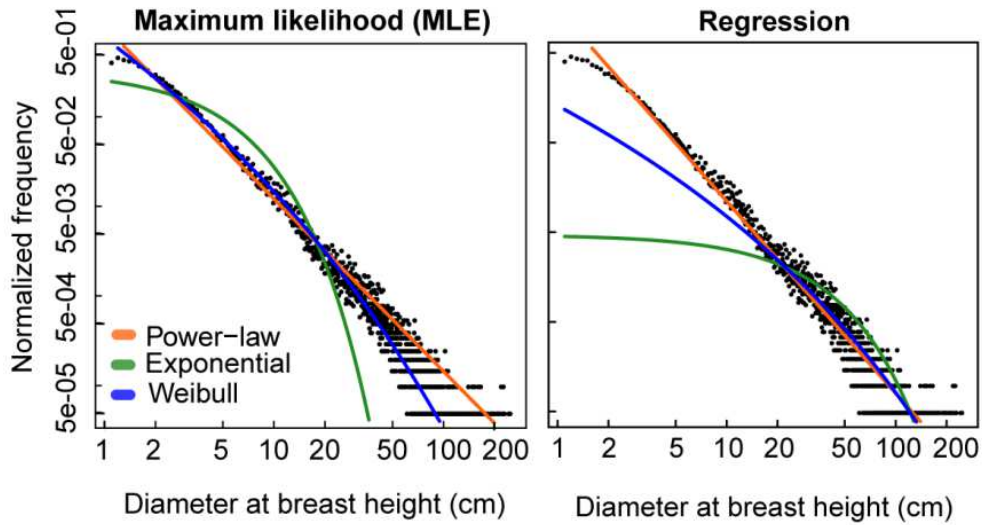


Figure A7.13: Log-log plots of the fits using regression (right) and *Gaussian MLE* (left). Data values (inventory data from Barro Colorado Island) of measured stem diameter (cm) at breast height (1.3 m) are shown as black points and fitted truncated distribution functions are represented by solid lines. The straight line denotes the power-law (orange), the slightly curved line refers to the Weibull distribution (blue) and the stronger curved line depicts the negative exponential distribution function (green). Estimated parameters are for (right) regression $\underline{\alpha} = 2.14$ (power-law), $\underline{\lambda} = 0.0374$ (exponential distribution), $\underline{\beta} = 1.08$ and $\underline{\gamma} = 0.352$ (Weibull distribution) and for (left) *Gaussian MLE* $\underline{\alpha} = 1.93$ (power-law), $\underline{\lambda} = 0.247$ (exponential distribution), $\underline{\beta} = 2.51$ and $\underline{\gamma} = 0.283$ (Weibull distribution).

Figures

Figure 1.1: Pictures of the three types of grasslands:.....	9
Figure 1.2: Schematic view of different management option affecting the diversity of grasslands.	13
Figure 2.1: The individual's and community architectural concept.....	34
Figure 2.2: Exemplary representation of an individual's traits characterizing its success in resource uptake and in competition with other individuals.....	39
Figure 3.1: Block diagram of one time step (one day) in Grassmind.	43
Figure 3.2: Flow diagram of one time step (one day) in Grassmind.....	44
Figure 3.3: Display of the state variables, which correspond with the geometrical characteristics of an individual.....	45
Figure 3.4: Illustration of light competition between individual species of different heights..	51
Figure 3.5: Illustration of the rooting zones of two different individuals.	55
Figure 3.6: Flow diagram of the interface program showing the scheduled exchange between the grassland model Grassmind and the soil model Candy as well as input by the database. .	65
Figure 4.1: Summary of the defined species groups and their change according to the reference species <i>Festuca pratensis</i>	72
Figure 4.2: Simulation of the parameterized species <i>Festuca pratensis</i> using the grassland model Grassmind compared to observation data for (A) density of individuals and (B) community cover of individuals.....	73
Figure 4.3: Comparison of the simulated and measured community leaf area index and maximum height of the sward for the parameterized species <i>Festuca pratensis</i>	74
Figure 4.4: Comparison of the monocultures with the 2-species-mixtures of the defined species groups for 50 m ²	75

Figure 5.1: Outline of tree size measurements in forests.	81
Figure 5.2: Scheme of the evaluation procedure of virtual data sets.	86
Figure 5.3: Analyses of binned virtual data using different bin widths..	88
Figure 5.4: Analyses of virtual data including different levels of measurement errors..	89
Figure 5.5: Effects of binning and random measurement errors on parameter estimation using different MLE methods..	91
Figure 5.6: Effect of errors on <i>Akaike weights</i> for the correct determination of the underlying distribution..	92
Figure A7.1: Comparison of observed and simulated community coverage.	109
Figure A7.2: Comparison of observed and simulated aboveground biomass..	109
Figure A7.3: Curves of leaf photosynthetic rate for different conditions of photosynthetic photon flux density PPFD.	112
Figure A7.4: Local sensitivity analysis for the response variable <i>aboveground biomass</i> of the specific measurement dates of the <i>Jena biodiversity experiment</i>	113
Figure A7.5: Local sensitivity analysis for the response variable <i>maximum sward height</i> of the specific measurement dates of the <i>Jena biodiversity experiment</i>	114
Figure A7.6: Local sensitivity analysis for the response variable <i>community coverage</i> of the specific measurement dates of the <i>Jena biodiversity experiment</i>	115
Figure A7.7: Local sensitivity analysis for the response variable <i>community coverage of green leaves</i> of the specific measurement dates of the <i>Jena biodiversity experiment</i>	116
Figure A7.8: Local sensitivity analysis for the response variable <i>community leaf area index</i> of the specific measurement dates of the <i>Jena biodiversity experiment</i>	117
Figure A7.9: Effect of binning on <i>Akaike weights</i> with increasing sample size using <i>standard MLE</i>	122

Figure A7.10: Effect of binning on <i>Akaike weights</i> with increasing sample size using multinomial MLE.....	123
Figure A7.11: Effect of random measurement errors on <i>Akaike weights</i> with increasing sample size using <i>standard MLE</i>	124
Figure A7.12: Effect of random measurement errors on <i>Akaike weights</i> with increasing sample size using <i>Gaussian MLE</i>	125
Figure A7.13: Log-log plots of the fits using regression (right) and <i>Gaussian MLE</i> (left).. .	126

Tables

Table 2.1: Overview of the reviewed models concerning time step, model structure, main variables and management activities considered.	26
Table 2.2: Overview of abiotic factors considered in the reviewed models, the resources species compete for and the number and type of species represented	27
Table 3.1: Technical parameters of the grassland model Grassmind.	61
Table 3.2: Geometrical parameters of the grassland model Grassmind.	61
Table 3.3: Process parameters of the grassland model Grassmind. Parameters, which are not species-specific, are written in bold.	61
Table 3.4: Soil parameters of the soil model Candy.....	63
Table 5.1: Presentation of the three assumed truncated frequency distributions $f(x;\theta)$ used in our investigations.	85
Table A7.1: List of geometrical parameters found in literature and estimated for the species <i>Festuca pratensis</i>	107
Table A7.2: List of process parameters found in literature and estimated for the species <i>Festuca pratensis</i>	107
Table A7.3: Summary of the important soil parameters used for the parameterization of the soil type in the model Candy.	111
Table A7.4: Display of specific key points evaluated during the assessment of maximum likelihood methods.	121

Bibliography

- Acevedo, M.F. and Raventós, J. (2002) Growth dynamics of three tropical savanna grass species: an individual-module model. *Ecological Modelling* 154:45-60.
- Amthor, J. S. (1984) The role of maintenance respiration in plant growth. *Plant, Cell and Environment* 7:561-569.
- Bailey, R.L. and Dell, T.R. (1973) Quantifying Diameter Distributions with the Weibull Function. *Forest Science* 19: 97-104.
- Beniston, M., Stephenson, D.B., Christensen, O.B., Ferro, C.A.T., Frei, C., Goyette, S. *et al.* (2007) Future extreme events in European climate: an exploration of regional climate model projections. *Climatic Change* 81:71–95.
- BMU (Bundesministerium für Umwelt, Naturschutz und Reaktorsicherheit), <http://www.bmu.de/themen/klima-energie/energiewende/kurzinfo/> [Accessed at 30 September 2013]
- Botkin, D.B., Janak, J.F. and Wallis, J.R. (1972) Some Ecological Consequences of a Computer Model of Forest Growth. *Journal of Ecology* 60: 849-872.
- Breckle, S.-W. (1999) Walter's Vegetation of the Earth. 4. Aufl., Stuttgart: Eugen Ulmer.
- Bugmann, H., Grote, R., Lasch, P., Lindner, M. and Suckow, F. (1997) A New Forest Gap Model to Study the Effects of Environmental Change on Forest Structure and Functioning. In Mohren, G.M.J, Kramer, K. and Sabaté, S., eds., *Global Change Impacts on Tree Physiology and Forest Ecosystems*. Kluwer Academic Publishers, pp. 255-261.
- Bugmann, H. (2001) A review of forest gap models. *Climatic Change* 51: 259-305.
- Burnham, K.P. and Anderson, D.R. (2002) Model selection and multimodel inference: a practical information-theoretic approach. New York: Springer.
- Byrd, R.H., Lu, P., Nocedal, J. and Zhu, C. (1995) A limited memory algorithm for bound constrained optimization. *SIAM Journal on Scientific Computing* 16: 1190-1208.
- Chave, J., Condit, R., Salomon, A., Hernandez, A., Lao, S. *et al.* (2004) Error propagating and scaling for tropical forest biomass estimates. *Philosophical Transactions of the Royal Society London B*. 359: 409–420.

- Clar, S., Drossel, B. and Schwabl, F. (1996) Forest fires and other examples of self-organized criticality. *Journal of Physics Condensed Matter* 8: 6803–6824.
- Clauset, A., Shalizi, C.R. and Newman, M.E.J. (2009) Power-law distribution in empirical data. *SIAM Review* 51: 661-703.
- Coffin, D.P. and Lauenroth, W.K. (1990) A gap dynamics simulation model of succession in a semiarid grassland. *Ecological Modelling* 49:229-266.
- Coffin, D.P. and Urban, D.L. (1993) Implications of natural history traits to system-level dynamics: comparison of a grassland and a forest. *Ecological Modelling* 67: 147-178.
- Condit, R. (1998) Tropical Forest Census Plots. Berlin and Georgetown, Texas: Springer and R.G. Landes Company.
- Coughenour, M.B., McNaughton, S.J. and Wallace, L.L. (1984) Modelling primary production of perennial graminoids – uniting physiological processes and morphometric traits. *Ecological Modelling* 23:101-134.
- Damgaard, C., Weiner, J. and Nagashima, H. (2002) Modelling individual growth and competition in plant populations: growth curves of *Chenopodium album* at two densities. *Journal of Ecology* 90:666-671.
- Damgaard, C. and Weiner, J. (2008) Modeling the growth of individuals in crowded plant populations. *Journal of Plant Ecology* 1: 111-116.
- Deák, B., Valkó, O., Kelemen, A., Török, P., Miglécz, T., Ölvedi, T. *et al.* (2011) Litter and graminoid biomass accumulation suppresses weedy forbs in grassland restoration. *Plant Biosystems* 145 (3): 730-737.
- de Groot, R.S., Wilson, M.A. and Boumans, R.M.J. (2002) A typology for the classification, description and valuation of ecosystem functions, goods and services. *Ecological Economics* 41: 393-408.
- Dengler, J., Bedall, P., Bruchmann, I., Hoefft, I. and Lang, A. (2004) Artenzahl-Areal-Beziehungen in uckermärkischen Trockenrasen unter Berücksichtigung von Kleinstflächen – eine neue Methode und erste Ergebnisse. *Kieler Notizen zur Pflanzenkunde in Schleswig-Holstein* 32: 20-25.
- Dengler, J. (2005) Zwischen Estland und Portugal – Gemeinsamkeiten und Unterschiede der Phytodiversitätsmuster europäischer Trockenrasen. *Tuexenia* 25: 387 – 405.

Detling, J.K., Parton, W.J. and Hunt, H.W. (1979) A Simulation Model of *Bouteloua gracilis* Biomass Dynamics on the North American Shortgrass Prairie. *Oecologia* 38:167-191.

Diemer, M., Joshi, J., Körner, C., Schmid, B. and Spehn, E. (1997) An experimental protocol to assess the effects of plant diversity on ecosystem functioning utilized in a European research network. *Bulletin of the Geobotanical Institute ETH* 63: 95-107.

Drossel, B. and Schwabl, F. (1992) Self-organized critical forest-fire model. *Physical Review Letters* 69: 1629-1632.

Duru, M., Ducrocq, H., Fabre, C. and Feuillerac, E. (2002) Modeling Net Herbage Accumulation of an Orchardgrass Sward. *Agronomy Journal* 94:1244-1256.

Duru, M., Adam, M., Cruz, P., Martin, G., Ansquer, P., Ducourtieux, C. *et al.* (2009) Modelling aboveground herbage mass for a wide range of grassland community types. *Ecological Modelling* 220:209-25.

Edwards, A.M., Phillips, R.A., Watkins, N.W., Freeman, M.P., Murphy, E.J. *et al.* (2007) Revisiting Lévy flight search patterns of wandering albatrosses, bumblebees and deer. *Nature* 449: 1044-1048.

Edwards, A.M. (2008) Using likelihood to test for Levy flight search patterns and for general power-law distributions in nature. *Journal of Animal Ecology* 77: 1212-1222.

Elberse, W. Th. and Berendse, F. (1993) A Comparative Study of the Growth and Morphology of Eight Grass Species from Habitats with Different Nutrient Availabilities. *Functional Ecology* 7:223-229.

Ellenberg, H., Weber, H.E., Düll, R., Wirth, V. and Werner, W. (1992) Zeigerwerte von Pflanzen in Mitteleuropa. Scripta Geobot. (Göttingen) 18. Datenbank.

Ellenberg, H. and Leuschner, C. (2010) Vegetation Mitteleuropas mit den Alpen. 6. Aufl. Eugen Ulmer.

Enquist, B.J. and Niklas, K.J. (2001) Invariant scaling relations across tree-dominated communities. *Nature* 410: 655-660.

Enquist, B.J., West, G.B. and Brown, J.H. (2009) Extensions and evaluations of a general quantitative theory of forest structure and dynamics. *Proceedings of the National Academy of Sciences USA* 106: 7046–7051.

Ernst-Abbe-Fachhochschule, Jena, Germany; <http://wetter.mb.fh-jena.de/station/>; [Accessed at 30 September 2013].

Eurostat Yearbook (2012) Europe in Figures, http://epp.eurostat.ec.europa.eu/cache/ITY_OFFPUB/KS-CD-12-001/EN/KS-CD-12-001-EN.PDF; [Accessed at 30 September 2013].

Fargione, J., Tilman, D., Dybzinski, R., Lambers, J.H.R., Clark, C., Harpole, W.S. *et al.* (2006) From selection to complementarity: shifts in the causes of biodiversity-productivity relationships in a long-term biodiversity experiment. *Proceedings of the Royal Society B*. 274: 871-876.

Farquhar, G.D., von Caemmerer, S. and Berry, J.A. (1980) A Biochemical Model of Photosynthetic CO₂ Assimilation in Leaves of C₃ Species. *Planta* 149:78-90.

Fischer, R., Armstrong, A.H., Shugart, H.H. and Huth, A. (2013) Potential Impacts of Reduced Rainfall in a Tropical Forest of Madagascar - A Simulation Study, *accepted*.

Flanagan, L.B., Wever, L.A. and Carlson, P.J. (2002) Seasonal and interannual variation in carbon dioxide exchange and carbon balance in a northern temperate grassland. *Global Change Biology* 8: 599-615.

FNR (Fachagentur Nachwachsende Rohstoffe e.V.), <http://energiepflanzen.fnr.de/pflanzen/mehrjaehrige/miscanthus/>, [Accessed at 30 September 2013]

Forsythe, W.C., Rykiel Jr, E.J., Stahl, R.S., Wu, H.I. and Schoolfield, R.M. (1995). A model comparison for daylength as a function of latitude and day of year. *Ecological Modelling* 80: 87-95.

Franko, U., Oelschlägel, B. and Schenk, S. (1995) Simulation of temperature-, water- and nitrogen dynamics using the model CANDY. *Ecological Modelling* 81:213-22.

Garwood, E.A. and Williams, T.E. (1967a) Soil water use and growth of a grass sward. *Journal of Agricultural Science* 68:281-292.

Garwood, E.A. and Williams, T.E. (1967b) Growth, Water use and nutrient uptake from subsoil by grass swards *Journal of Agricultural Science* 69:125-130.

Gelfand, I., Sahajpal, R., Zhang, X., Izaurralde, R.C., Gross, K.L. and Robertson, G.P. (2013) Sustainable bioenergy production from marginal lands in the US Midwest. *Nature* 493: 514–517

- Gerwitz, A. and Page, E.R. (1974) An Empirical Mathematical Model to Describe Plant Root Systems. *Journal of Applied Ecology* 11:773-781.
- Grace, J.B., Anderson, T.M., Smith, M.D., Seabloom, E., Andelman, S.J., Meche, G. *et al.* (2007) Does species diversity limit productivity in natural grassland communities? *Ecology Letters* 10:680-689.
- Granier, A., Breda, N., Biron, P. and Villette, S. (1999) A lumped water balance model to evaluate duration and intensity of drought constraints in forest stands. *Ecological Modelling* 116: 269-283.
- Grime, J.P. (1981) *Plant Strategies and Vegetation Processes*. J. Wiley, Chichester.
- Grimm, V. and Railsback, S.F. (2012) Pattern-oriented modelling: a “multiscope” for predictive systems ecology. *Philosophical Transactions Royal Society London B* 367: 298-310
- Gutenberg, B. and Richter, C.F. (1954) *Seismicity of the Earth and Associated Phenomena*. Princeton: Princeton University Press.
- Hartig, F., Calabrese, J.M., Reineking, B., Wiegand, T. and Huth, A. (2011) Statistical inference for stochastic simulation models – theory and application. *Ecology Letters* 14: 816-827.
- Hauck, B., Gay, A.P., Macduff, J., Griffiths, C.M. and Thomas, H. (1997) Leaf senescence in a non-yellowing mutant of *Festuca pratensis*: implications of the stay-green mutation for photosynthesis, growth and nitrogen nutrition. *Plant, Cell and Environment* 20:1007–1018.
- Heath, M.T. (2002) *Scientific Computing: An Introductory Survey*. New York: McGraw-Hill.
- Hector, A., Schmid, B., Beierkuhnlein, C., Caldeira, M.C., Diemer, M., Dimitrakopoulos, P.G. *et al.* (1999) Plant diversity and productivity experiments in European grasslands. *Science* 286:1123-1127.
- Heisse, K., Roscher, C., Schumacher, J. and Schulze, E.-D. (2007) Establishment of grassland species in monocultures: different strategies lead to success. *Oecologia* 152: 435-447.
- Hernández-Garay, A., Matthew, C. and Hodgson, J. (1999) Tiller size/density compensation in perennial ryegrass miniature swards subject to differing defoliation heights and a proposed productivity index. *Grass and Forage Science* 54:347-56.
- Hooper, D.U. and Vitousek, P.M. (1997) The effects of plant composition and diversity on ecosystem processes. *Science* 277: 1302-1305.

- Hooper, D.U. and Vitousek, P.M. (1998) Effects of plant composition and diversity on nutrient cycling. *Ecological Monographs* 68: 121-149.
- Hubbell, S.P., Foster, R.B., O'Brien, S.T., Harms, K.E., Condit, R. *et al.* (1999) Light gap disturbances, recruitment limitation, and tree diversity in a neotropical forest. *Science* 283: 554-557.
- Hubbell, S.P., Condit, R. and Foster, R.B. (2005) Barro Colorado Forest Census Plot Data. Available: <https://ctfs.arnarb.harvard.edu/webatlas/datasets/bci>. [Accessed at 27 June 2012].
- Hunt, H.W., Trlica, M.J., Redente, E.F., Moore, J.C., Detling, J.K., Kittel, T.G.F. *et al.* (1991) Simulation model for the effects of climate change on temperate grassland ecosystems. *Ecological Modelling* 53:205-246.
- Huth, A., Ditzer, T and Bossel, H. (1998) The Rain Forest Growth Model FORMIX3 – Model Description and Analysis of Forest Growth and Logging Scenarios for the Deramakot Forest Reserve (Malaysia), Göttingen : Erich Goltze Publishers.
- IPCC, Climate Change. (2007) Synthesis Report. Intergovernmental Panel on Climate Change. Cambridge: Cambridge University Press.
- Jordan, N., Boody, G., Broussard, W., Glover, J.D., Keeney, D., McCown, B.H. *et al.* (2007) Sustainable Development of the Agricultural Bio-Economy. *Science* 316:1570-1571.
- Kays, S. and Harper, J.L. (1974) The Regulation of Plant and Tiller Density in a Grass Sward. *Journal of Ecology* 62:97-105.
- Keel, A. (1995) Vegetationskundlich-ökologische Untersuchungen und Bewirtschaftungsexperimente in Halbtrockenwiesen (Mesobromion) auf dem Schaffhauser Randen. Veröff. Geobot. Inst. ETH, Stiftg. Rübel, Zürich 124: 1-181.
- Kiefer, J. (1953) Sequential minimax search for a maximum. *Proceedings of the American Mathematical Society* 4: 502–506.
- Kieseppä, I.A. (1997) Akaike Information Criterion, Curve-fitting, and the Philosophical Problem of Simplicity. *British Journal of Philosophical Science* 48: 21-48.
- Kinzig, A.P., Pacala, S. and Tilman, D. (2002) The Functional Consequences of Biodiversity: Empirical Progress and Theoretical Extensions. Princeton: Princeton University Press.
- Klapp, E. (1971) Wiesen und Weiden. 4. Aufl., Berlin-Hamburg: Verlag Paul Parey.

- Koh, L.P. and Ghazoul, J. (2008) Biofuels, biodiversity, and people: Understanding the conflicts and finding opportunities, *Biological Conservation* 141: 2450-2460.
- Köhler, P. and Huth, A. (2004) Simulating Growth Dynamics in a South-Eats Asian Rainforest Threatened by Recruitment Shortage and Tree Harvesting. *Climatic Change* 67: 95-117.
- Kohyama, T. (1991) Simulating Stationary Size Distribution of Trees in Rain Forests. *Annals of Botany* 68: 173-180.
- Kohyama, T. (1993) Size-structured tree populations in gap-dynamic forest – the forest architecture hypothesis for the stable coexistence of species. *Journal of Ecology* 81:131-143.
- Kohyama, T. and Shigesada, N. (1995) A size-distribution-based model of forest dynamics along a latitudinal environmental gradient. *Vegetatio* 121: 117-126.
- Kohyama, T., Suzuki, E., Partomihardjo, T., Yamada, T. and Kubo, T. (2003) Tree species differentiation in growth, recruitment and allometry in relation to maximum height in a Bornean mixed dipterocarp forest. *Journal of Ecology* 91: 797-806.
- Kühn, I., Durka, W. and Klotz, S. (2004) BiolFlor - a new plant-trait database as a tool for plant invasion ecology. *Diversity and Distributions* 10:363-365.
- Lantinga, E.A., Nassiri, M. and Kropff, M.J. (1999) Modelling and measuring vertical light absorption within grass-clover mixtures. *Agricultural and Forest Meteorology* 96:71-83.
- Larcher, W. (1976) *Ökologie der Pflanzen*. 2. Aufl. Stuttgart: Eugen Ulmer.
- Larcher, W. (2001) *Ökophysiologie der Pflanzen*. 6.Aufl. Verlag Eugen Ulmer.
- Lawton, J.H., Naeem, S., Thompson, L.J., Hector, A. and Crawley, M.J. (1998) Biodiversity and ecosystem functioning: getting the Ecotron experiment in its correct context. *Functional Ecology* 12: 848-852.
- Leemans, R. and Prentice, I.C. (1989) FORSKA, a General Forest Succession Model, Uppsala: Institute of Ecological Botany.
- Liu, Y., Wu, L., Baddeley, J.A. and Watson, C.A. (2011) Models of biological nitrogen fixation of legumes. A review. *Agronomy for Sustainable Development* 31:155-72.
- Lonsdale, W.M. and Watkinson, A.R. (1982) Light and Self-Thinning. *New Phytologist* 90: 431-445.

- Lonsdale, W.M. and Watkinson, A.R. (1983) Tiller dynamics and self-thinning in grassland habitats. *Oecologia* 60: 390-395.
- Loreau, M. and Hector, A. (2001) Partitioning selection and complementarity in biodiversity experiments. *Nature* 412: 72-76.
- Loreau, M., Naeem, S., Inchausti, P., Bengtsson, J., Grime, J.P., Hector, A. *et al.* (2001) Biodiversity and Ecosystem Functioning: Current Knowledge and Future Challenges. *Science* 294: 804-808.
- Maidment, D.R. (1993) Handbook of Hydrology. McGraw-Hill.
- Marquard, E., Weigelt, A., Temperton, V.M., Roscher, C., Schumacher, J., Buchmann, N. *et al.* (2009a) Plant species richness and functional composition driveoveryielding in a six-year grassland experiment. *Ecology* 90(12): 3290-3302.
- Marquard, E., Weigelt, A., Roscher, C., Gubsch, M., Lipowsky, A. and Schmid, B. (2009b) Positive biodiversity-productivity relationships due to increased plant density. *Journal of Ecology* 97: 696-704.
- Matthew, C., Lemaire, G., Hamilton, N.R.S. and Hernandez-Garay, A. (1995) A Modified Self-Thinning Equation to Describe Size/Density Relationships for Defoliated Swards. *Annals of Botany* 76: 579-587.
- McKendry, P. (2002a) Energy production from biomass (part1): overview of biomass. *Bioresource Technology* 83: 37-46.
- McKendry, P. (2002b) Energy production from biomass (part 2): conversion technologies. *Bioresource Technology* 83: 47-54.
- McNaughton, S.J. (1993) Biodiversity and function of grazing ecosystems. In E.-D. Schulze and H.A. Mooney, eds., *Biodiversity and Ecosystem Function*, 361-383. Berlin: Springer-Verlag.
- Monsi, M. and Saeki, T. (1953) Über den Lichtfaktor in den Pflanzengesellschaften und seine Bedeutung für die Stoffproduktion, *Japanese Journal of Botany* 14: 22-52.
- MPI for Biogeochemistry, Jena, Germany; <http://www.bgc-jena.mpg.de/wetter>. [Accessed at 30 September 2013]

Mulder, C.P.H., Koricheva, J., Huss-Danell, K., Högberg, P. and Joshi, J. (1999) Insects affect relationships between plant species richness and ecosystem processes. *Ecology Letters* 2: 237-246.

Muller-Landau, H.C., Condit, R.S., Harms, K.E., Marks, C.O., Thomas, S.C. *et al.* (2006) Comparing tropical forest tree size distributions with the predictions of metabolic ecology and equilibrium models. *Ecology Letters* 9: 589-602.

Müller, I., Schmid, B. and Weiner, J. (2000) The effect of nutrient availability on biomass allocation patterns in 27 species of herbaceous plants. *Perspectives in Plant Ecology, Evolution and Systematics* 3: 115-127

Naeem, S., Thompson, L.J., Lawler, S.P., Lawton, J.H. and Woodfin, R.M. (1995) Empirical evidence that declining species diversity may alter the performance of terrestrial ecosystems. *Philosophical Transactions of the Royal Society of London, B*. 347: 249-262.

Naeem, S., Hakansson, K., Thompson, L.J., Lawton, J.H. and Crawley, M.J. (1996) Biodiversity and plant productivity in a model assemblage of plant species. *Oikos* 76: 259-264.

Nagashima, H. and Terashima, I. (1995) Relationships between Height, Diameter and Weight Distributions of *Chenopodium album* Plants in Stands: Effects of Dimension and Allometry. *Annals of Botany* 75: 181-188.

Nelder, J.A. and Mead, R. (1965) A simplex algorithm for function minimization. *Computer Journal* 7: 308-313.

Newman, M.E.J. (2005) Power laws, Pareto distribution and Zipf's law. *Contemporary Physics* 46: 323-351.

Niklas, K.J. (1995) Plant Height and the Properties of Some Herbaceous Stems. *Annals of Botany* 75: 133-142.

Niklas, K.J., Midgley, J.J. and Rand, R.H. (2003) Tree size frequency distributions, plant density, age and community disturbance. *Ecology Letters* 6: 405-411.

Niklas, K.J. (2005) Modelling Below- and Above-ground Biomass for Non-woody and Woody Plants. *Annals of Botany* 95:315-321.

Nitsche, S. and Nitsche, L. (1994) Extensive Grünlandnutzung. Radebeul: Neumann Verlag GmbH.

- Nocedal, J. and Wright, S.J. (2006) Numerical Optimization. Springer, 664 p.
- Oelmann, Y., Kreuziger, Y., Bol, R and Wilcke, W. (2007) Nitrate leaching in soil: Tracing the NO₃- sources with the help of stable N and O isotopes. *Soil Biology and Biochemistry* 39: 3024-3033.
- Pacala, S.W., Canham, C.D. and Silander Jr., J.A. (1993) Forest Models Defined by Field Measurements: I. The Design of a Northeastern Forest Simulator. *Canadian Journal of Forest Research* 23: 1980-1988.
- Pacala, S.W., Canham, C.D., Saponara, J., Silander, J.A., Kobe, R.K. and Ribbens, E. (1996) Forest Models Defined by Field Measurements: Estimation, Error Analysis and Dynamics. *Ecological Monographs* 66:1-43.
- Peppler-Lisbach, C. and Petersen, J. (2001) Synopsis der Pflanzengesellschaften Deutschlands. Heft 8: Calluno-Ulicetea (G3). Teil 1: Nardetalia strictae. Borstgrasrasen. Göttingen.
- Pott, R. and Hüppe, J. (1991) Die Hudelandschaften Nordwestdeutschlands. Abh. Westfäl. Mus. Naturk. (Münster/W.) 53: 1-313.
- Pretzsch, H., Biber, P. and Dursky, J. (2002) The single tree-based stand simulator SILVA: construction, application and evaluation. *Forest Ecology and Management* 162:3-21.
- R Development Core Team (2009) R: A language and environment for statistical computing. R Foundation for Statistical Computing, Vienna, Austria. Available: <http://www.r-project.org>. [Accessed at 27 June 2012].
- Reed, W.J. and McKelvey, K.S. (2002) Power law behaviour and parametric models for the size distribution of forest fires. *Ecological Modelling* 150: 239–254.
- Reich, P.B. (1998) Variation among plant species in leaf turnover rates and associated traits: implications for growth at all life stages. In: *Inherent Variation in Plant Growth: Physiological Mechanisms and Ecological Consequences*. Backhuys Pub., Leiden, The Netherlands.
- Reich, P.B., Knops, J., Tilman, D., Craine, J., Ellsworth, D., Tjoelker, M. *et al.* (2001) Plant diversity enhances ecosystem responses to elevated CO₂ and nitrogen deposition. *Nature* 410: 809-810.

- Reich, P.B., Buschena, C., Tjoelker, M.G., Wrage, K., Knops, J., Tilman, D. *et al.* (2003) Variation in growth rate and ecophysiology among 34 grassland and savannah species under contrasting N supply: a test of functional group differences. *New Phytologist* 157: 617-631.
- Reich, P.B., Hobbie, S.E., Lee, T., Ellsworth, D.S., West, J.B., Tilman, D. *et al.* (2006) Nitrogen limitation constrains sustainability of ecosystem response to CO₂. *Nature* 440: 922-925.
- Reich, P.B., Tilman, D., Isbell, F., Mueller, K., Hobbie, S.E., Flynn, D.F.B. *et al.* (2012) Impacts of Biodiversity Loss Escalate Through Time as Redundancy Fades. *Science* 336: 589-592.
- Rennolls, K., Geary, D.N. and Rollinson, T.J.D. (1985) Characterizing Diameter Distributions by use of the Weibull Distribution. *Forestry* 58: 57-66.
- Reuss, J.O. and Innis, G.S. (1977) A Grassland Nitrogen Simulation Model. *Ecology* 58:379-88.
- Reynolds, A.M., Swain, J.L., Smith, A.D., Martin, A.P. and Osborne, J.L. (2009) Honeybees use a Lévy flight search strategy and odour-mediated anemotaxis to relocate food sources. *Behavioral Ecology and Sociobiology* 64: 115-123.
- Reynolds, A.M. (2012) Distinguishing between Lévy walks and strong alternative models. *Ecology* 93: 1228-1233.
- Riedo, M., Grub, A., Rosset, M. and Fuhrer, J. (1998) A pasture simulation model for dry matter production, and fluxes of carbon, nitrogen, water and energy. *Ecological Modeling* 105:141-183.
- Riedo, M., Gyalistras, D. and Fuhrer, J. (2000) Net primary production and carbon stocks in differently managed grasslands: simulation of site-specific sensitivity to an increase in atmospheric CO₂ and to climate change. *Ecological Modelling* 134:207-27.
- Roscher, C., Schumacher, J., Baade, J., Wilcke, W., Gleixner, G., Weisser W.W., Schmid, B. and Schulze, E.-D. (2004) The role of biodiversity for element cycling and trophic interactions: an experimental approach in a grassland community. *Basic and Applied Ecology* 5: 107-121.
- Running, S.W. and Gower, S.T. (1991) FOREST-BGC: A general model of forest ecosystem processes for regional applications. II. Dynamic carbon allocation and nitrogen budgets. *Tree Physiology* 9:147-160.

- Ryser, P. and Urbas, P. (2000) Ecological significance of leaf life span among Central European grass species. *Oikos* 91: 41-50.
- Sato, H., Itoh, A. and Kohyama, T. (2007) SEIB-DGVM: A new Dynamic Global Vegetation Model using a spatially explicit individual-based approach. *Ecological Modelling* 200: 279-307.
- Schapendonk, A.H.C.M, Stol, W., van Kraalingen, D.W.G. and Bouman, B.A.M. (1998) LINGRA, a sink/source model to simulate grassland productivity in Europe. *European Journal of Agronomy* 9:87-100.
- Schenk, H.J. and Jackson, R.B. (2002) Rooting depths, lateral root spreads and below-ground/above-ground allometries of plants in water-limited ecosystems. *Journal of Ecology* 90:480-494.
- Scherer-Lorenzen, M. (1999) Effects of plant diversity on ecosystem processes in experimental grassland communities. *Bayreuther Forum Ökologie* 75: 1-195.
- Schippers, P. and Olf, H. (2000) Biomass partitioning, architecture and turnover of six herbaceous species from habitats with different nutrient supply. *Plant Ecology* 149: 219-231.
- Schippers, P. and Kropff, M.J. (2001) Competition for Light and Nitrogen among Grassland Species: A Simulation Analysis. *Functional Ecology* 15:155-164.
- Shimano, K. (2000) A power function for forest structure and regeneration pattern of pioneer and climax species in patch mosaic forests. *Plant Ecology* 146: 207-220.
- Shinozaki, K., Yoda, K., Hozumi, K. and Kira, T. (1964) A quantitative analysis of plant form – the pipe model theory II. Further evidence of the theory and its application in forest ecology. *The Ecological Society of Japan* 14: 133-139.
- Shugart, H.H. (1998) *Terrestrial Ecosystems in Changing Environments*. Cambridge University Press.
- Siehoff, S., Lennartz, G., Heilburg, I.C., Roß-Nickoll, M., Ratte, H.T. and Preuss, T.G. (2011) Process-based modelling of grassland dynamics built on ecological indicator values for land use. *Ecological Modelling* 222:3854-3868.
- Sims, D.W., Southall, E.J., Humphries, N.E., Hays, G.C., Bradshaw, C.J. *et al.* (2008) Scaling laws of marine predator search behaviour. *Nature* 451: 1098-1102.

Sitch, S., Smith, B., Prentice, C., Arneeth, A., Bondeau, A., Cramer, W. *et al.* (2003) Evaluation of ecosystem dynamics, plant geography and terrestrial carbon cycling in the LPJ dynamic global vegetation model. *Global Change Biology* 9:161-185.

Smith, B., Prentice, I.C. and Sykes, M.T. (2001) Representation of vegetation dynamics in the modelling of terrestrial ecosystems: comparing two contrasting approaches within European climate space. *Glob Ecology and Biogeography* 10:621–637.

Spehn, E.M., Joshi, J., Schmid, B., Alpehi, J. and Körner, C. (2000a) Plant diversity effects on soil heterotrophic activity in experimental grassland systems. *Plant and Soil* 224: 217-230.

Spehn, E.M., Joshi, J., Schmid, B., Diemer, M. and Körner, C. (2000b) Above-ground resource use increases with plant species richness in experimental grassland ecosystems. *Functional Ecology* 14: 326-337.

Spehn, E.M., Hector, A., Joshi, J., Scherer-Lorenzen, M., Schmid, B., Bazeley-White, E. *et al.* (2005) Ecosystem effects of biodiversity manipulations in European grasslands. *Ecological Monographs* 75(1): 37-63.

Stegen, J.C. and White, E.P. (2008) On the relationship between mass and diameter distributions in tree communities. *Ecology Letters* 11: 1287-1293.

Steinbeiss, S., Beßler, H., Engels, C., Temperton, V.M., Buchmann, N., Roscher, C. *et al.* (2008) Plant diversity positively affects short-term soil carbon storage in experimental grasslands. *Global Change Biology* 14: 2937-2949.

Swift, M.J. and Anderson, J.M. (1993) Biodiversity and ecosystem function in agricultural systems. In E.-D. Schulze and H.A. Mooney, eds., *Biodiversity and Ecosystem Function*, 15-41. Berlin: Springer-Verlag.

Symstad, A.J., Tilman, D., Willson, J. and Knops, J.M.H. (1998) Species loss and ecosystem functioning: effects of species identity and community composition. *Oikos* 81: 389-397.

Taubert, F., Frank, K. and Huth, A. (2012) A review of grassland models in the biofuel context. *Ecological Modelling* 245: 84-93.

TEEB (2010), The Economics of Ecosystems and Biodiversity Ecological and Economic Foundations. Edited by Pushpam Kumar. Earthscan, London and Washington

Temperton, V.M., Mwangi, P.N., Scherer-Lorenzen, M., Schmid, B. and Buchmann, N. (2007) Positive interactions between nitrogen-fixing legumes and four different neighbouring species in a biodiversity experiment. *Oecologia* 151:190–205.

- Thornley, J.H.M and Verberne, E.L.J. (1989) A model of nitrogen flows in grassland. *Plant, Cell and Environment* 12:863-886.
- Thornley, J.H.M and Johnson, I.R. (1990) Plant and crop modelling – a mathematical approach to plant and crop physiology. Oxford: Clarendon Press.
- Thornley, J.H.M. (1998) Grassland dynamics: an ecosystem simulation model. CAB International.
- Thornley, J.H.M. and Cannell, M.G.R. (2000) Modelling the Components of Plant Respiration: Representation and Realism. *Annals of Botany* 85:55-67.
- Thornley, J.H.M. and France, J. (2007) Mathematical Models in Agriculture: Quantitative Methods for the Plant, Animal and Ecological Sciences. CAB International.
- Tilman, D. (1988) Plant Strategies and the Dynamics and Structure of Plant Communities. Princeton: Princeton University Press.
- Tilman, D., Knops, J., Wedin, D., Reich, P., Ritchie, M. and Siemann, E. (1997) The Influence of Functional Diversity and Composition on Ecosystem Processes. *Science* 277: 1300-1302.
- Tilman, D., Reich, P.B., Knops, J., Wedin, D., Mielke, T. and Lehman, C. (2001) Diversity and productivity in a long-term grassland experiment. *Science* 294: 843-845.
- Tilman, D., Reich, P.B. and Knops, J. (2006a) Biodiversity and ecosystem stability in a decade-long grassland experiment. *Nature* 441: 629-632.
- Tilman, D., Hill, J. and Lehman, C. (2006b) Carbon-Negative Biofuels from Low-Input High-Diversity Grassland Biomass. *Science* 314: 1598-1600.
- Tjoelker, M.G., Craine, J.M., Wedin, D., Reich, P.B. and Tilman, D. (2005). Linking leaf and root trait syndromes among 39 grassland and savannah species. *New Phytologist* 167(2):493-508.
- Török, P., Vida, E., Deák, B., Lengyel, Sz. and Tóthmérész, B. (2011) Grassland restoration on former croplands in Europe: an assessment of applicability of techniques and costs. *Biodiversity and Conservation* 20: 2311-2332.
- Troumbis, A.Y. and Memtas, D. (2000) Observational evidence that diversity may increase productivity in Mediterranean shrublands. *Oecologia* 125: 101-108.

- Turcotte, D.L. and Malamud, B.D. (2004) Landslides, forest fires, and earthquakes: examples of self-organized critical behaviour. *Physica A: Statistical Mechanics and its Application* 340: 580-589.
- Turner, M.D. and Rabinowitz, D. (1983) Factors Affecting Frequency Distributions of Plant Mass: The Absence of Dominance and Suppression in Competing Monocultures of *Festuca Paradoxa*. *Ecology* 64: 469-475.
- Virkar, Y. and Clauset, A. (2012) Power-law distributions in binned empirical data. arXiv: 1208.3524. Available: <http://arxiv.org/abs/1208.3524>. [Accessed at 12 November 2012].
- Wang, X., Hao, Z., Zhang, J., Lian, J., Li, B. *et al.* (2009) Tree size distributions in an old-growth temperate forest. *Oikos* 118: 25-36.
- Weigelt, A., Weisser, W.W., Buchmann, N. and Scherer-Lorenzen, M. (2009) Biodiversity for multifunctional grasslands: equal productivity in high-diversity low-input and low-diversity high-input systems. *Biogeosciences* 6: 1695-1706.
- Weigelt, A., Marquard, E., Temperton, V.M., Roscher, C., Scherber, C., Mwangi, P.N. *et al.* (2010) The Jena Experiment: six years of data from a grassland biodiversity experiment. *Ecology* 91:929.
- West, G.B., Enquist, B.J. and Brown, J.H. (2009) A general quantitative theory of forest structure and dynamics. *Proceedings of the National Academy of Sciences USA* 106: 7040-7045.
- White, E.P., Ernest, S.K.M., Kerkhoff, A.J. and Enquist, B.J. (2007) Relationships between body size and abundance in ecology. *Trends in Ecology and Evolution* 22: 323-330.
- White, E.P., Enquist, B.J. and Green, J.L. (2008) On Estimating the Exponent of Power-Law Frequency Distributions. *Ecology* 89: 905-912.
- Wilson, J.B., Peet, R.K., Dengler, J. and Pärtel, M. (2012) Plant species richness: the world records. *Journal of Vegetation Science* 23: 796-802.
- Yamakura, T., Hagihara, A., Sukardjo, S. and Ogawa, H. (1986) Aboveground biomass of tropical rain forest stands in Indonesian Borneo. *Vegetatio* 68: 71-82.
- Yan, H.P., Kang, M.Z., de Reffye, P. and Dingkuhn, M. (2004) A Dynamic, Architectural Plant Model Simulating Resource-dependent Growth. *Annals of Botany* 93:591-602.

Yoda, K., Kira, T., Ogawa, H. and Hozumi, H. (1963) Intraspecific competition among higher plants. XI. Self-thinning in overcrowded pure stands under cultivated and natural conditions. *Journal of Biology, Osaka City University* 14:107-29.

Danksagung

An dieser Stelle möchte ich mich ganz herzlich bei allen Personen bedanken, die zum Gelingen dieser Arbeit beigetragen haben.

Mein besonderer Dank gilt meinen Betreuern Prof. Dr. Andreas Huth und Prof. Dr. Karin Frank, die mir dieses Projekt anvertrauten. Bereits an meinem ersten Tag im Department Ökologische Systemanalyse am UFZ lernte ich die kreative, herzliche und enthusiastische Atmosphäre des Departments kennen, welche sich ebenfalls durch die gesamte Zeit als Doktorandin fortsetzte. Dies ist in erster Linie der hervorragenden Betreuung zu verdanken. Vor allem bedanke ich mich bei meinen beiden Betreuern für die uneingeschränkte Unterstützung, ihr Vertrauen, den eingeräumten Freiheiten für eine kreative Modellierung sowie anregenden und inspirierenden Gesprächen. Besonders bei Prof. Dr. Andreas Huth möchte ich mich für seine richtungsweisende und ideenreiche Betreuung bedanken, mit der er mich bereits bei der ersten Kontaktaufnahme sofort für die Ökologische Modellierung begeistern konnte. Seit nunmehr 5 ½ Jahren während meiner Diplomanden-, Master- und Doktorandenzeit unter Prof. Dr. Andreas Huths Betreuung habe ich die Möglichkeit bekommen zahlreich für meinen weiteren wissenschaftlichen Werdegang zu lernen.

Besonders möchte ich mich auch bei Dr. Uwe Franko für die Bereitstellung des Bodenmodells Candy und für die uneingeschränkte Unterstützung und Hilfsbereitschaft beim Kopplungsprozess zwischen Grassmind und Candy bedanken. Mein Dank geht auch an Thomas Banitz, Florian Hartig, Oliver Jakoby, Michael Müller, Claudia Dislich, Rico Fischer, Jürgen Groeneveld, Friedrich Bohn und allen aktuellen und ehemaligen Mitgliedern des Departments Ökologische Systemanalyse am UFZ, mit denen ich stets interessante und produktive Diskussionen führen konnte. Besonders bedanken möchte ich mich bei Thomas Banitz, der Teile meiner Arbeit kommentierte und zur Verbesserung beigetragen hat. Des Weiteren danke ich Michael Müller, Thomas Banitz und Claudia Dislich sehr für ihre uneingeschränkte Hilfsbereitschaft und Unterstützung bei jeglichen Fragen und Herausforderungen während der Promotionszeit. Ebenfalls gilt mein besonderer Dank Oliver Jakoby und Florian Hartig, welche stets für spannende Diskussionen zu meinem Promotionsthema offen waren und mir mit ihrem Wissen und ihrer Kreativität neue Sichtweisen bereiteten. Ebenso danke ich auch Gaby, Heike und Andreas für ihre technische und administrative Unterstützung.

Ganz herzlich möchte ich mich auch bei meiner Familie und meinen Freunden bedanken, die stets großes Interesse an meinen Voranschreiten während der Promotionszeit hatten und mich besonders in der letzten Phase der Fertigstellung der Arbeit tatkräftig unterstützten und motivierten.

Außerdem danke ich dem Helmholtz-Zentrum für Umweltforschung – UFZ sowie der Helmholtz Interdisciplinary Graduate School for Environmental Research (HIGRADE).

Erklärung über die Eigenständigkeit der erbrachten wissenschaftlichen Leistung

Ich erkläre hiermit, dass ich die vorliegende Arbeit ohne unzulässige Hilfe Dritter und ohne Benutzung anderer als der angegebenen Hilfsmittel angefertigt habe. Die aus anderen Quellen direkt oder indirekt übernommenen Daten und Konzepte sind unter Angabe der Quelle gekennzeichnet.

Bei der Auswahl und Auswertung folgenden Materials haben mir die nachstehend aufgeführten Personen in der jeweils beschriebenen Weise entgeltlich / unentgeltlich geholfen.

Kapitel 2: Ko-Autoren des veröffentlichten Artikels: Karin Frank, Andreas Huth

Taubert, Franziska, Frank, Karin & Huth, Andreas: A review of grassland models in the biofuel context. Ecological Modelling 245 (2012) 84-93.

Kapitel 5: Ko-Autoren des veröffentlichten Artikels: Florian Hartig, Hans-Jürgen Dobner, Andreas Huth

Taubert, Franziska, Hartig, Florian, Dobner, Hans-Jürgen & Huth, Andreas: On the Challenge of Fitting Tree Size Distributions in Ecology. PLoS ONE 8(2): e58036. doi:10.1371/journal.pone.0058036

Weitere Personen waren an der inhaltlichen materiellen Erstellung der vorliegenden Arbeit nicht beteiligt. Insbesondere habe ich hierfür nicht die entgeltliche Hilfe von Vermittlungs- bzw. Beratungsdiensten (Promotionsberater oder andere Personen) in Anspruch genommen. Niemand hat von mir unmittelbar oder mittelbar geldwerte Leistungen für Arbeiten erhalten, die im Zusammenhang mit dem Inhalt der vorgelegten Dissertation stehen.

Die Arbeit wurde bisher weder im In- noch im Ausland in gleicher oder ähnlicher Form einer anderen Prüfungsbehörde vorgelegt.

Ort, Datum

Unterschrift